Jet evolution in heavy ion collisions

MITP OQS Program, 24th April 2026

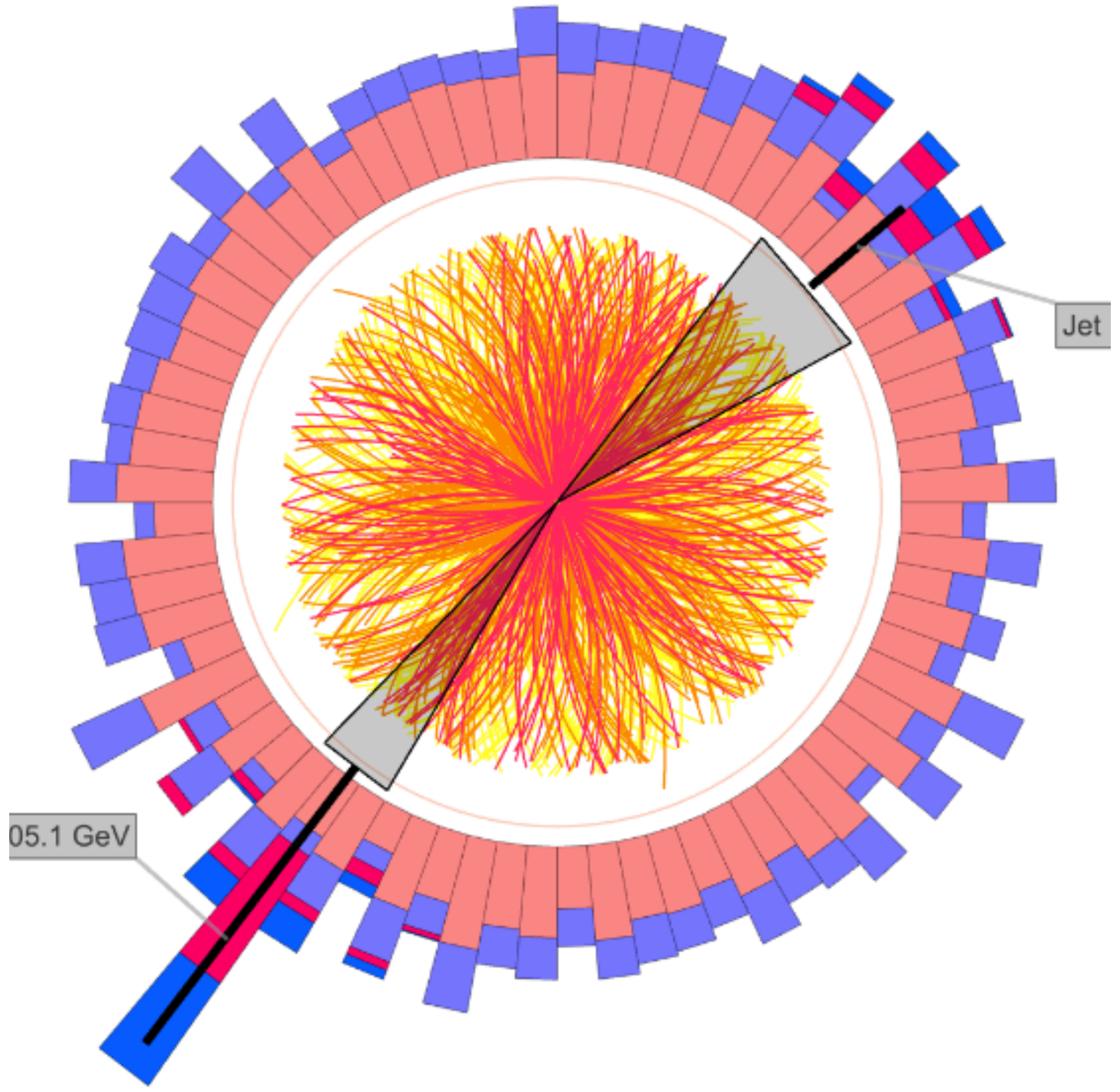

João Barata, CERN-TH

Why Heavy Ion collisions (HICs) ?

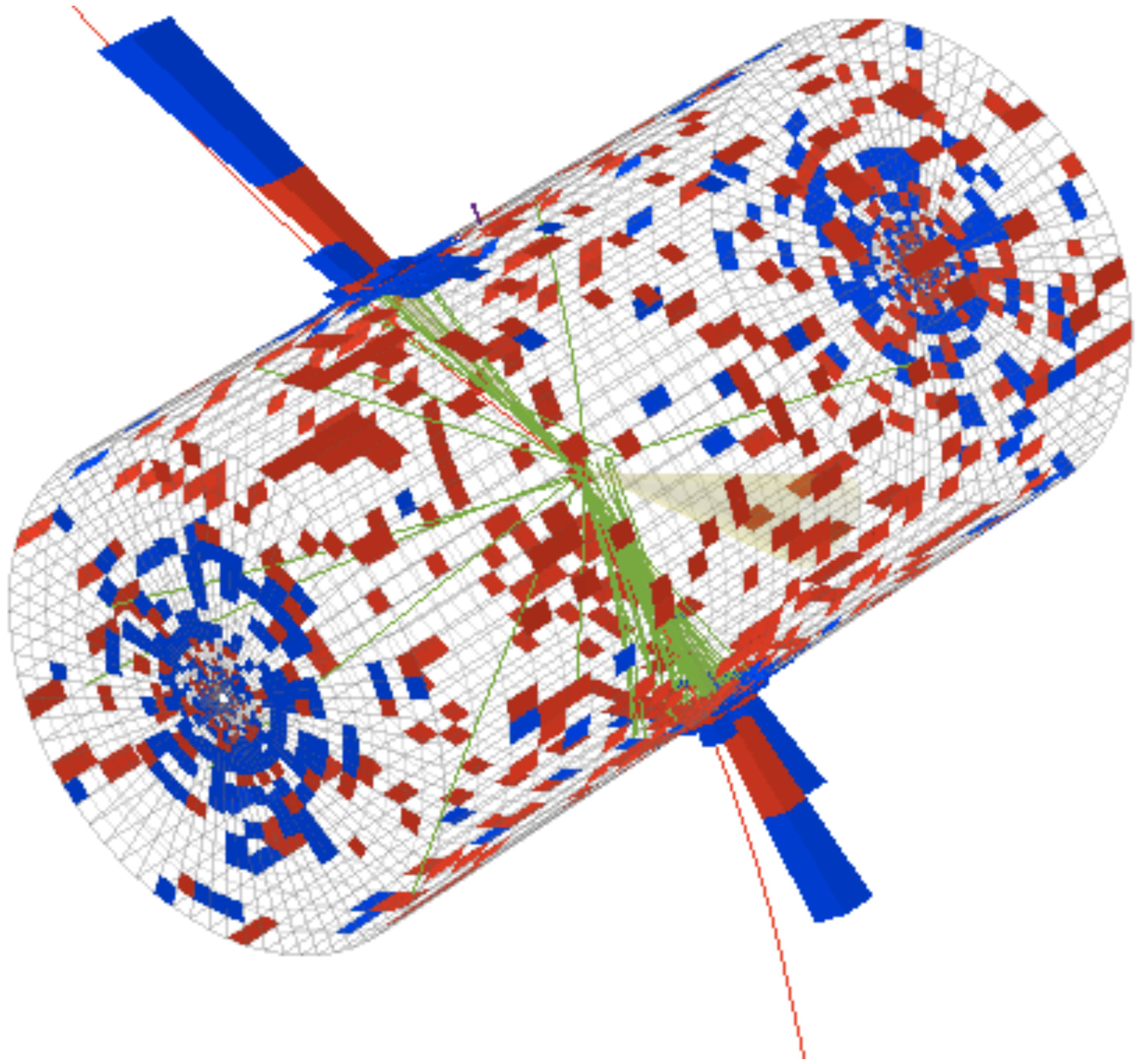

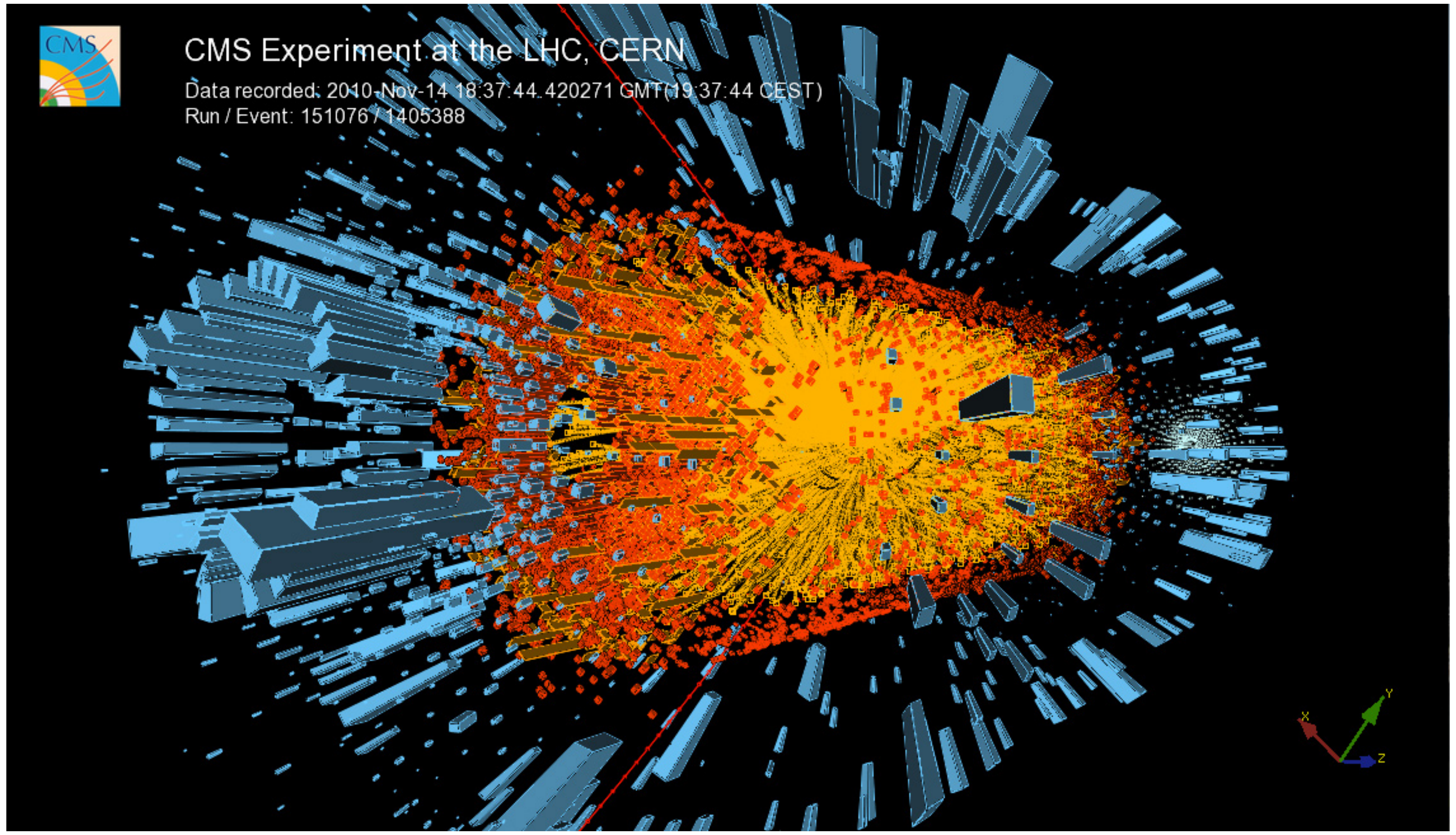

pp collision: a few particles are detected

Precision tests of QCD

AA collision: thousands of detected particles

Emergent many-body properties of QCD

The Standard Model of heavy ion collisions

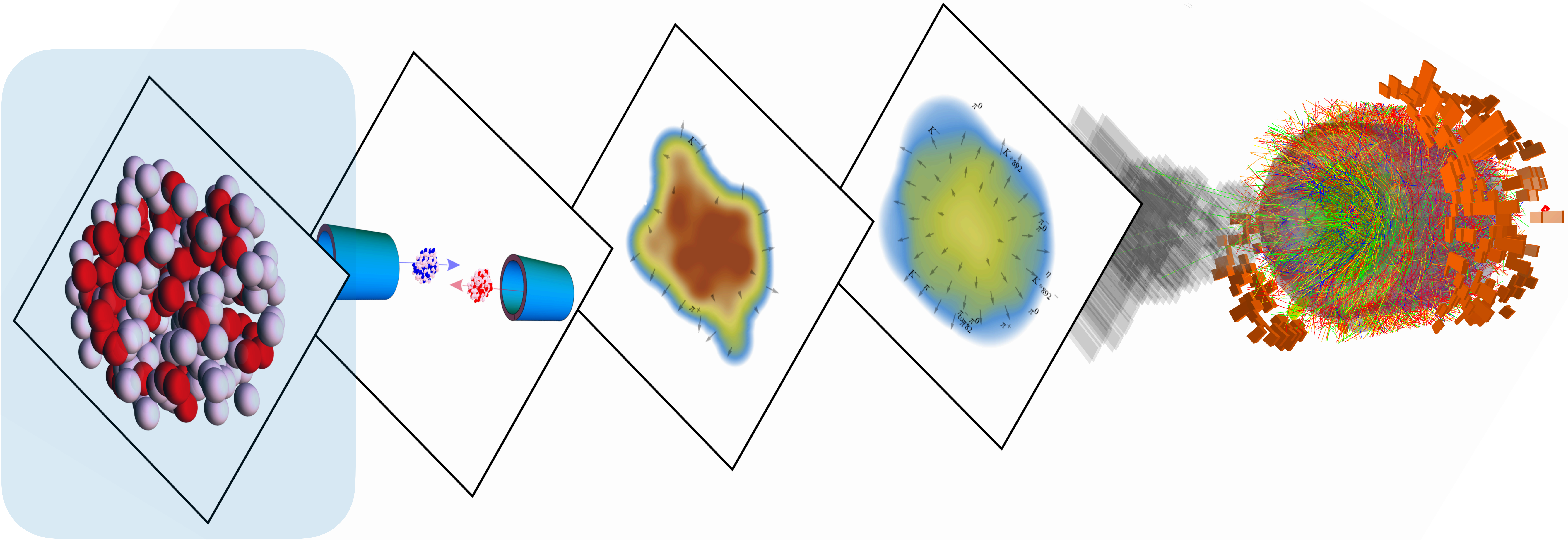

CGC, IS models, nPDFs, ...

The Standard Model of heavy ion collisions

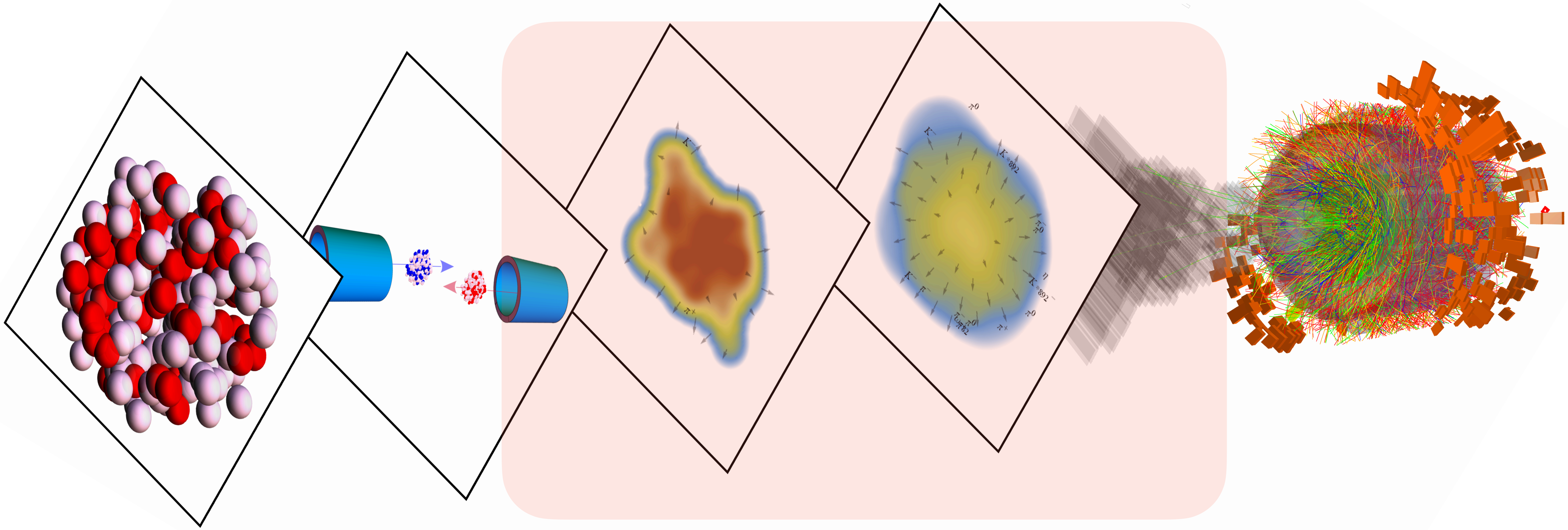

Kinetic theory, hydro, ...

The Standard Model of heavy ion collisions

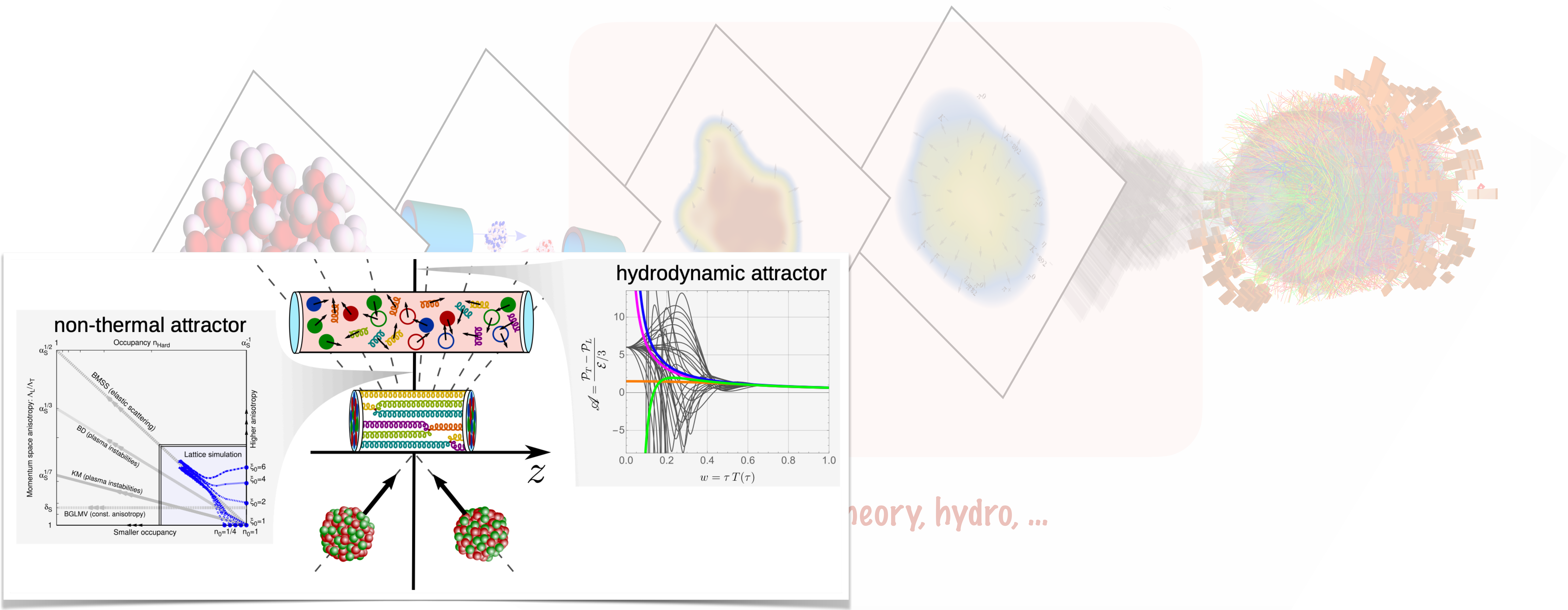

[Berges, Heller, Mazeliauskas, Venugopalan, 2005.12299]

The Standard Model of heavy ion collisions

The Quark Gluon Plasma

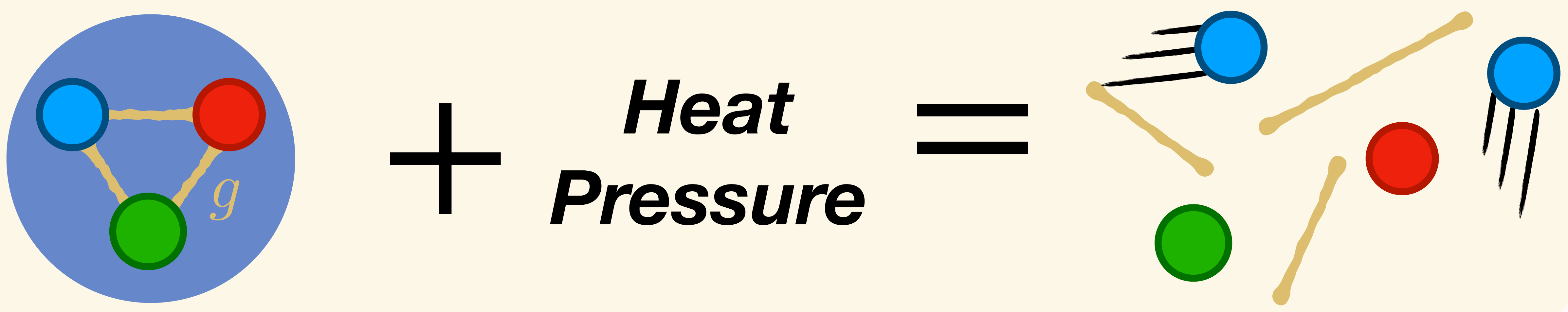

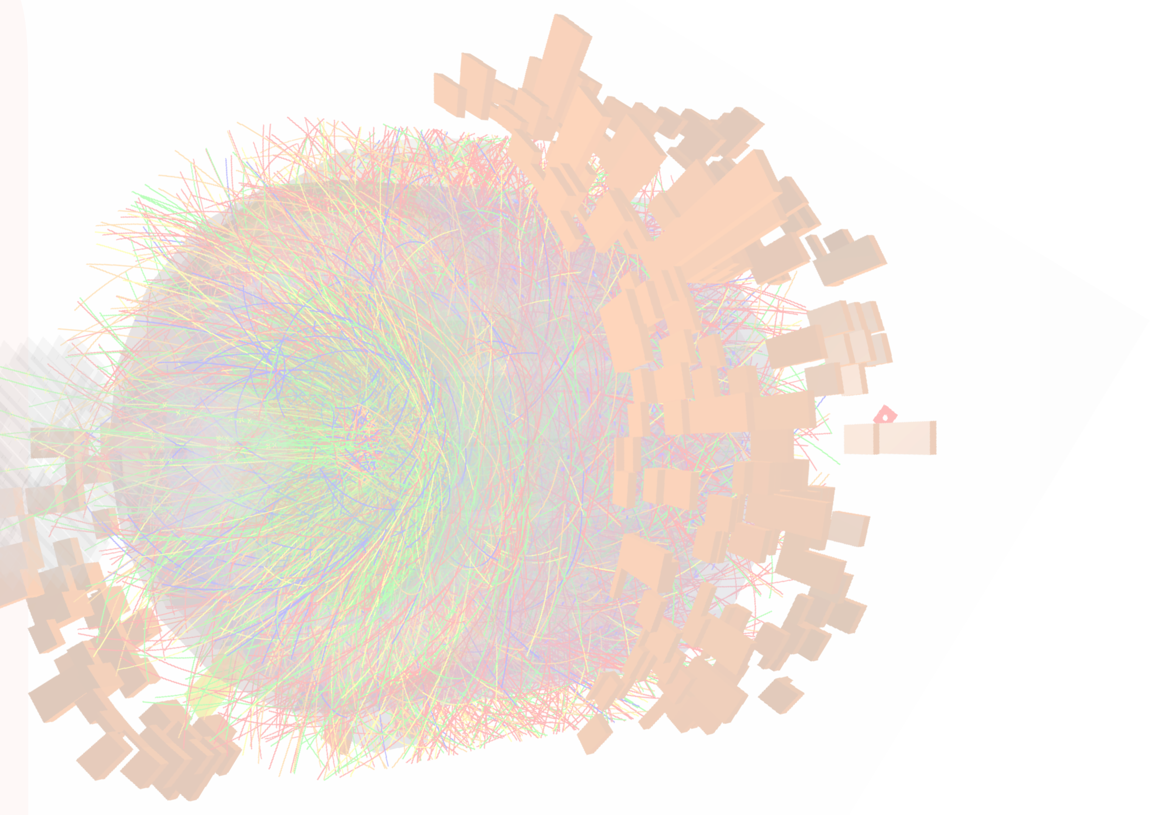

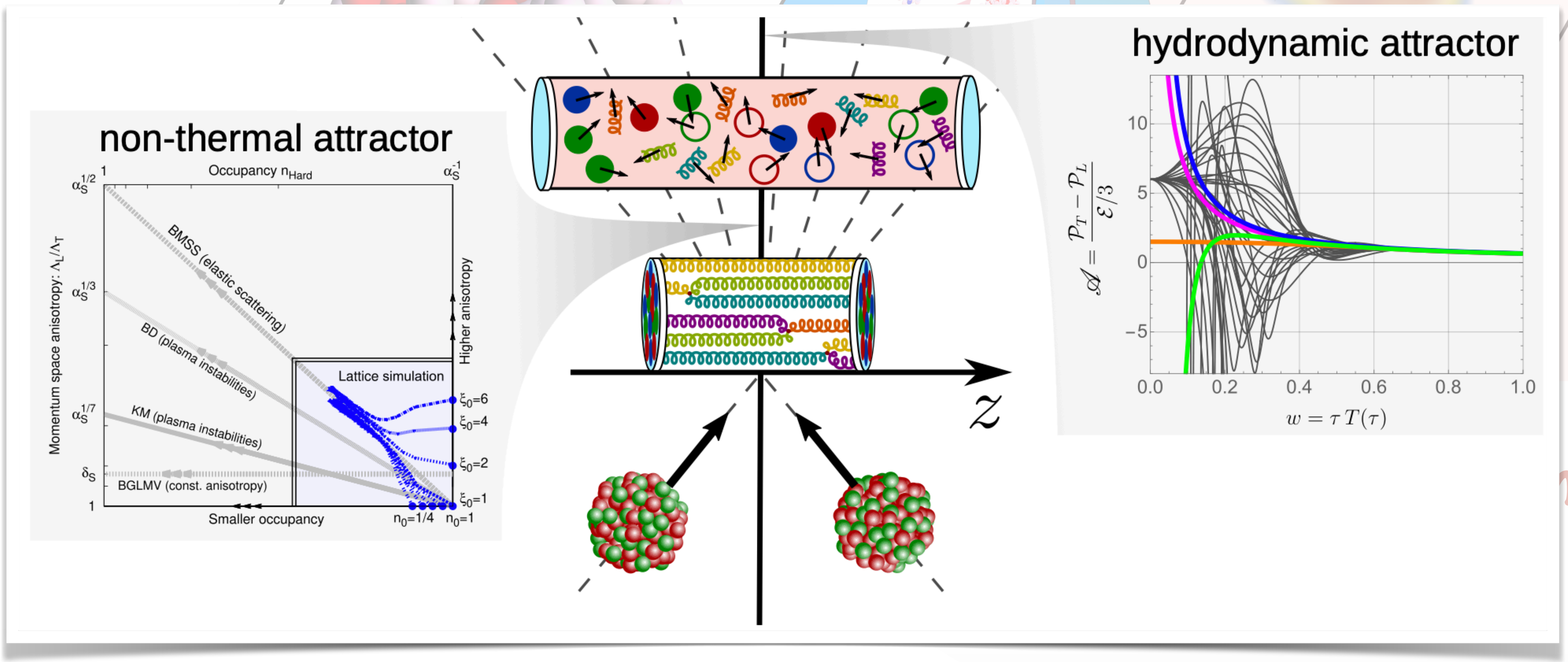

heory, hydro, ...

[Berges, Heller, Mazeliauskas, Venugopalan, 2005.12299]

The Standard Model of heavy ion collisions

The Quark Gluon Plasma

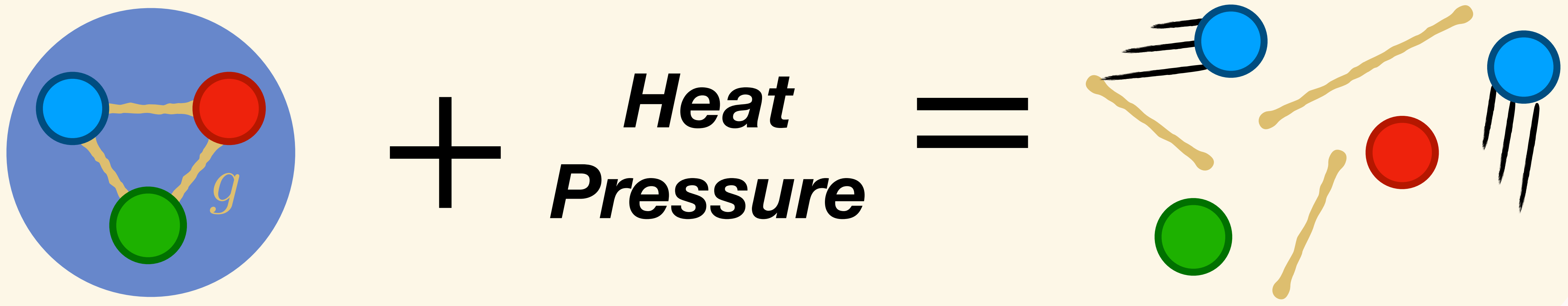

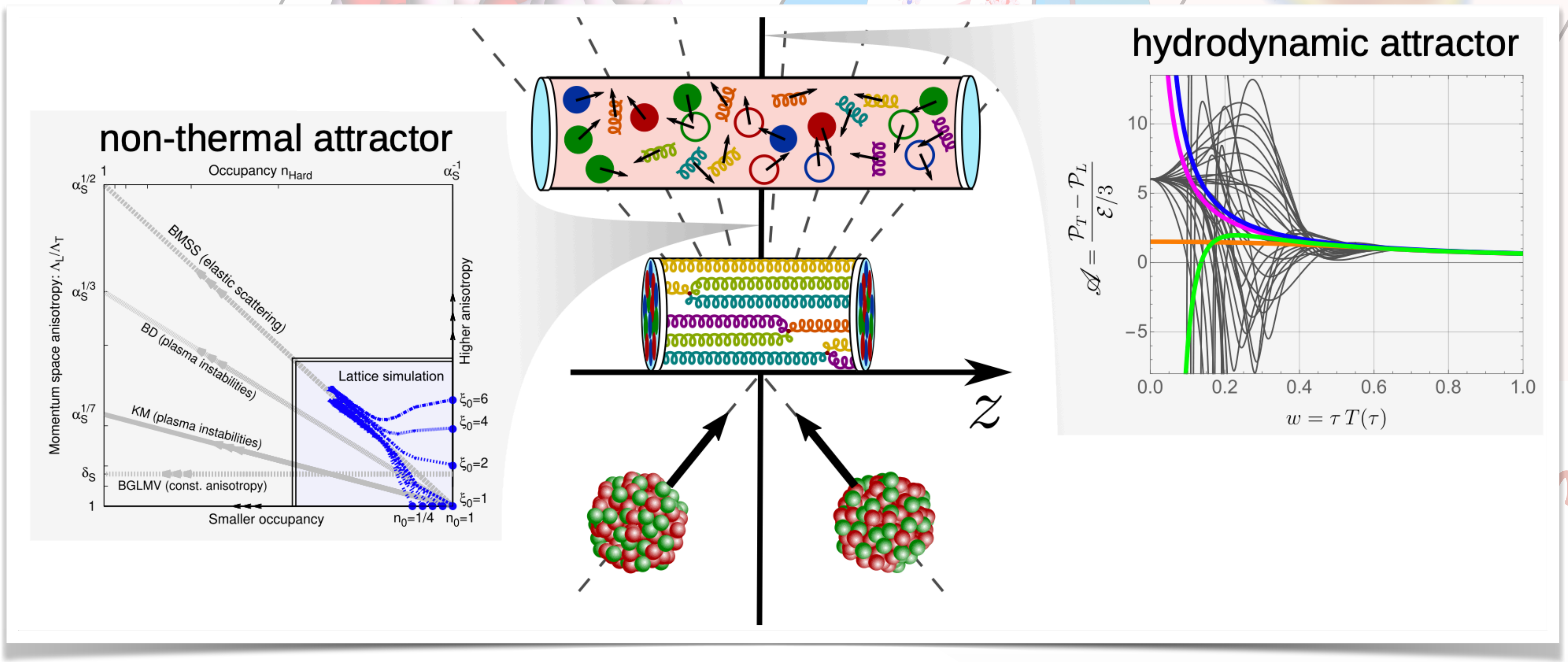

[Berges, Heller, Mazeliauskas, Venugopalan, 2005.12299]

[PHENIX collaboration, 2018]

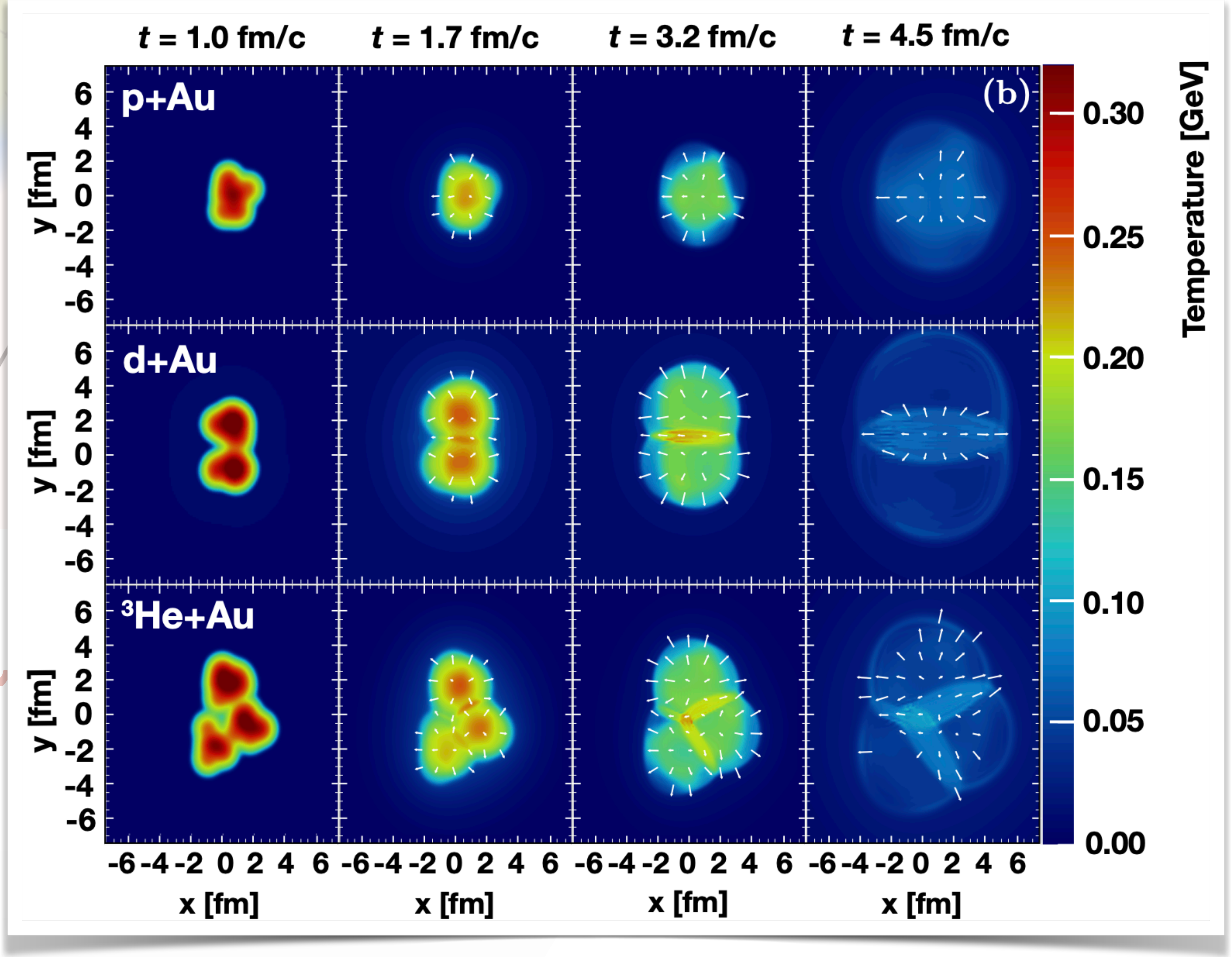

The Standard Model of heavy ion collisions

*Many questions remain open about **validity and emergence** of this "Standard Model" picture of HICs from the QFT and experimental perspectives*

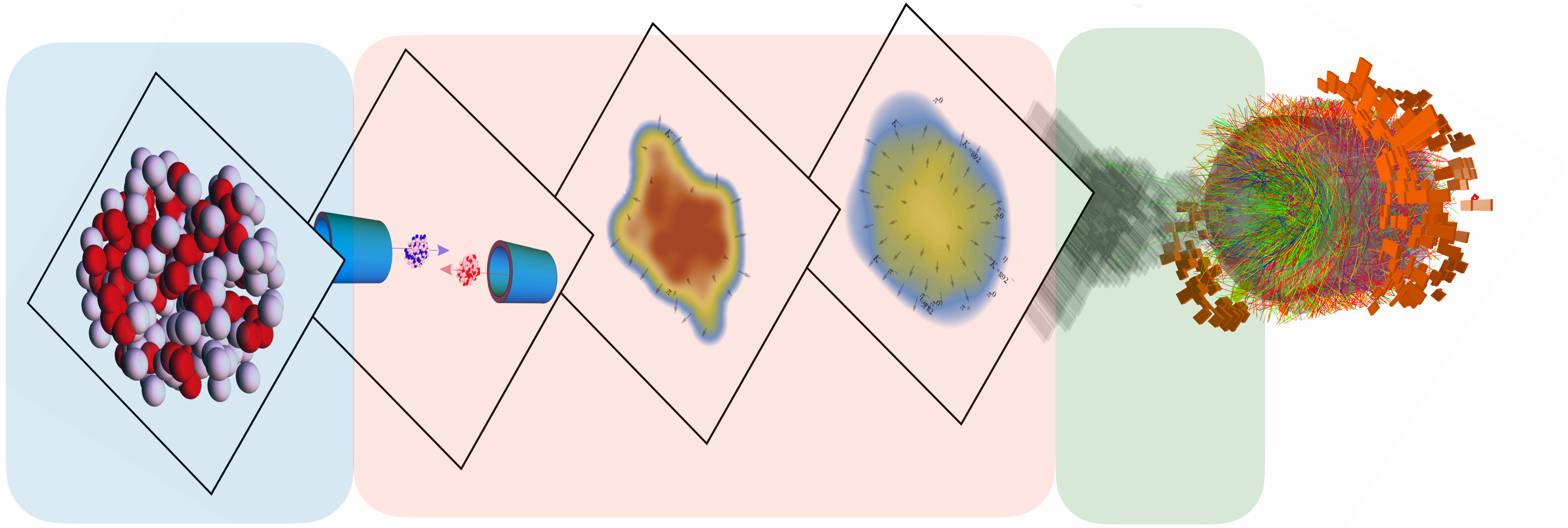

CGC, IS models, …

Kinetic theory, hydro, …

Hadronic transport, …

No confirmation of saturation/ CGC picture	*No test of out of equilibrium dynamics*	*Lacking connection between observables and theory*

Probing heavy ion collisions using jets

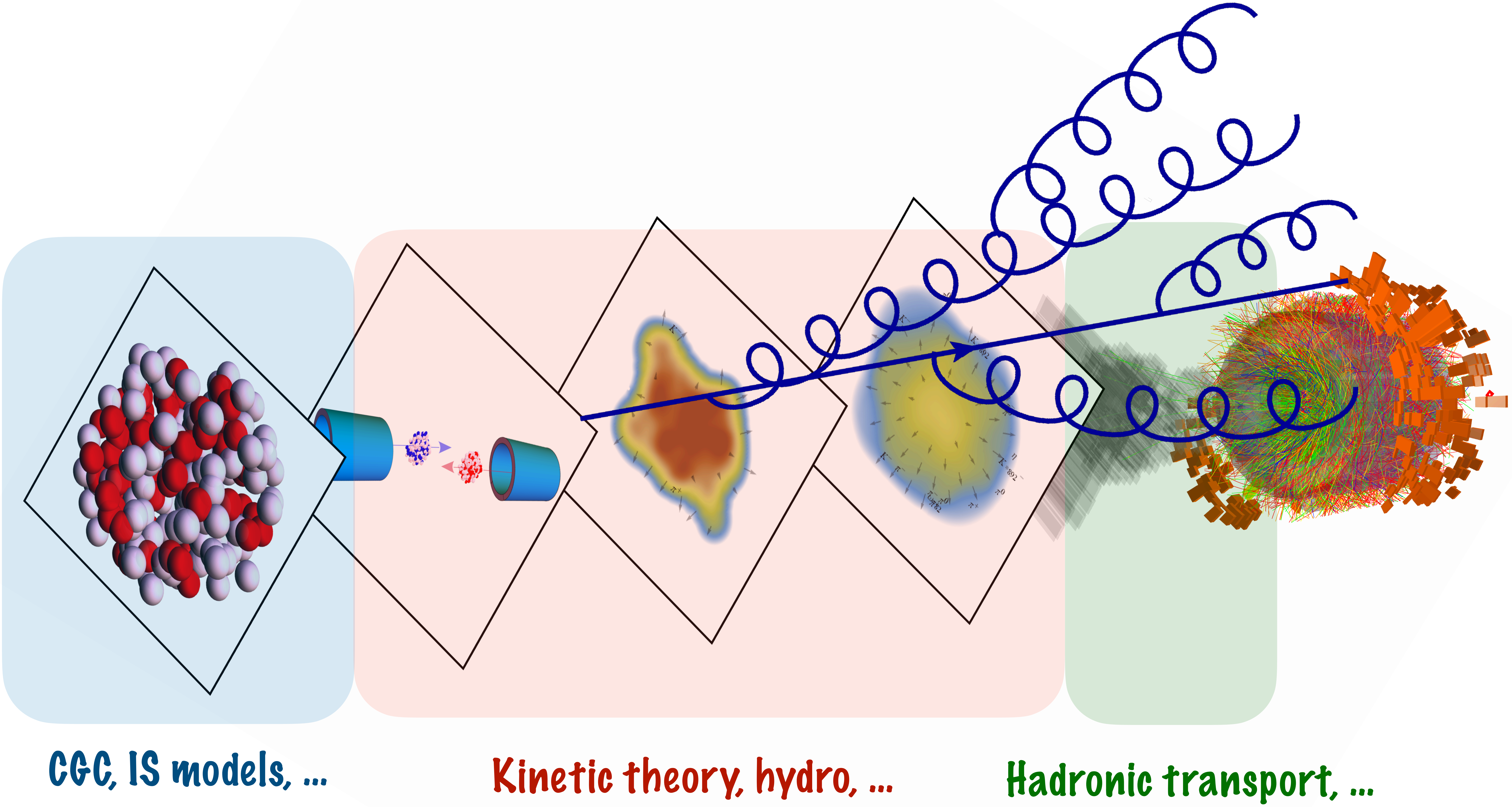

Jets allow for a QCD driven exploration of the intermediate matter states in HIs

Probing heavy ion collisions using jets

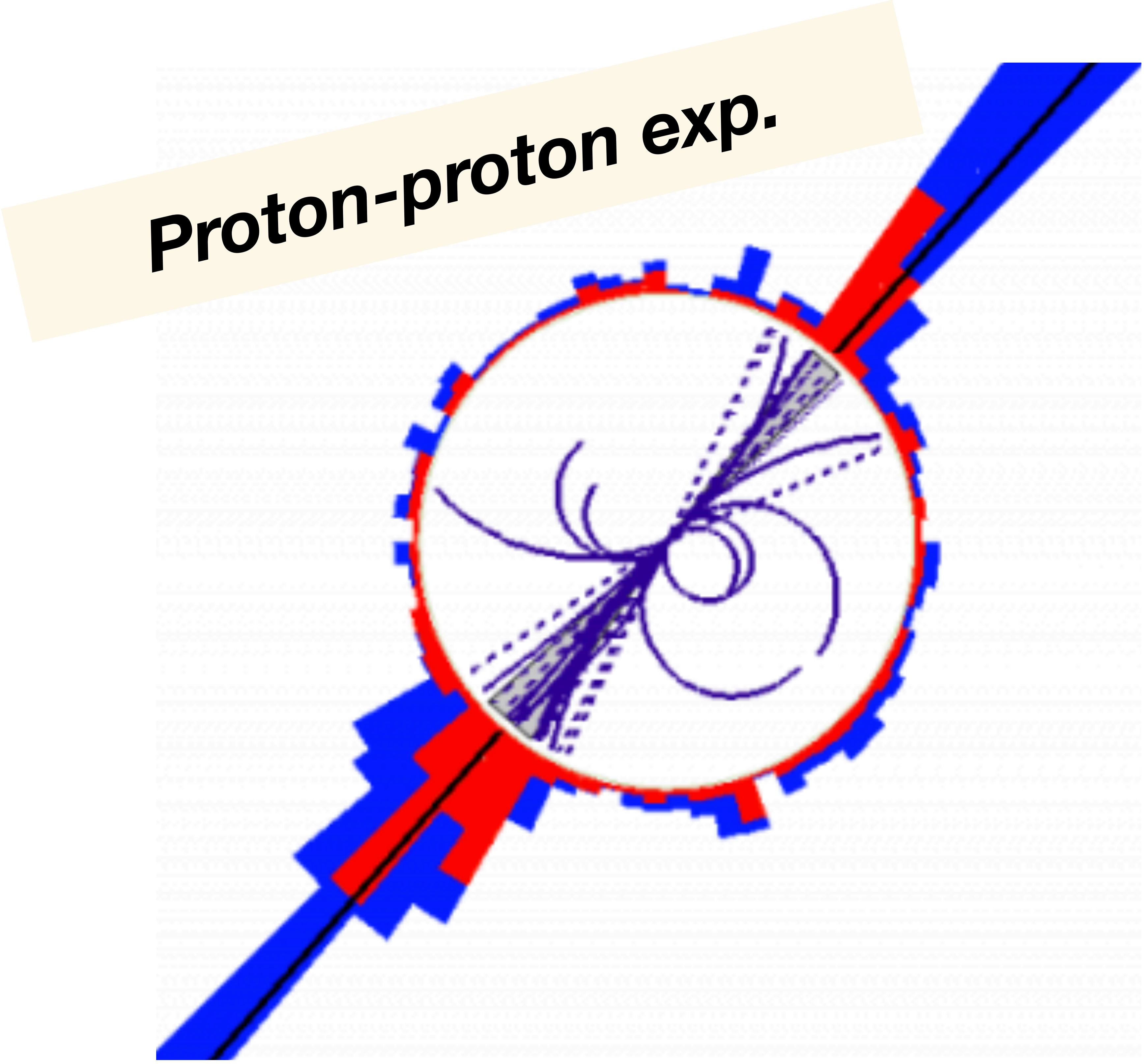

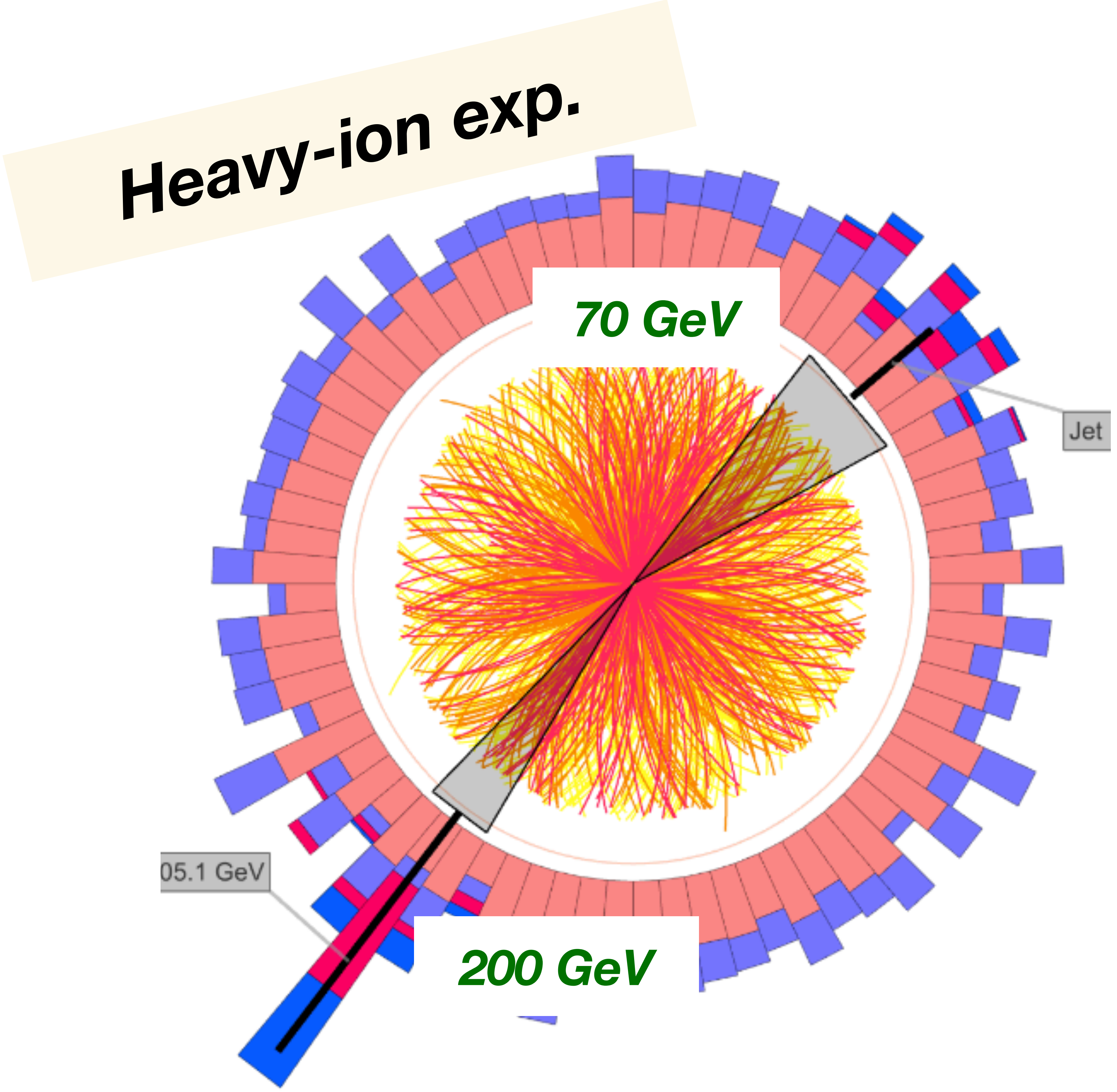

Probing heavy ion collisions using jets

Initial blue quark

Final red quark

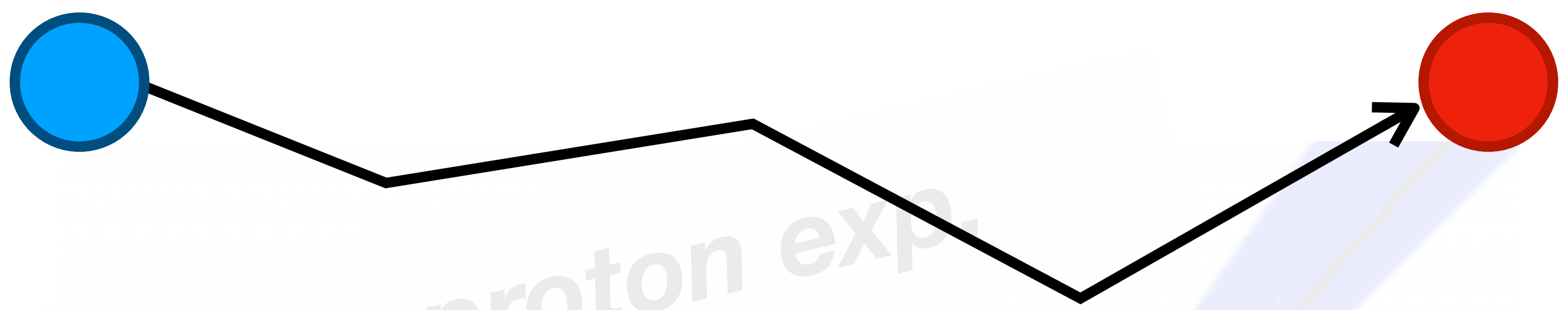

Momentum broadening

$$\langle \boldsymbol{k} \rangle = 0$$

$$\langle \boldsymbol{k}^2 \rangle \sim \hat{q} L$$

Jet transport coefficient, diffusion constant

Light-cone time evolved in matter

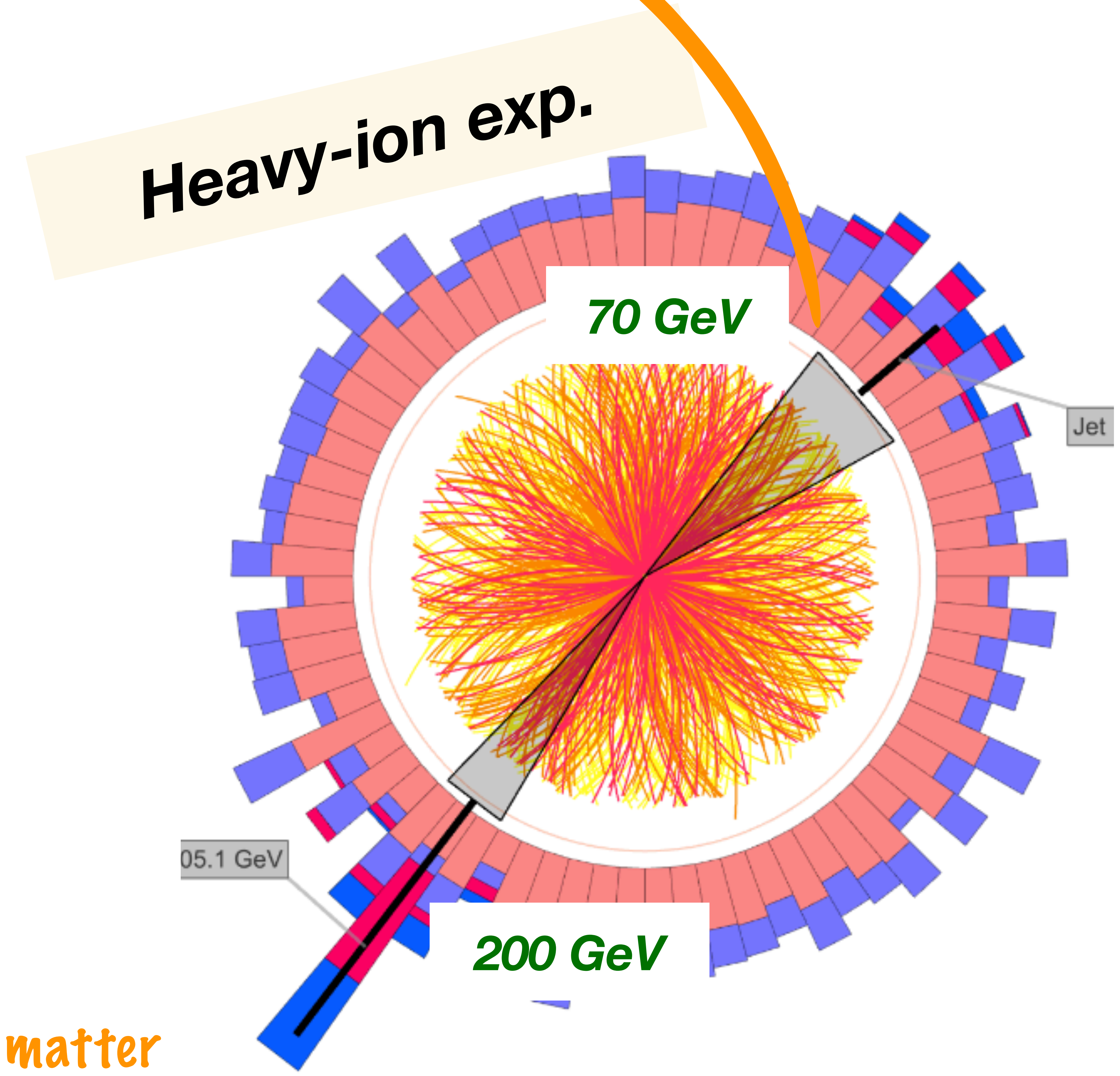

Probing heavy ion collisions using jets

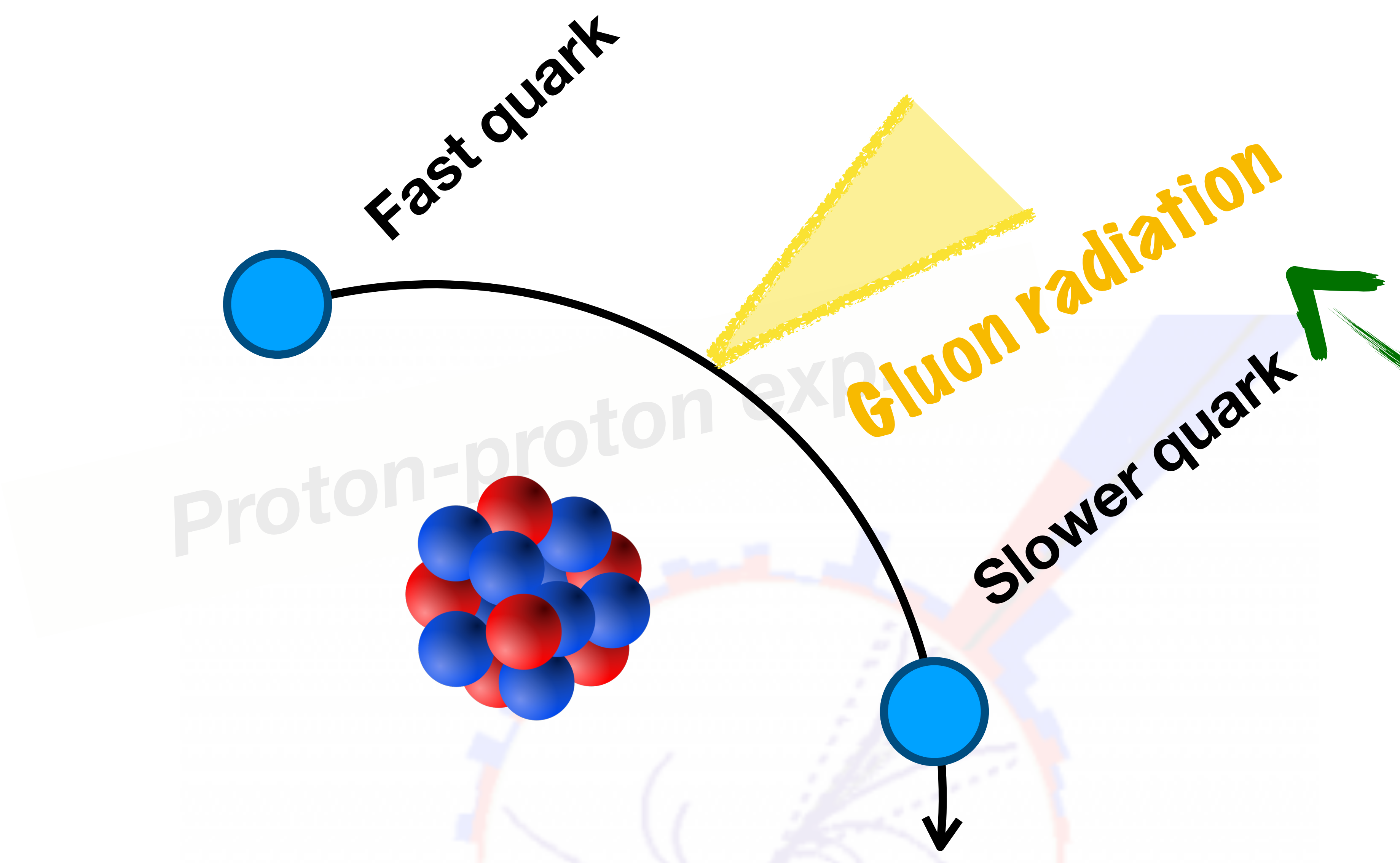

Radiative energy loss

$$\omega \frac{dI}{d\omega} \sim \alpha_s \frac{L}{t_f} \sim \alpha_s \sqrt{\frac{\hat{q}L^2}{\omega}}$$

LPM QCD effect

Energy depletion driven by soft gluon cascades

vs

$$\omega \frac{dI}{d\omega} \sim \alpha_s \frac{\mu^2 L}{\omega}$$

Bethe-Heitler "classical" rate

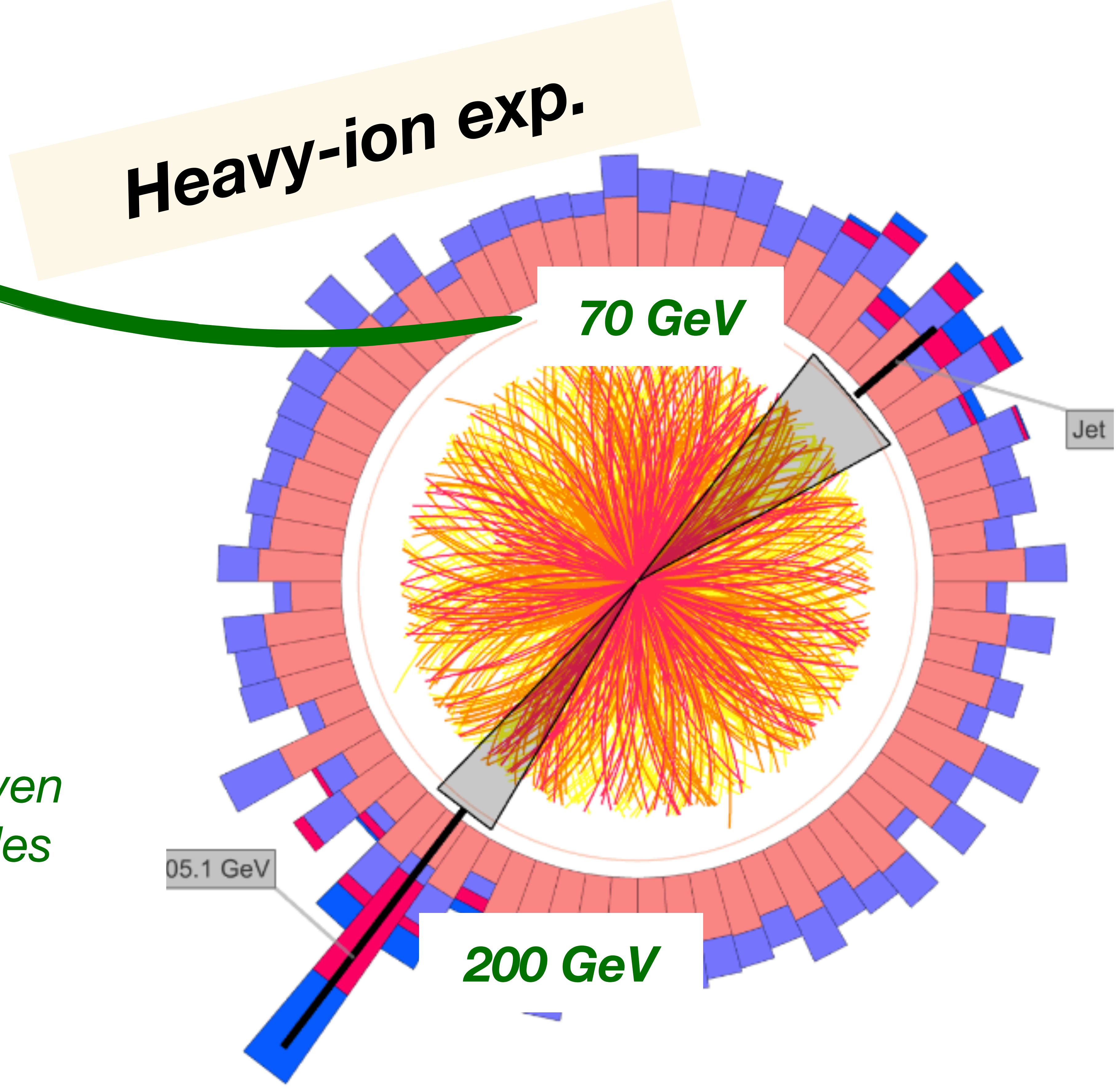

Probing heavy ion collisions using jets

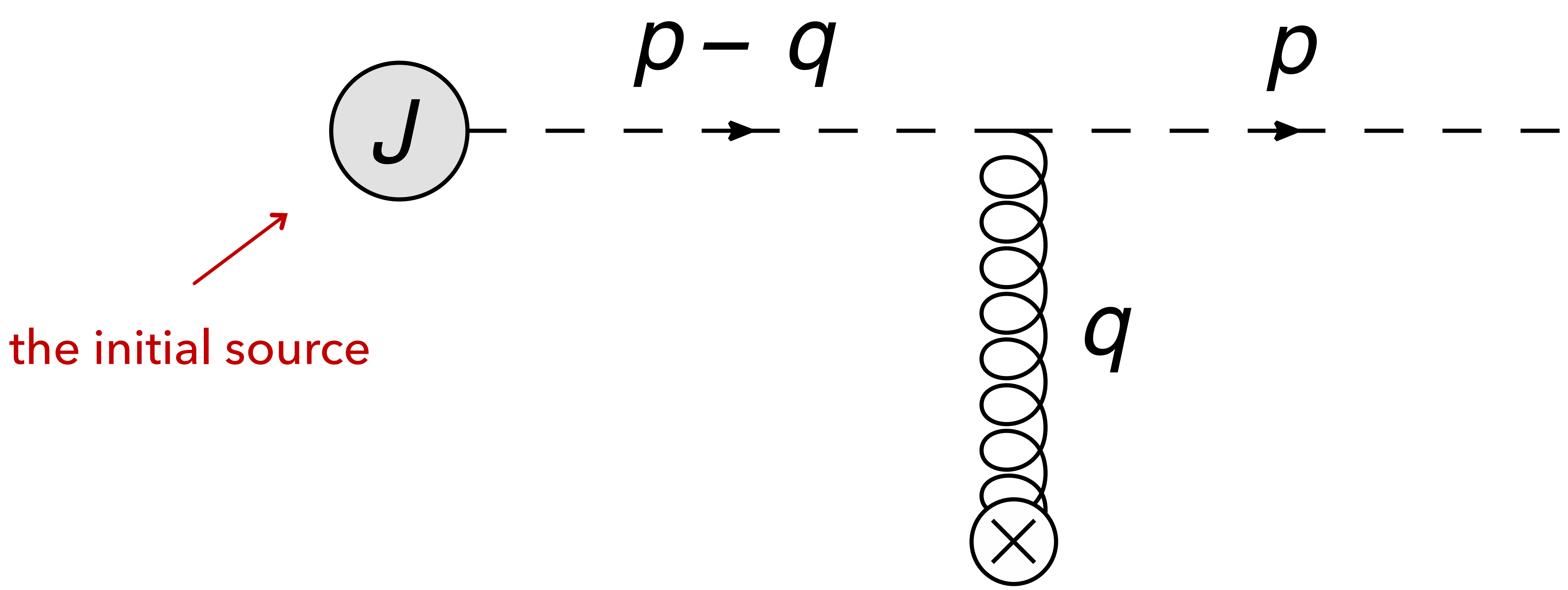

the initial source

$$iM_1(p) = \int \frac{d^4q}{(2\pi)^4} \left[ig\, t^a_{\rm proj} A^{\mu a}_{\rm ext}(q)\, (2p-q)_\mu \right] \left[\frac{i}{(p-q)^2 + i\epsilon} \right] J(p-q)$$

Probing heavy ion collisions using jets

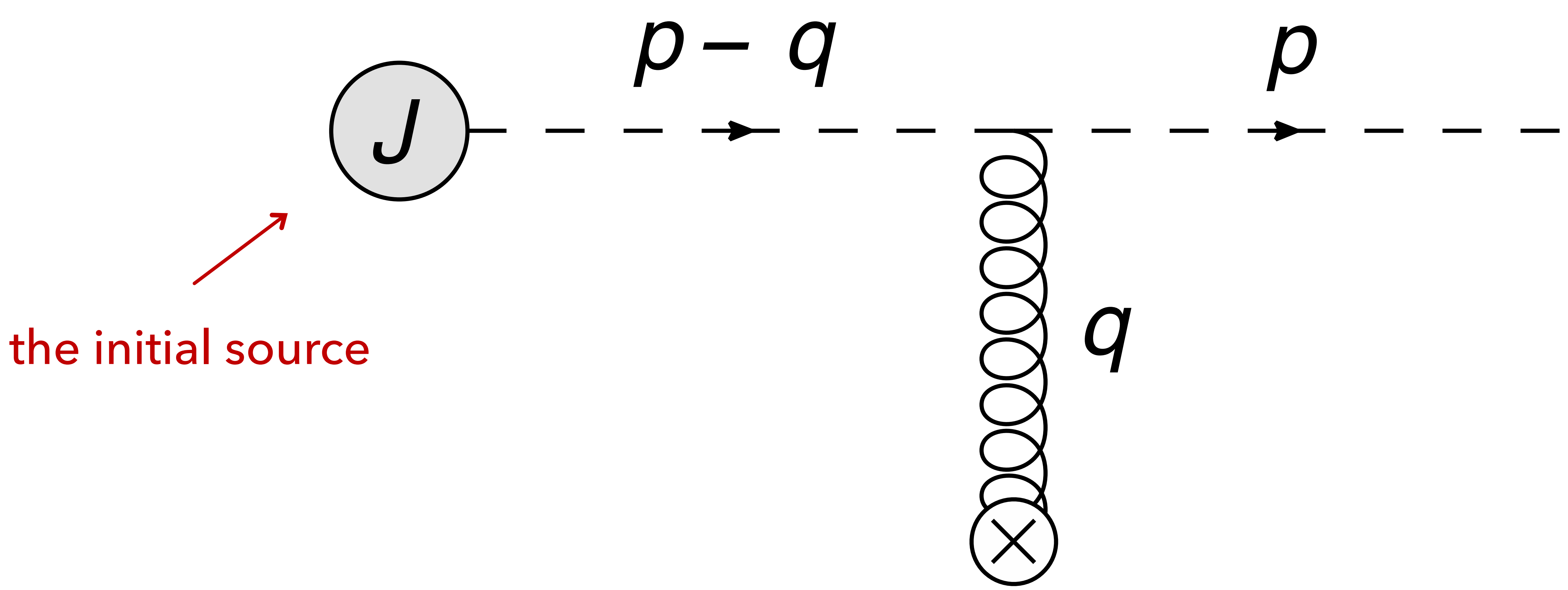

the initial source

$$iM_1(p) = \int \frac{d^4q}{(2\pi)^4}\left[ig\, t^a_{\rm proj} A^{\mu a}_{\rm ext}(q)\,(2p-q)_\mu\right]\left[\frac{i}{(p-q)^2+i\epsilon}\right] J(p-q)$$

$$gA^{\mu a}_{ext}(q) = \sum_i e^{iq\cdot x_i}\, t^a_i\, u^\mu_i\, v_i(q)\,(2\pi)\,\delta\left(q^0\right)$$

color sources

Probing heavy ion collisions using jets

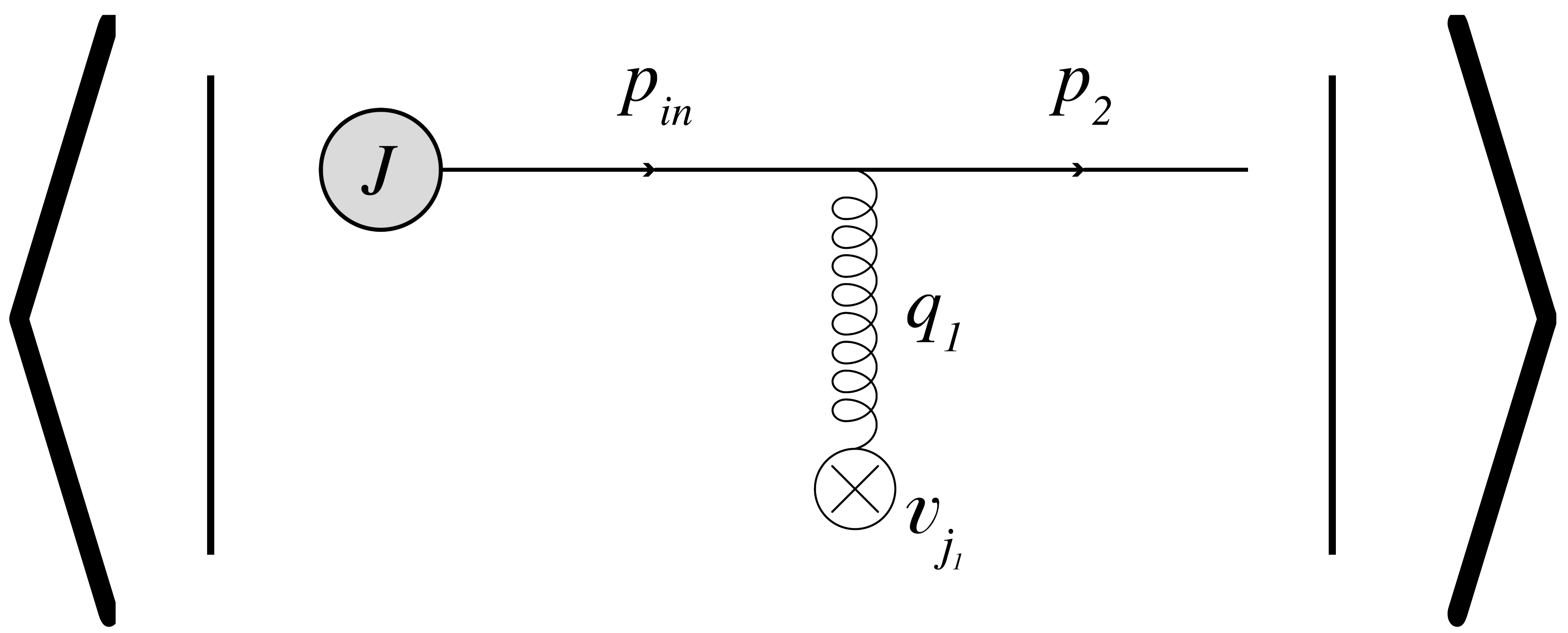

$$\langle t_i^a t_j^b \rangle = \mathcal{C}\delta_{ij}\delta^{ab}$$

color neutrality

$$\sum_i = \int d^3x\, \rho(\vec{x})$$

source averaging

Probing heavy ion collisions using jets

$$E\frac{d\mathcal{N}}{d^3p} \simeq f(E)\delta^{(2)}(\mathbf{p}) + \Big\langle$$

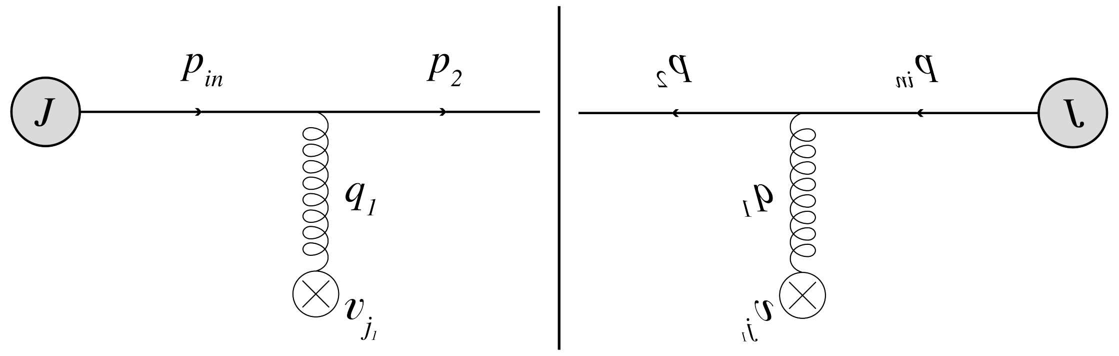

$$\Big\rangle + \Big\langle$$

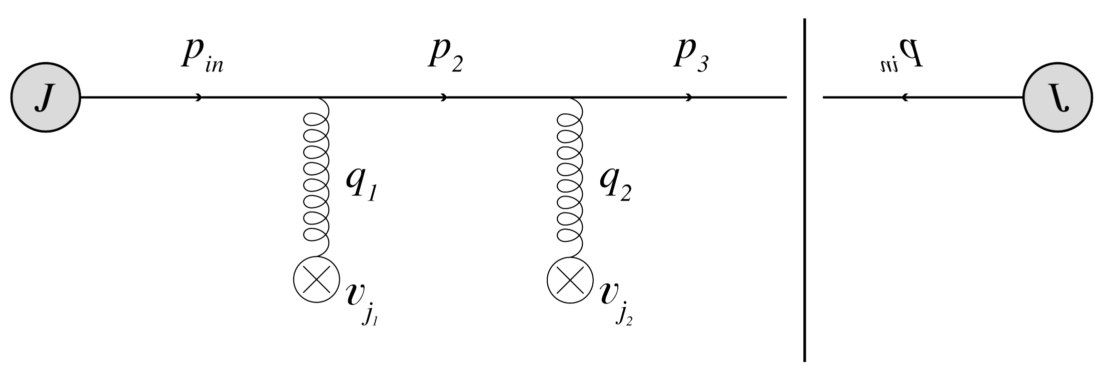

$$\Big\rangle$$

$$\mathcal{V}(\mathbf{q}) = -\mathcal{C}\rho\left(|v(\mathbf{q})|^2 - \delta^{(2)}(\mathbf{q})\int_l |v(\mathbf{l})|^2\right)$$

$$E\frac{d\mathcal{N}^{(1)}}{d^3p} = \int_0^L dz \int_q \mathcal{V}(\mathbf{q})\, f(E)\delta^{(2)}(\mathbf{p}-\mathbf{q})$$

$$\hat{q} = \frac{\partial}{\partial L}\langle p_\perp^2\rangle = \frac{\mathcal{C}g^4\rho}{4\pi\mu^2}L\,\frac{\mu^2}{L}\log\frac{E}{\mu}$$

opacity

Probing heavy ion collisions using jets

Interactions with medium can be described via exchanges of soft gluons

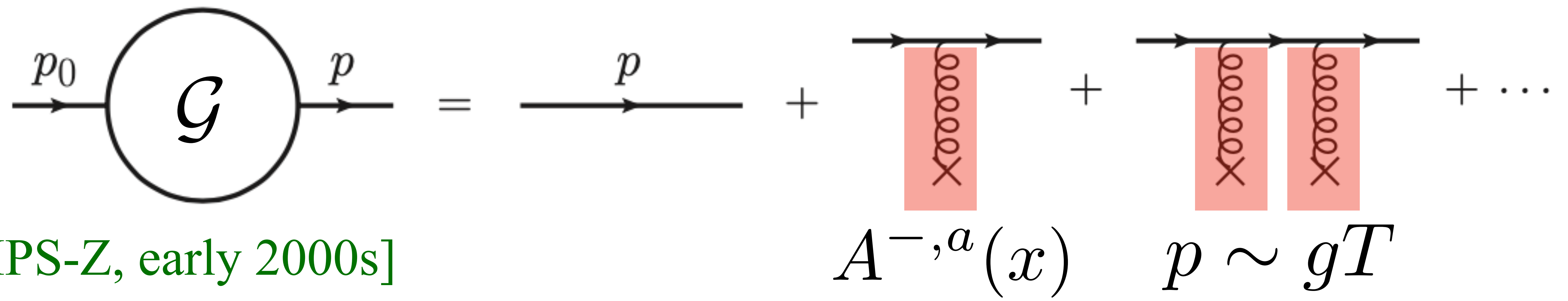

[BDMPS-Z, early 2000s]

At high energies this is equivalent to 2d non-rel. QM: [Susskind, 1960s]

$$\mathcal{G}(\boldsymbol{x}_2, t_2; \boldsymbol{x}_1, t_1) = \int_{\boldsymbol{x}_1}^{\boldsymbol{x}_2} \mathcal{D}\boldsymbol{r} \exp\left(\frac{i\omega}{2}\int_{t_1}^{t_2} dt\, \dot{\boldsymbol{r}}^2\right) \mathcal{W}_{\boldsymbol{r}}$$

Wilson line along forward light-cone

Motion in transverse direction;
partial sub-eikonal order effect

Probing heavy ion collisions using jets

Interactions with medium can be described via exchanges of soft gluons

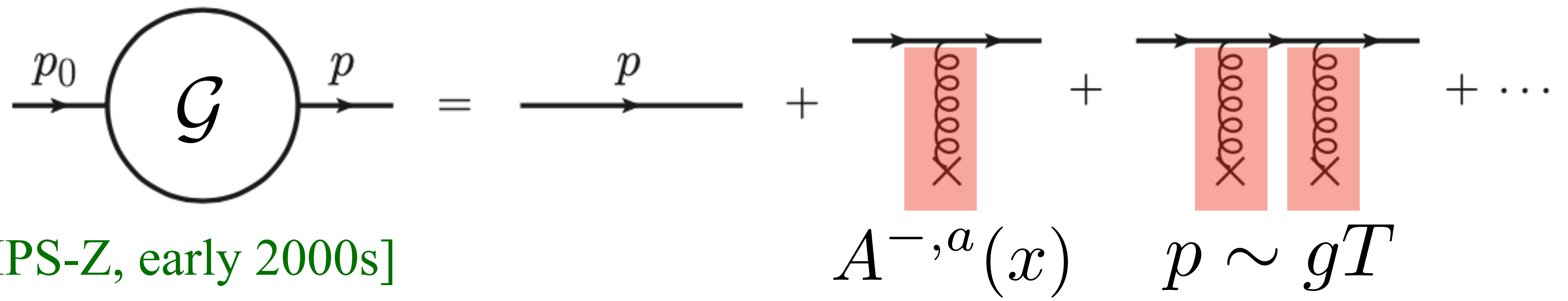

[BDMPS-Z, early 2000s]

At high energies this is equivalent to 2d non-rel. QM: [Susskind, 1960s]

$$\mathcal{G}(\boldsymbol{x}_2, t_2; \boldsymbol{x}_1, t_1) = \int_{\boldsymbol{x}_1}^{\boldsymbol{x}_2} \mathcal{D}\boldsymbol{r} \exp\left(\frac{i\omega}{2}\int_{t_1}^{t_2} dt\, \dot{\boldsymbol{r}}^2\right) \mathcal{W}_{\boldsymbol{r}}$$

Wilson line along forward light-cone

Motion in transverse direction;
partial sub-eikonal order effect

Any cross-section boils down to computing correlation functions of such objects

QCD vertices

$$d\sigma \sim \langle \mathcal{T} \prod \{\mathcal{G}, \Gamma\} \rangle_{\text{matter}}$$

Single particle density matrix evolution

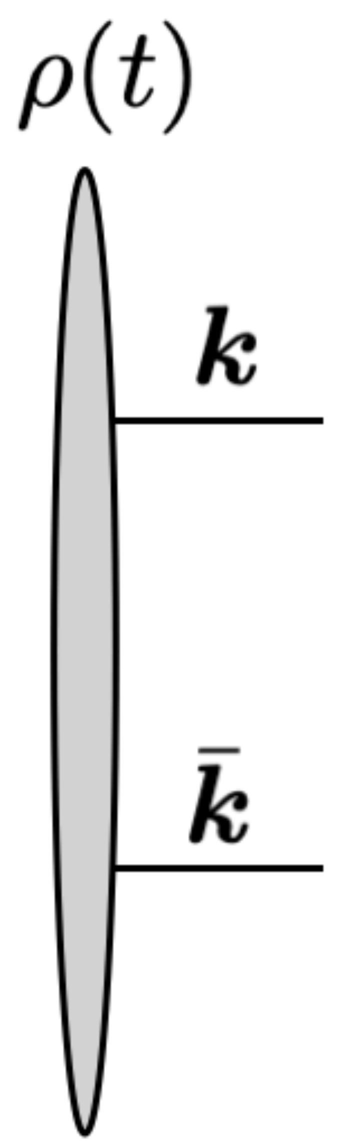

Single particle density matrix evolution in HICs

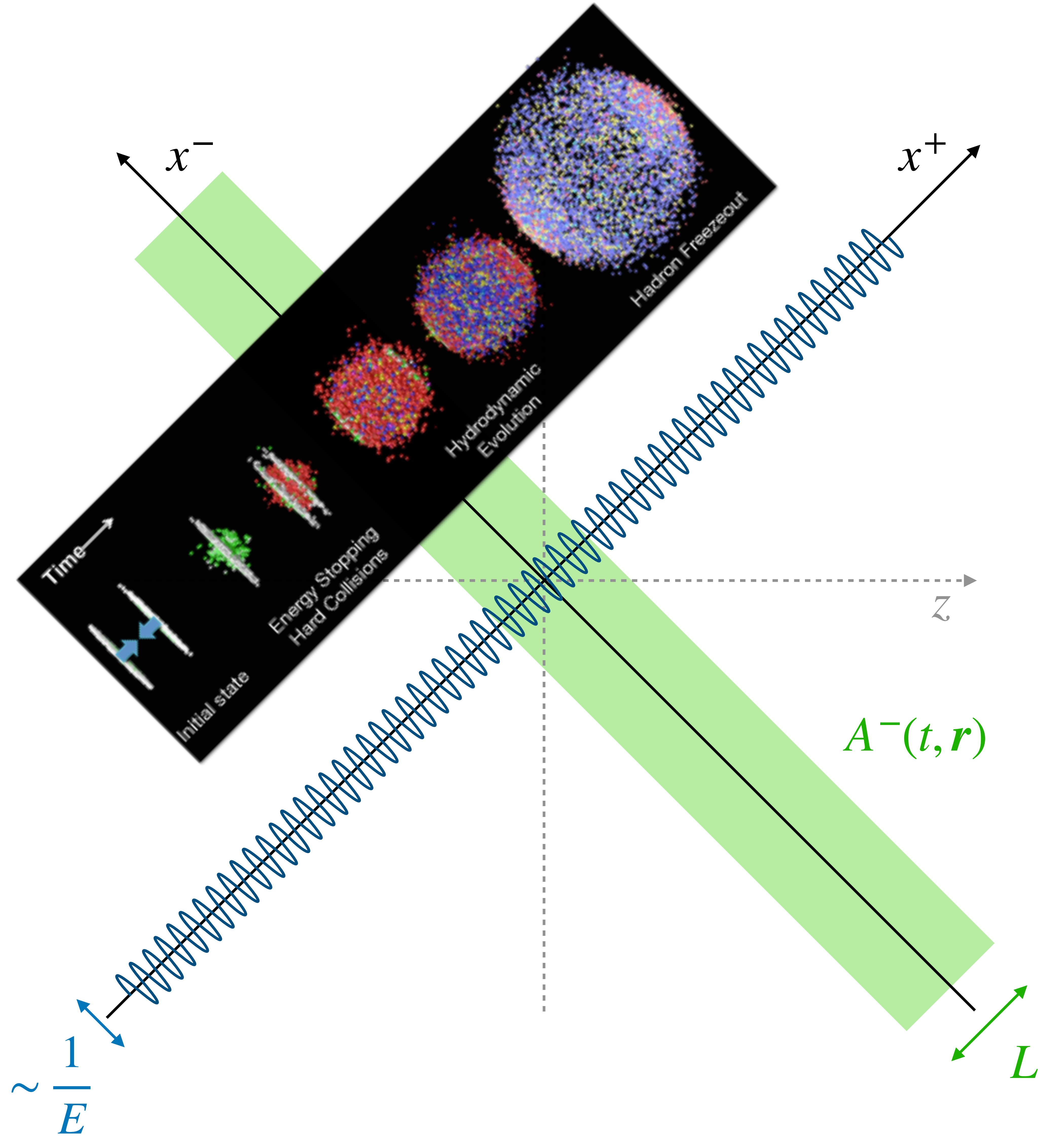

The single parton wave function satisfies

$$\left[i\partial_t + \frac{\partial_\perp^2}{2E} + gA(\boldsymbol{r},t)\right]\psi(\boldsymbol{r},t) = 0$$

The reduced density matrix can be defined as

$$\mathcal{H} = \mathcal{H}_{jet} \otimes \mathcal{H}_{bulk}$$

$$\rho \equiv \mathrm{tr}_A(\rho[A]) = \Big\langle |\psi_A(t)\rangle\langle\psi_A(t)| \Big\rangle_A$$

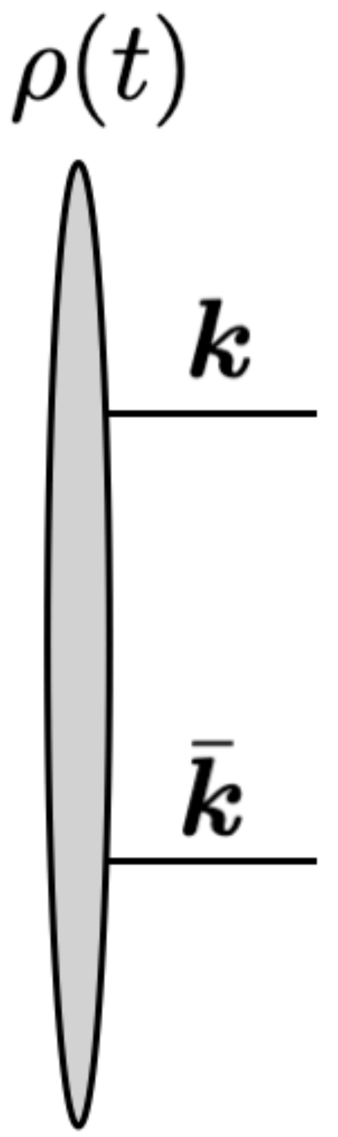

Single particle density matrix evolution in HICs

[JB, Blaizot, Mehtar-Tani, 2305.10476]

$$3 \otimes \bar{3} = 1 \oplus 8$$

$$\rho(t) \equiv \rho_s + t^a \rho_o^a = \frac{1}{N_c} \mathrm{Tr}_c(\rho) + 2\, t^a \mathrm{Tr}_c(t^a \rho)$$

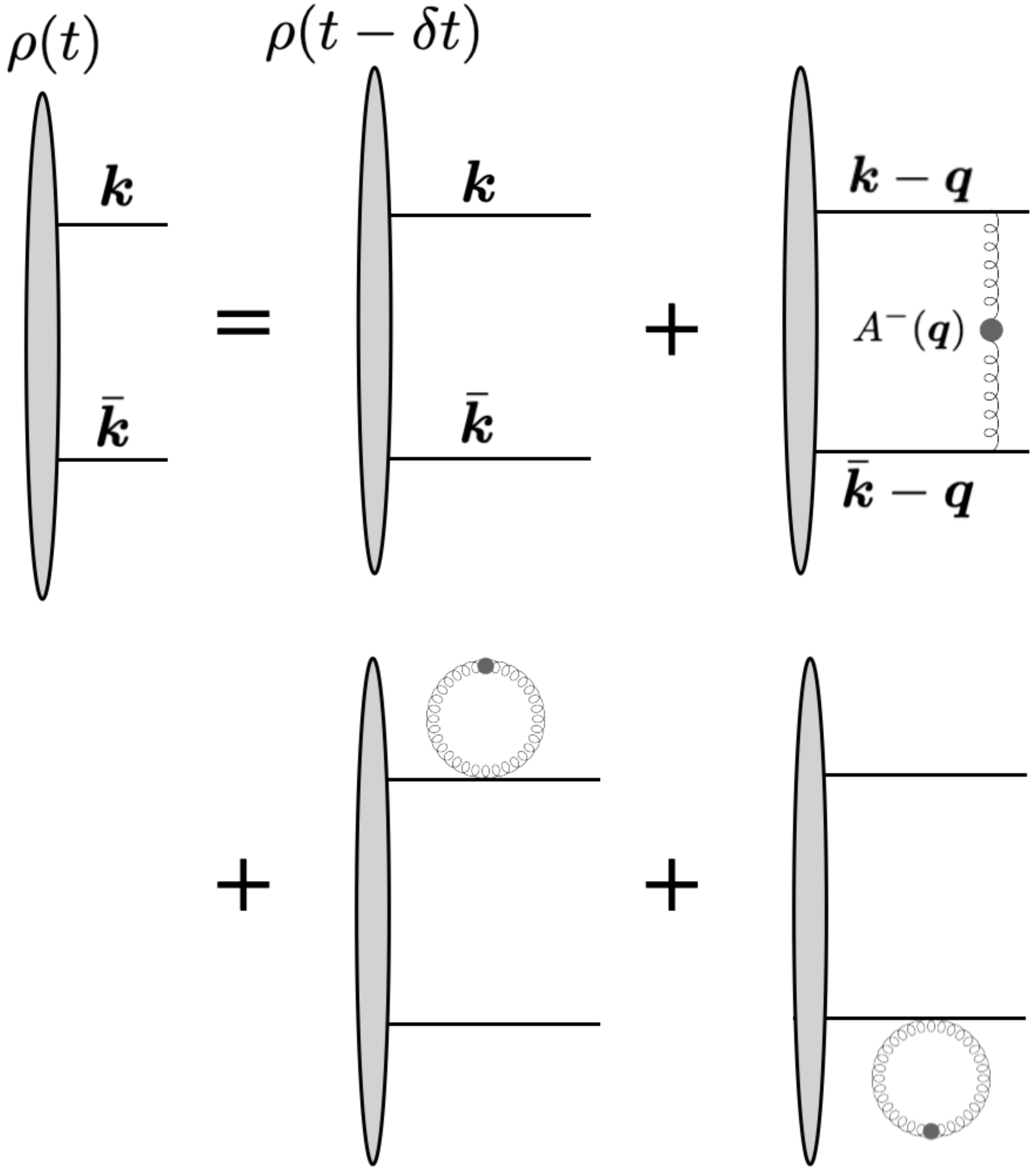

Single particle density matrix evolution in HICs

[JB, Blaizot, Mehtar-Tani, 2305.10476]

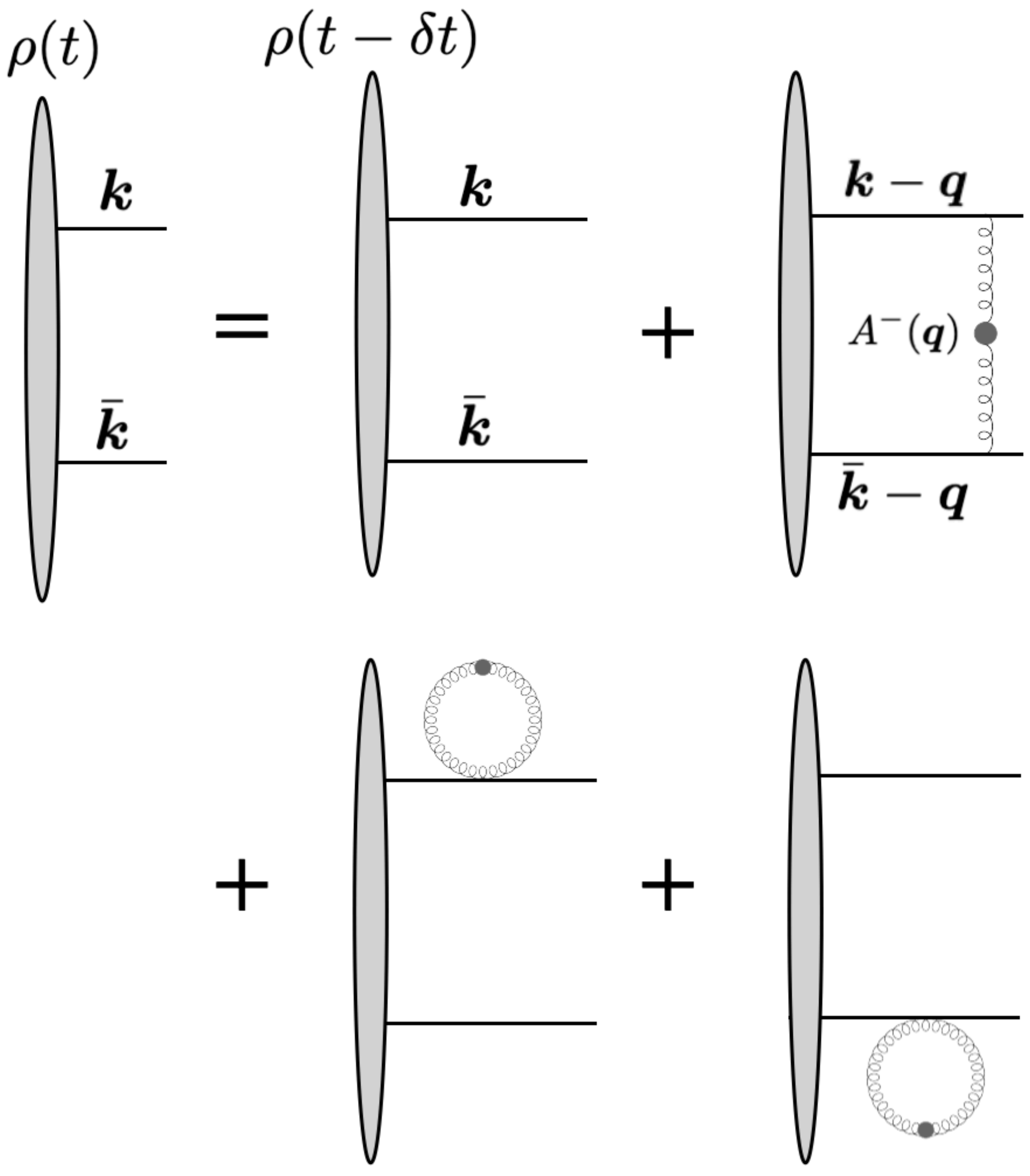

$$3 \otimes \bar{3} = 1 \oplus 8$$

$$\rho(t) \equiv \rho_s + t^a \rho_o^a = \frac{1}{N_c}\mathrm{Tr}_c(\rho) + 2\, t^a \mathrm{Tr}_c(t^a \rho)$$

For color singlet:

$$\langle \boldsymbol{k}|\rho_s(t)|\bar{\boldsymbol{k}}\rangle = C_F \int_{\boldsymbol{q}} \int_0^t dt'\, e^{i\frac{(\boldsymbol{k}^2-\bar{\boldsymbol{k}}^2)}{2E}(t-t')} \times \gamma(\boldsymbol{q}) \left[\langle \boldsymbol{k}-\boldsymbol{q}|\rho_s(t')|\bar{\boldsymbol{k}}-\boldsymbol{q}\rangle - \langle \boldsymbol{k}|\rho_s(t')|\bar{\boldsymbol{k}}\rangle\right]$$

For color octet:

$$\langle \boldsymbol{k}|\rho_o(t)|\bar{\boldsymbol{k}}\rangle = C_F \int_{\boldsymbol{q}} \int_0^t dt'\, e^{i\frac{(\boldsymbol{k}^2-\bar{\boldsymbol{k}}^2)}{2E}(t-t')} \times \gamma(\boldsymbol{q}) \left[\langle \boldsymbol{k}-\boldsymbol{q}|\rho_o(t')|\bar{\boldsymbol{k}}-\boldsymbol{q}\rangle + \frac{1}{2N_cC_F}\langle \boldsymbol{k}|\rho_o(t')|\bar{\boldsymbol{k}}\rangle\right]$$

Single particle density matrix evolution in HICs

[JB, Blaizot, Mehtar-Tani, 2305.10476]

The matrix elements of the singlet and octet components satisfy Boltzmann transport

$$\gamma(\boldsymbol{q}) \approx g^4 n/\boldsymbol{q}^4$$

$$\partial_t \rho_{\rm s,o}(\boldsymbol{\ell}, \boldsymbol{x}, t) = -\left[\frac{\boldsymbol{\ell}\cdot\partial_{\boldsymbol{x}}}{E} + \Gamma_{\rm s,o}(\boldsymbol{x})\right]\rho_{\rm s,o}(\boldsymbol{\ell}, \boldsymbol{x}, t)$$

$$\Gamma_{\rm s}(\boldsymbol{x}) = C_F \int_{\boldsymbol{q}} \left(1 - e^{i\boldsymbol{q}\cdot\boldsymbol{x}}\right)\gamma(\boldsymbol{q})\,,$$

$$\Gamma_{\rm o}(\boldsymbol{x}) = \int_{\boldsymbol{q}} \left(C_F + \frac{1}{2N_c} e^{i\boldsymbol{q}\cdot\boldsymbol{x}}\right)\gamma(\boldsymbol{q})$$

Single particle density matrix evolution in HICs

[JB, Blaizot, Mehtar-Tani, 2305.10476]

The matrix elements of the singlet and octet components satisfy Boltzmann transport $\gamma(\boldsymbol{q}) \approx g^4 n/\boldsymbol{q}^4$

$$\partial_t \rho_{\rm s,o}(\boldsymbol{\ell}, \boldsymbol{x}, t) = -\left[\frac{\boldsymbol{\ell}\cdot\partial_{\boldsymbol{x}}}{E} + \Gamma_{\rm s,o}(\boldsymbol{x})\right]\rho_{\rm s,o}(\boldsymbol{\ell}, \boldsymbol{x}, t)$$

$$\Gamma_{\rm s}(\boldsymbol{x}) = C_F \int_{\boldsymbol{q}} \left(1 - e^{i\boldsymbol{q}\cdot\boldsymbol{x}}\right)\gamma(\boldsymbol{q}) \,,$$

$$\Gamma_{\rm o}(\boldsymbol{x}) = \int_{\boldsymbol{q}} \left(C_F + \frac{1}{2N_c} e^{i\boldsymbol{q}\cdot\boldsymbol{x}}\right)\gamma(\boldsymbol{q})$$

This form allows to settle the evolution in color space $\rho_{\rm s,o}(\boldsymbol{b}, \boldsymbol{x}, t) = \rho^{(0)}_{\rm s,o}(\boldsymbol{b}, \boldsymbol{x})\, {\rm e}^{-t\,\Gamma_{\rm s,o}(\boldsymbol{x})}$

$$\Gamma_{\rm s}(\boldsymbol{x}) \approx 4\pi\alpha_s^2 C_F n \log\left(\frac{Q^2}{m_D^2}\right)\frac{\boldsymbol{x}^2}{4} \equiv \frac{\hat{q}}{4}\boldsymbol{x}^2 \,,$$

$$\Gamma_{\rm o}(\boldsymbol{x}) \approx \frac{4\pi\alpha_s^2 C_A n}{m_D^2}$$

$\boldsymbol{x} \to 0$ ⟶

Singlet ⟶ Neutral to matter

Blaizot, Iancu, Braaten, Pisarski, …

Octet ⟶ Damping

One can also show that singlet subspaces become equally probable Zakharov, Blaizot, Escobedo, …

Single particle density matrix evolution in HICs

[JB, Blaizot, Mehtar-Tani, 2305.10476]

$$t_1 \simeq 0.06 \text{ fm} \quad t_2 \simeq 22.80 \text{ fm} \quad t_0 \simeq 444.44 \text{ fm}$$

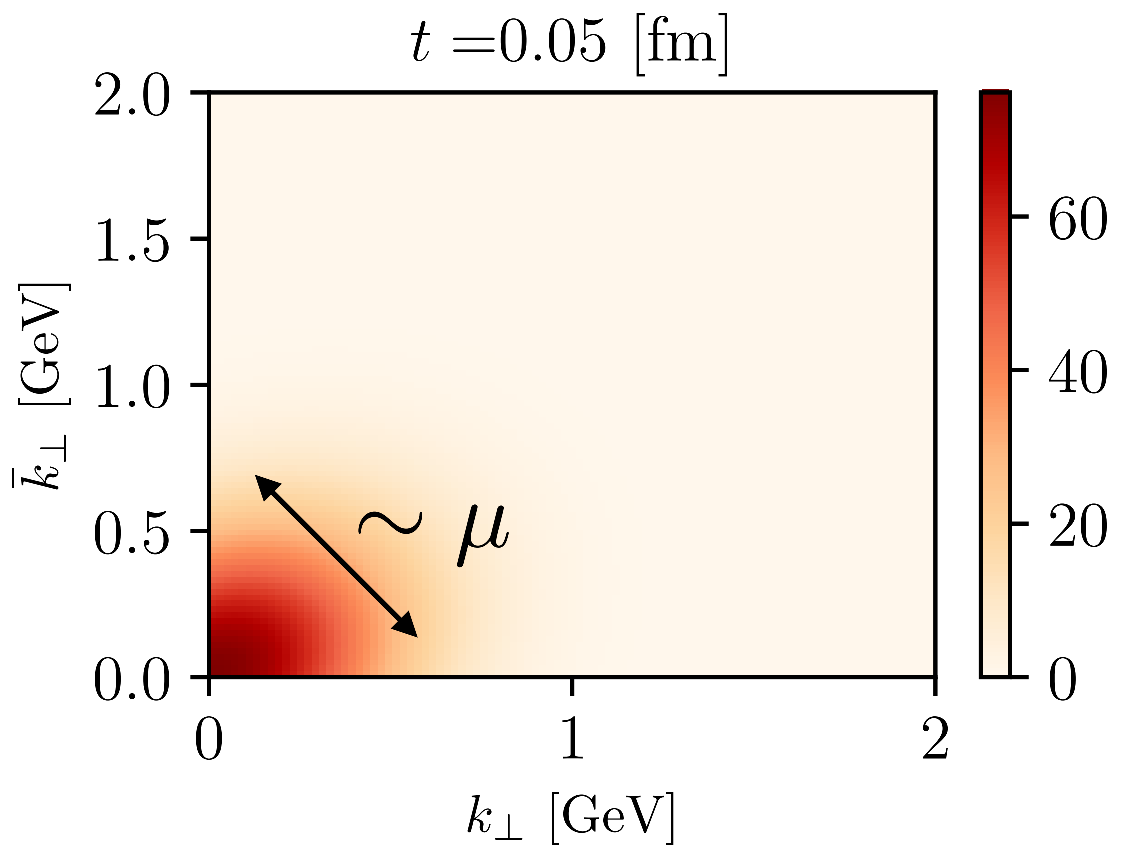

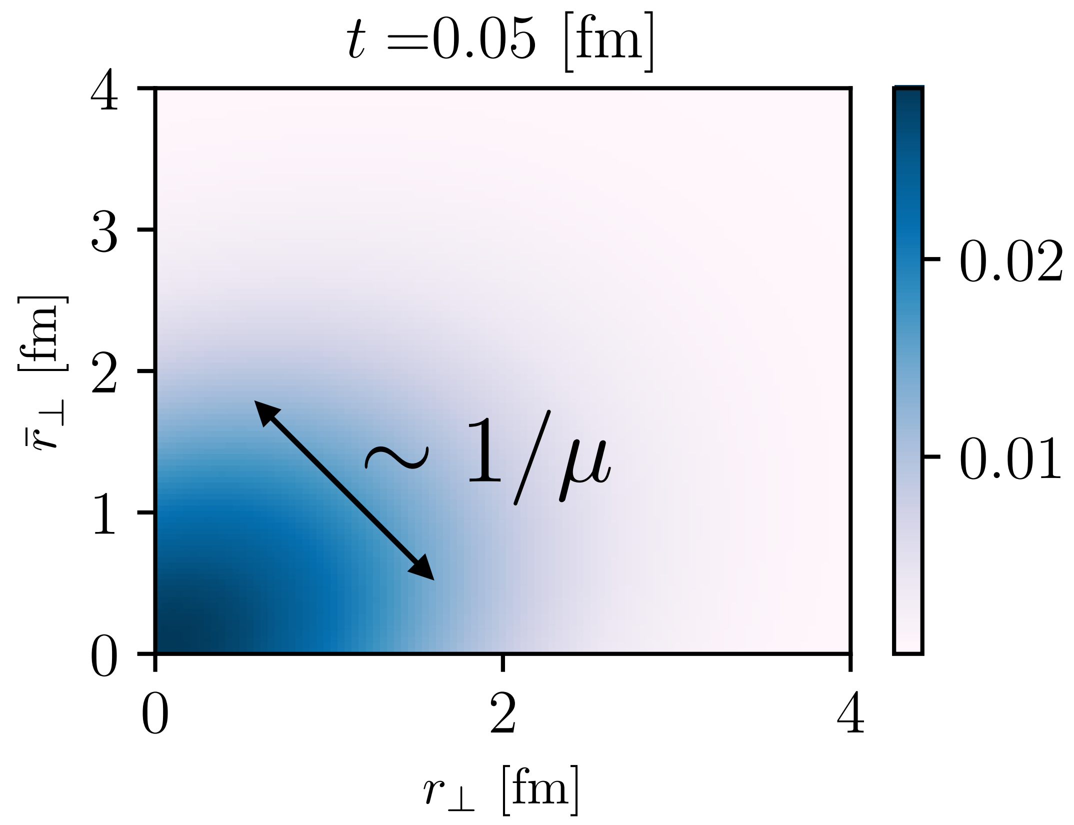

Single particle density matrix evolution in HICs

[JB, Blaizot, Mehtar-Tani, 2305.10476]

$t_1 \simeq 0.06$ fm $\quad t_2 \simeq 22.80$ fm $\quad t_0 \simeq 444.44$ fm

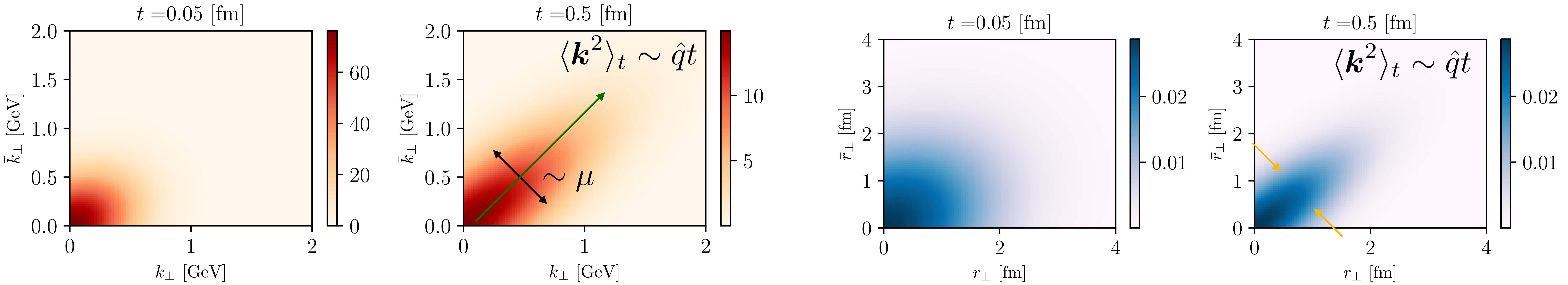

Single particle density matrix evolution in HICs

[JB, Blaizot, Mehtar-Tani, 2305.10476]

$t_1 \simeq 0.06$ fm $\quad t_2 \simeq 22.80$ fm $\quad t_0 \simeq 444.44$ fm

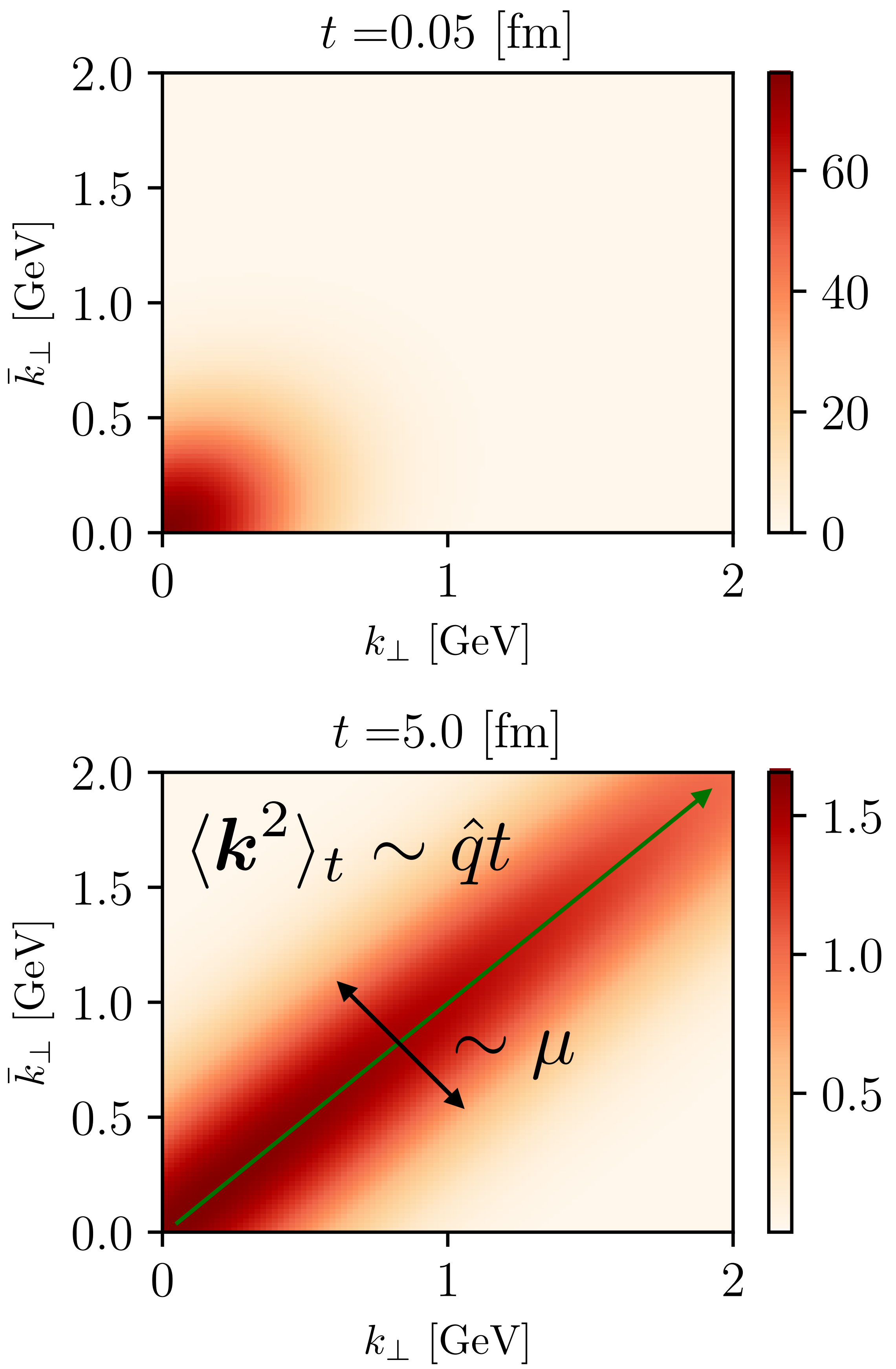

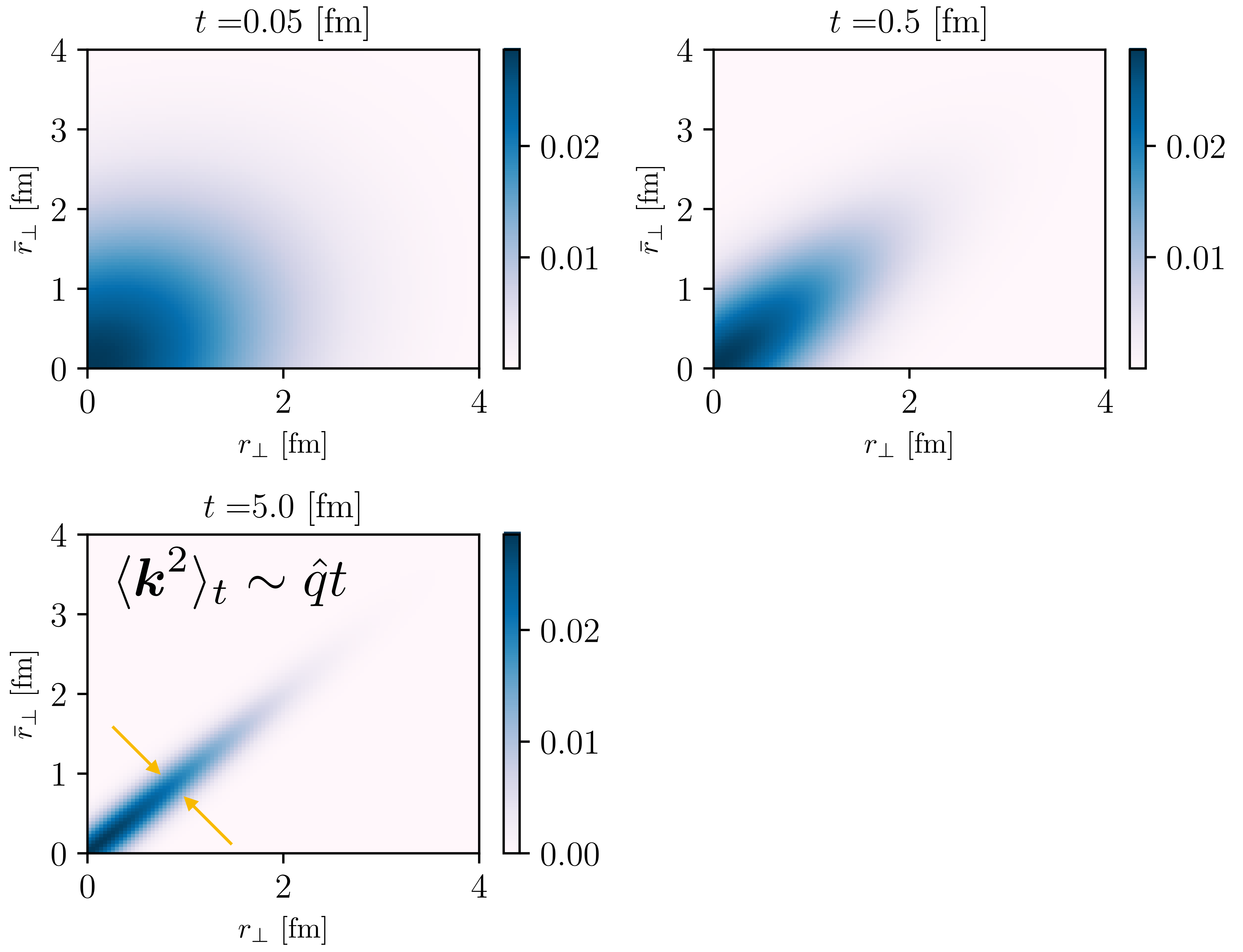

Single particle density matrix evolution in HICs

[JB, Blaizot, Mehtar-Tani, 2305.10476]

$t_1 \simeq 0.06$ fm $\quad t_2 \simeq 22.80$ fm $\quad t_0 \simeq 444.44$ fm

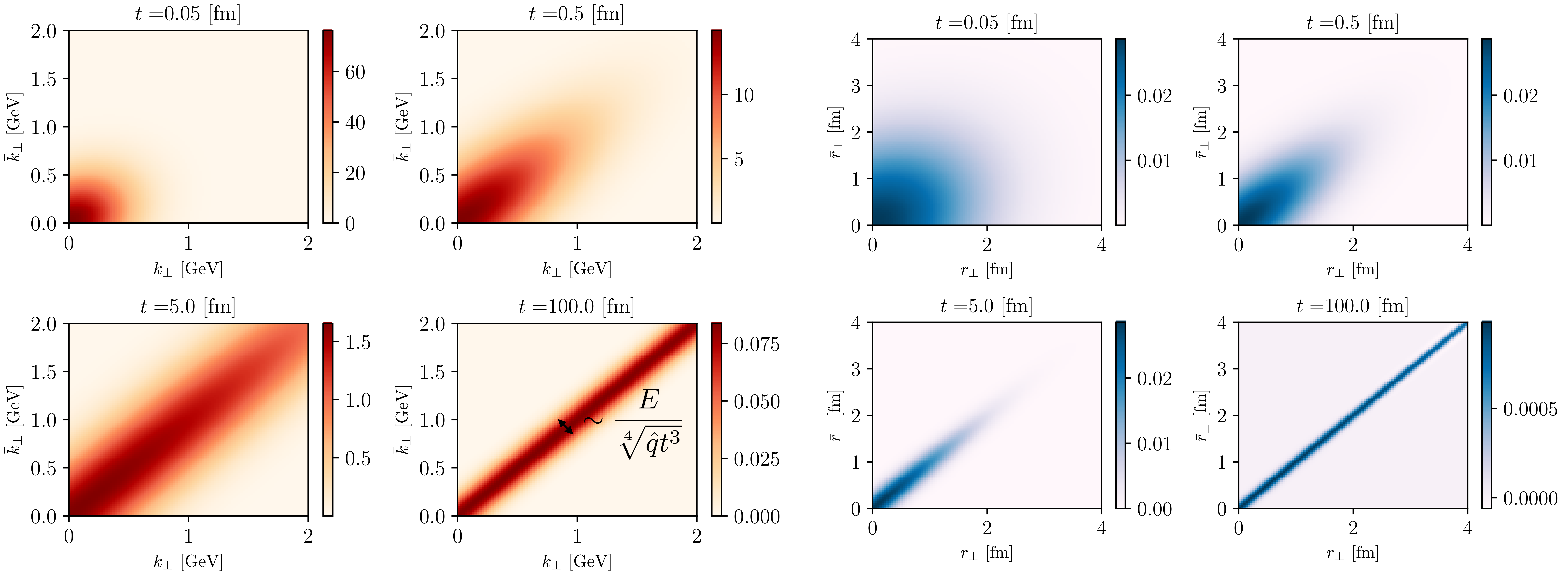

Single particle density matrix evolution in HICs

Similar evolution to that seen in quarkonia

$\mathcal{D}_s$ T = 300 MeV initial P-like octet

Delorme, Gousset, Katz, Gossiaux

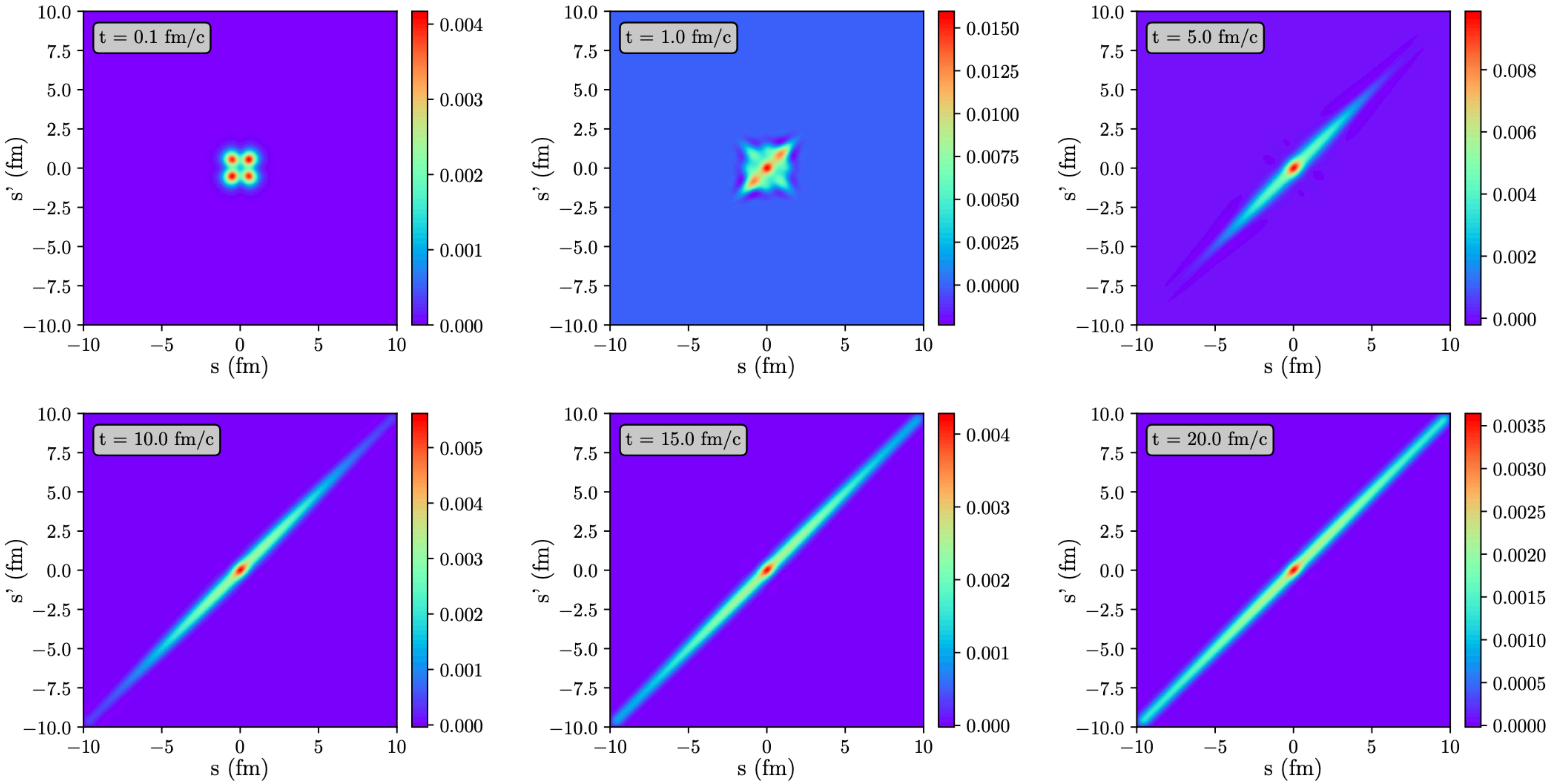

$$\frac{d}{dt}\begin{pmatrix}\mathcal{D}_s\\ \mathcal{D}_o\end{pmatrix} = \mathcal{L}\begin{pmatrix}\mathcal{D}_s(\mathbf{s},\mathbf{s}',t)\\ \mathcal{D}_o(\mathbf{s},\mathbf{s}',t)\end{pmatrix}$$

$$\mathcal{L} = \begin{pmatrix}\mathcal{L}_{ss} & \mathcal{L}_{so}\\ \mathcal{L}_{os} & \mathcal{L}_{oo}\end{pmatrix}$$

Single particle density matrix evolution in HICs

$t_1 \simeq 0.06$ fm $t_2 \simeq 22.80$ fm $t_0 \simeq 444.44$ fm $t_{\rm rel} \simeq 66.7$ fm

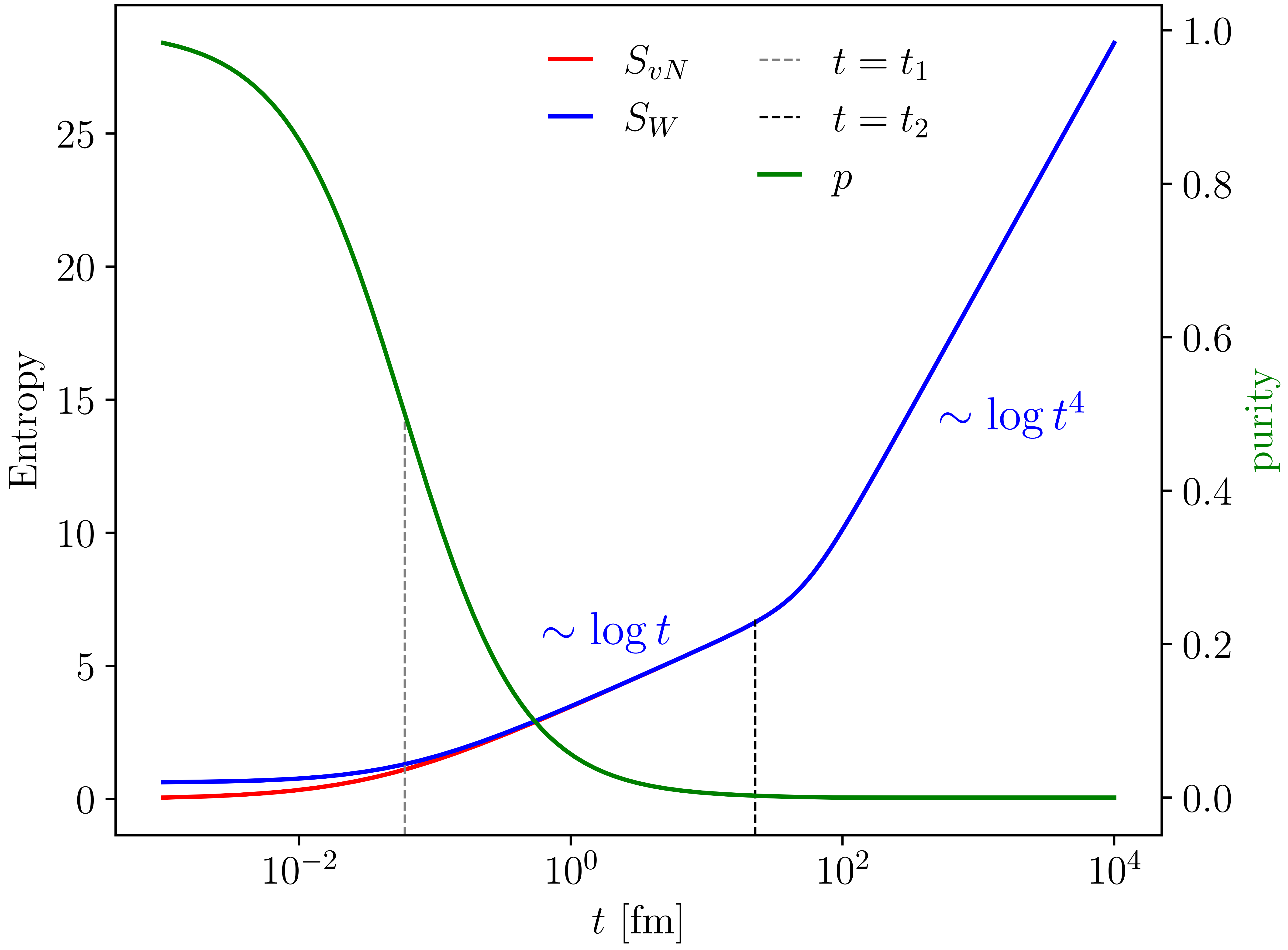

Asymptotically, one has that

$$\frac{S_{\rm w} - S_{\rm vN}}{S_{\rm w}} \approx \frac{\sqrt{p}}{\ln(1/p)}$$

thus, the **entropy content of the density matrix coincides with that of a classical distribution**

$$S_{\rm vN}[\rho] = -{\rm Tr}\rho \ln \rho$$

$$S_{\rm w} \equiv -\int_{\boldsymbol{K},\boldsymbol{b}} \rho_{\rm w}(\boldsymbol{b},\boldsymbol{K}) \log \rho_{\rm w}(\boldsymbol{b},\boldsymbol{K})$$

Single particle density matrix evolution in HICs

$$S_{\rm vN}[\rho] = -{\rm Tr}\rho \ln \rho \qquad S_{\rm w} \equiv -\int_{\boldsymbol{K},\boldsymbol{b}} \rho_{\rm w}(\boldsymbol{b},\boldsymbol{K}) \log \rho_{\rm w}(\boldsymbol{b},\boldsymbol{K})$$

$t_1 \simeq 0.06$ fm $\quad t_2 \simeq 22.80$ fm $\quad t_0 \simeq 444.44$ fm $\quad t_{\rm rel} \simeq 66.7$ fm

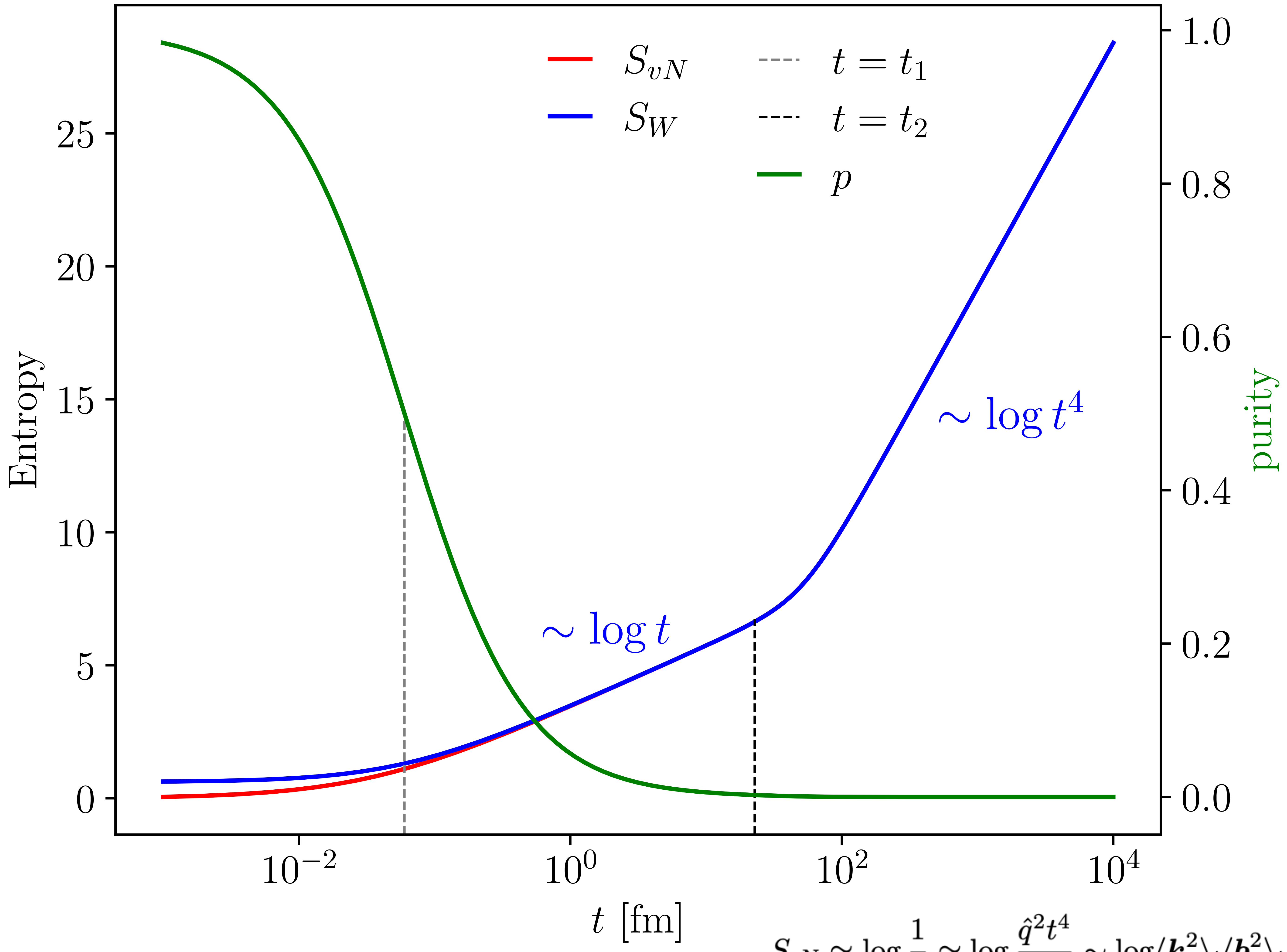

$$S_{\rm vN} \simeq \log \frac{1}{p} \simeq \log \frac{\hat{q}^2 t^4}{E^2} \sim \log \langle \boldsymbol{k}^2 \rangle_t \langle \boldsymbol{b}^2 \rangle_t$$

Asymptotically, one has that

$$\frac{S_{\rm w} - S_{\rm vN}}{S_{\rm w}} \approx \frac{\sqrt{p}}{\ln(1/p)}$$

thus, the **entropy content of the density matrix coincides with that of a classical distribution**

In reality, the entropy growth is bounded

$$\left[\frac{\partial}{\partial t} - \frac{\partial}{\partial \boldsymbol{K}}\left(\frac{\hat{q}}{4}\frac{\partial}{\partial \boldsymbol{K}} + \gamma_f \frac{\boldsymbol{K}}{E}\right)\right] \mathcal{P}(\boldsymbol{K}, t) = 0$$

This occurs roughly after a time $\gamma_f = \hat{q}/4T \sim T^2$

$$t_{\rm rel} \equiv ET/\hat{q}$$

Real-time evolution for hard probes

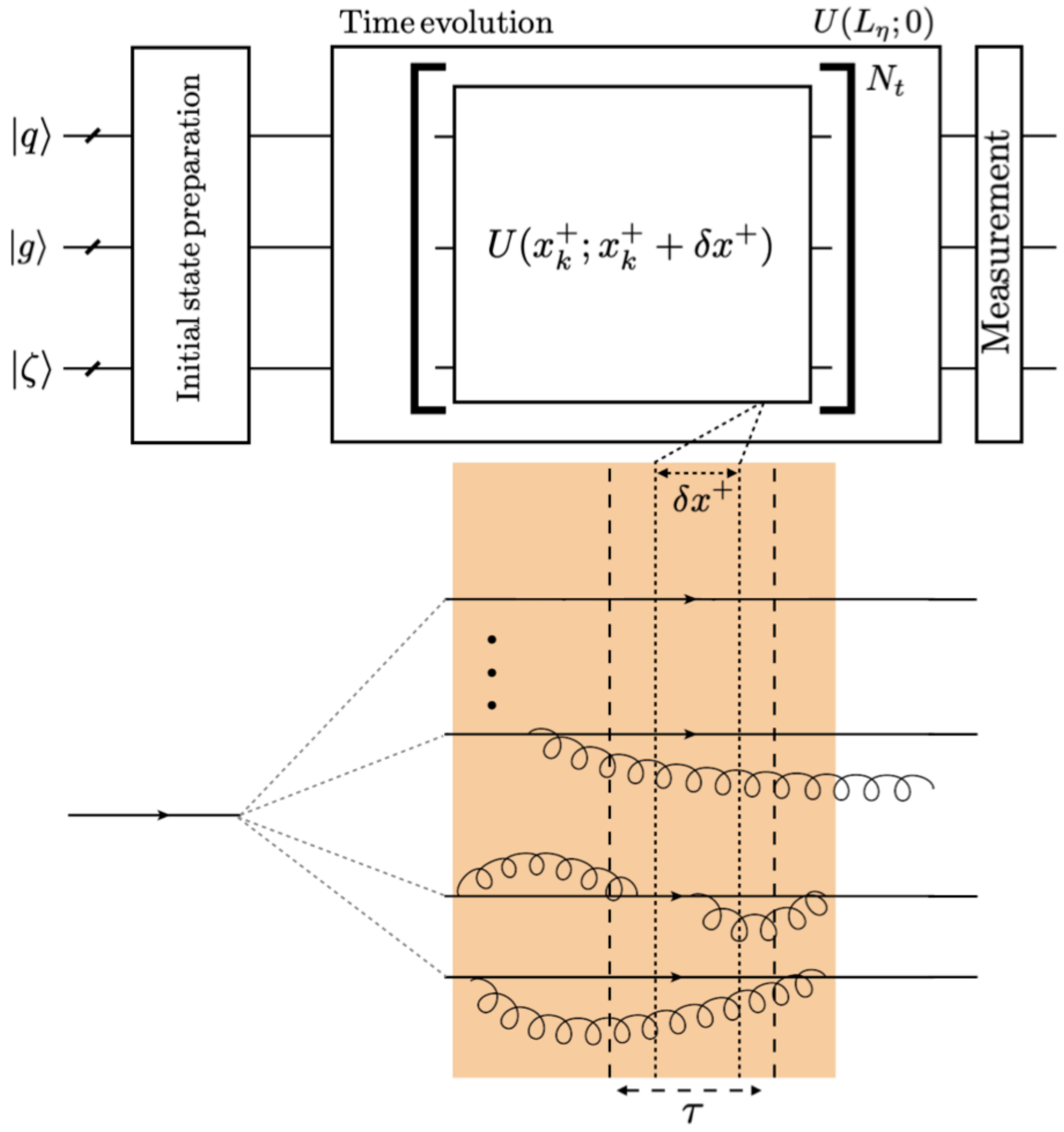

Real-time simulation of hard probes

[JB et al, 2104.04661, 2208.06750, 2307.01792]
[Qian, Li, Salgado, Kreshchuk, 2411.09762]

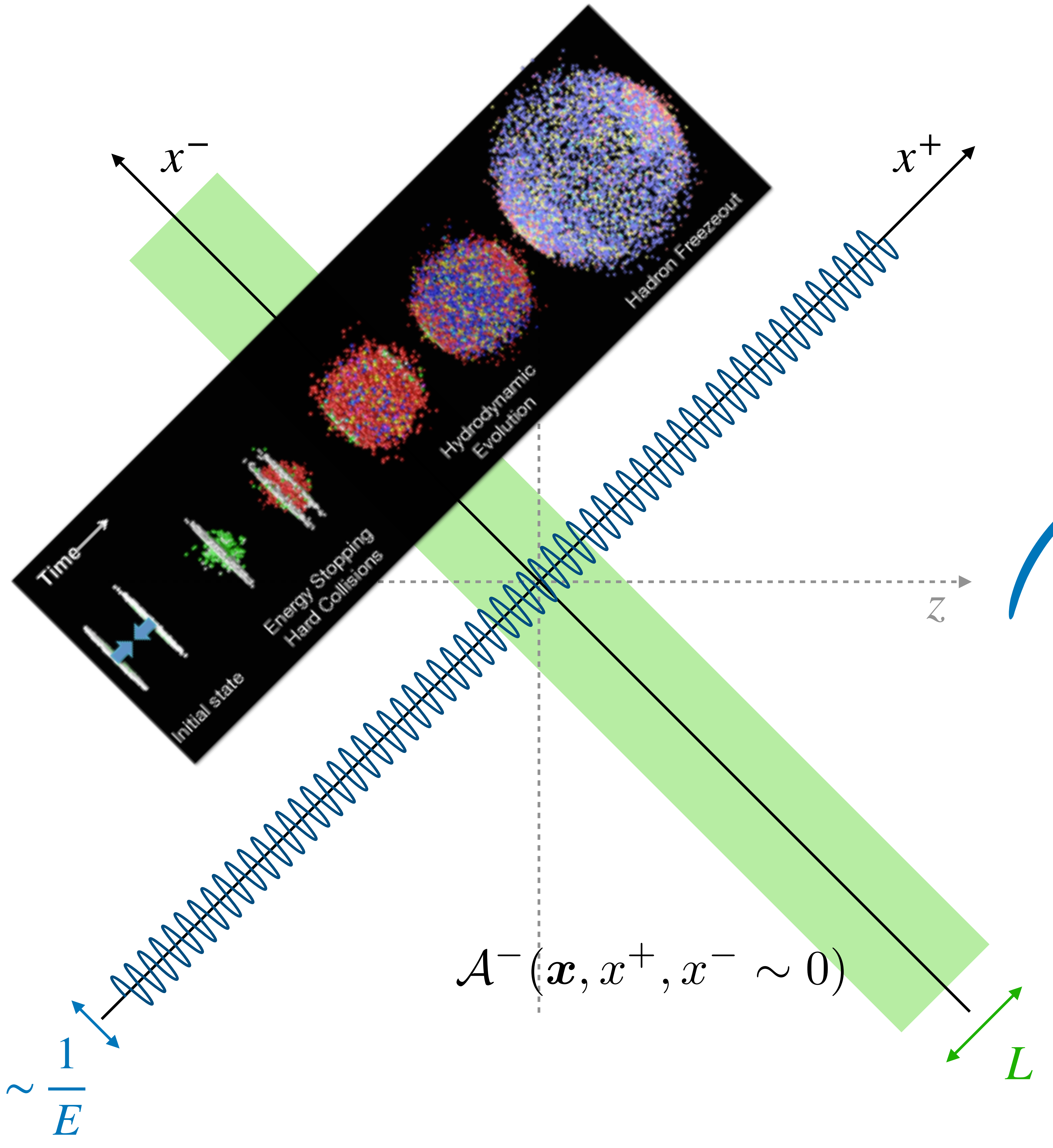

[Susskind, 1960s]

Dynamics of high energy particles map to non-rel. 2d QM problem

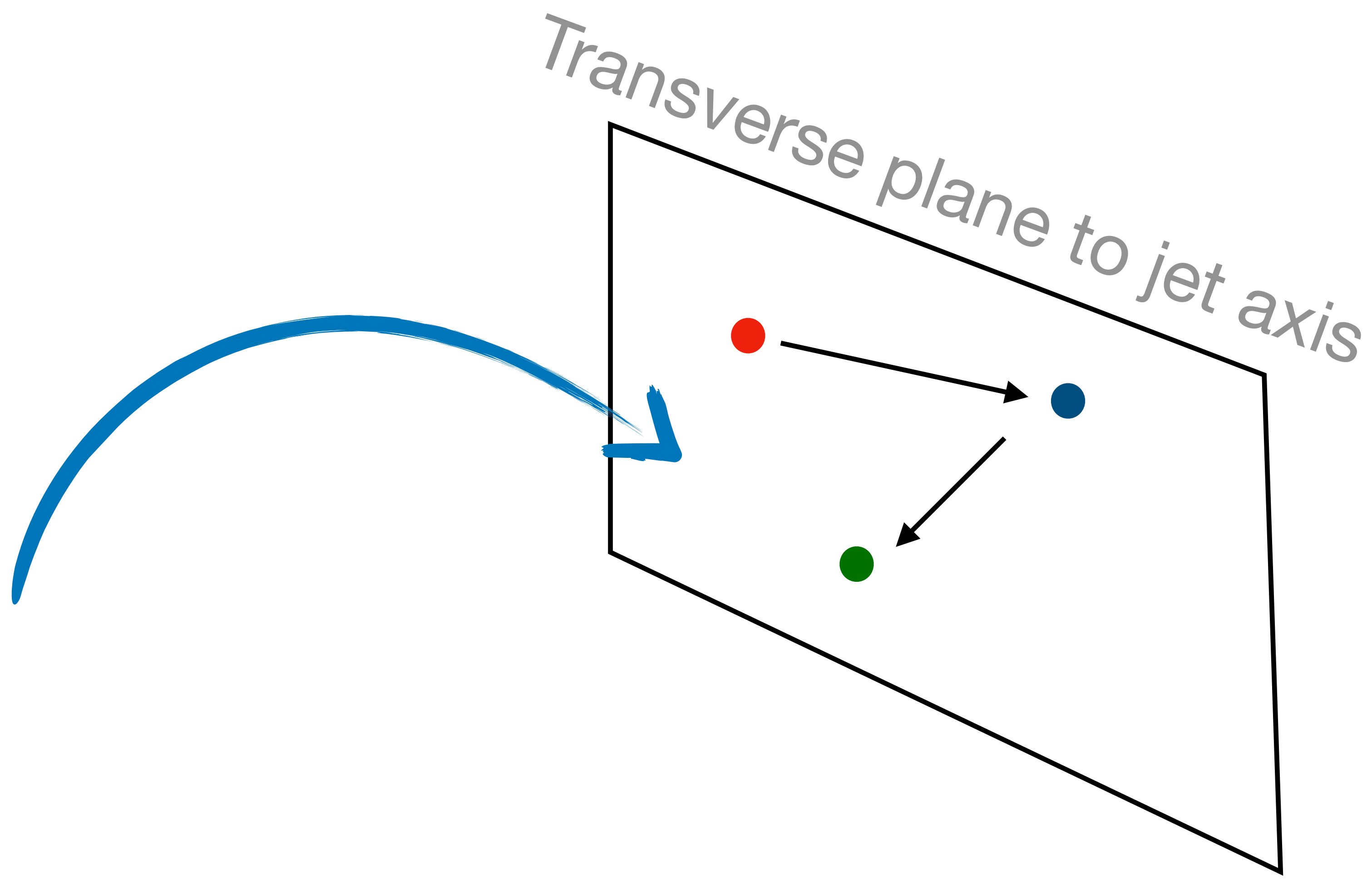

Real-time simulation of hard probes

[JB et al, 2104.04661, 2208.06750, 2307.01792]
[Qian, Li, Salgado, Kreshchuk, 2411.09762]

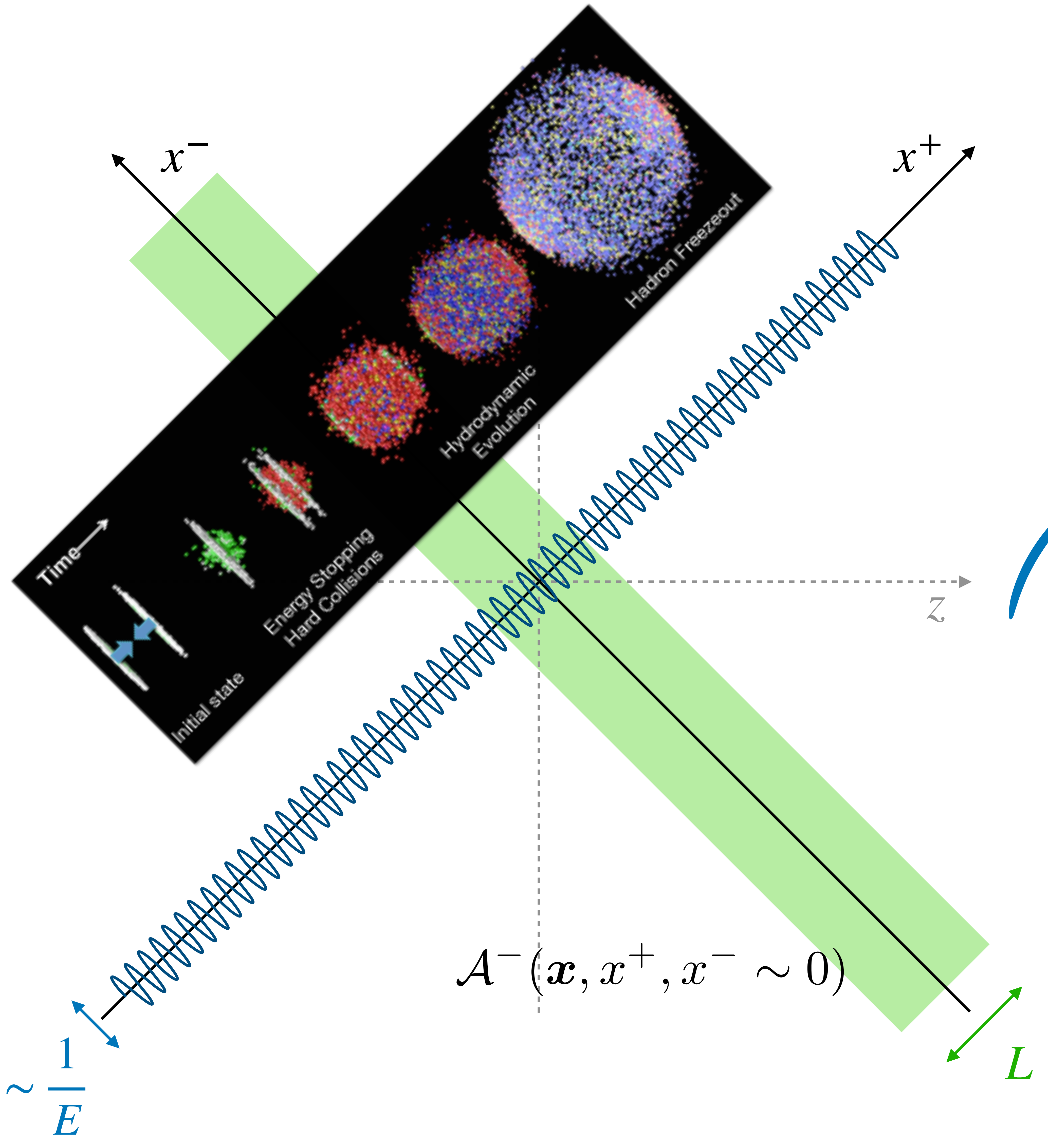

[Susskind, 1960s]

Dynamics of high energy particles map to non-rel. 2d QM problem

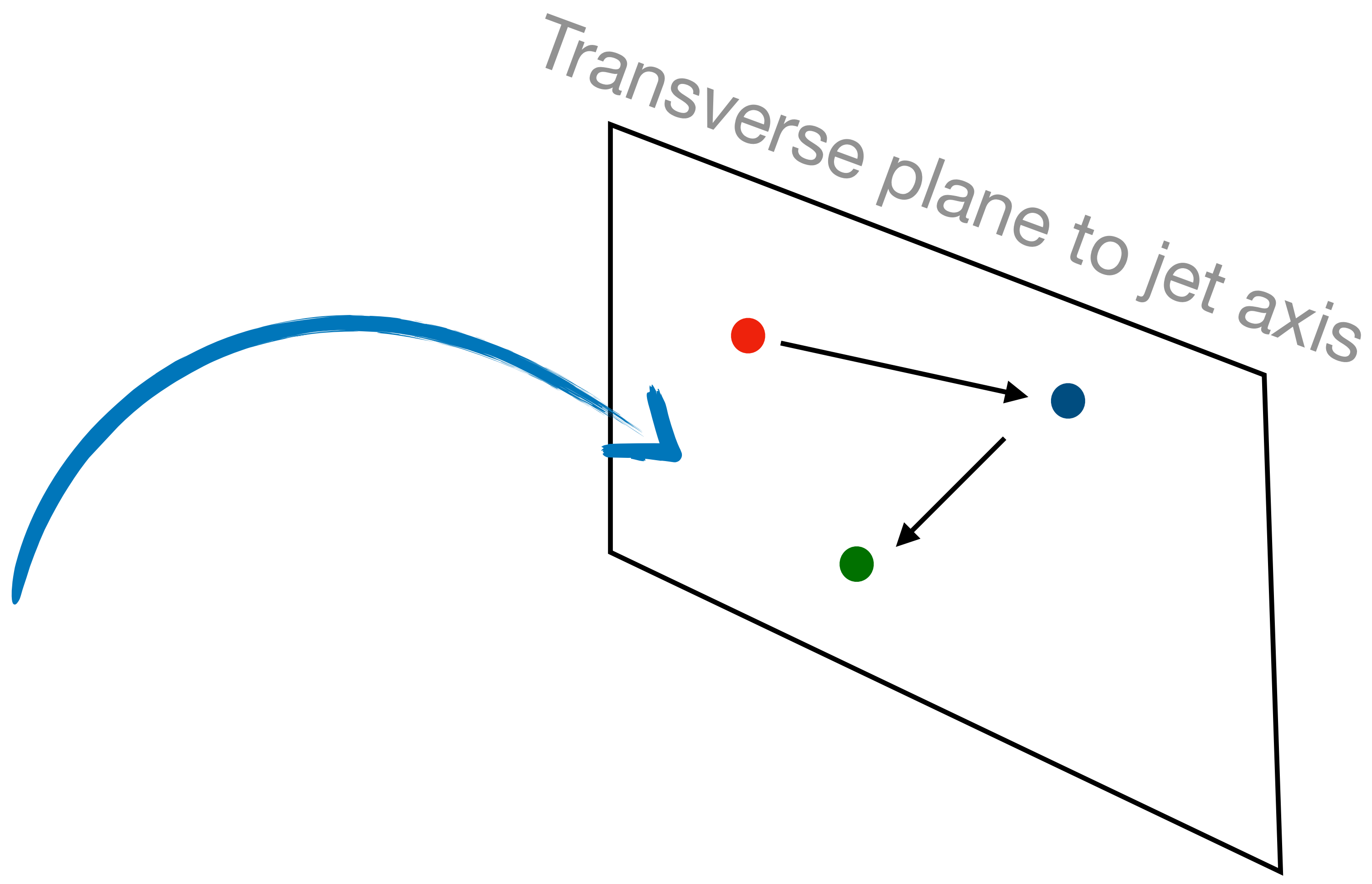

+ **Classical and non-dynamical approximation for background matter**

$$|\psi_{\text{jet}}\rangle = e^{-iH(\text{QGP})t}|\psi_{\text{jet}}(t=0)\rangle$$

$$\text{Observable} = \Big\langle \langle\psi_{\text{jet}}|\hat{O}|\psi_{\text{jet}}\rangle \Big\rangle_{\text{QGP}}$$

Real-time simulation of hard probes

[JB et al, 2104.04661, 2208.06750, 2307.01792]
[Qian, Li, Salgado, Kreshchuk, 2411.09762]

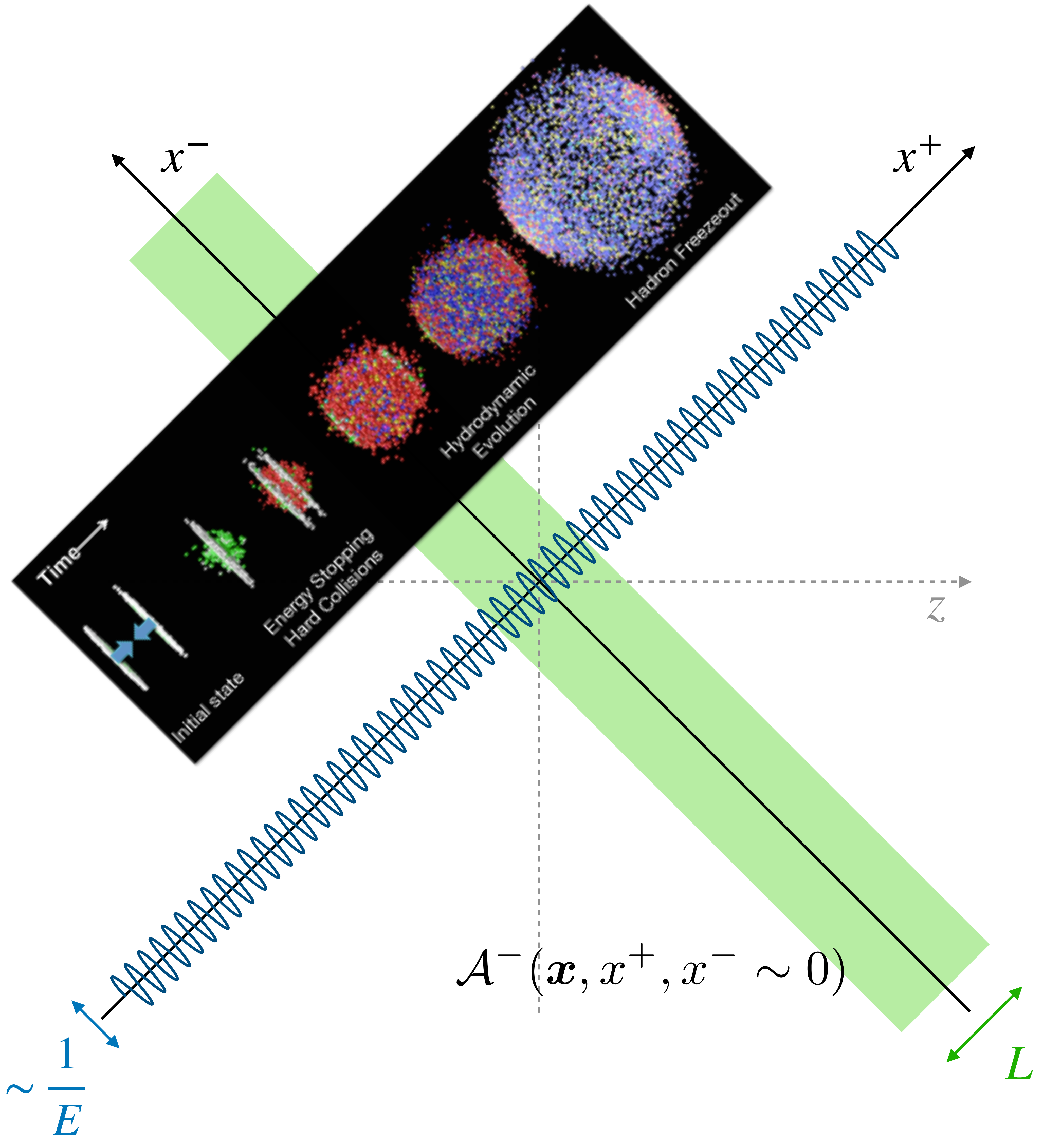

Integrating out x^- the quark propagator satisfies

$$\left(i\partial_t + \frac{\partial_{\boldsymbol{x}}^2}{2\omega} + g\mathcal{A}^-(t,\boldsymbol{x})\cdot T\right) G(t,\boldsymbol{x};0,\boldsymbol{y}) = i\delta(t)\delta(\boldsymbol{x}-\boldsymbol{y})$$

or

$$\mathcal{H}(t) = \underbrace{\frac{\boldsymbol{p}^2}{2\omega}}_{\text{p-space}} + \underbrace{g\mathcal{A}^-(t,\boldsymbol{x})\cdot T}_{\text{x-space}} = \mathcal{H}_K + \mathcal{H}_\mathcal{A}(t)$$

+vertices

Real-time simulation of hard probes

[JB et al, 2104.04661, 2208.06750, 2307.01792]
[Qian, Li, Salgado, Kreshchuk, 2411.09762]

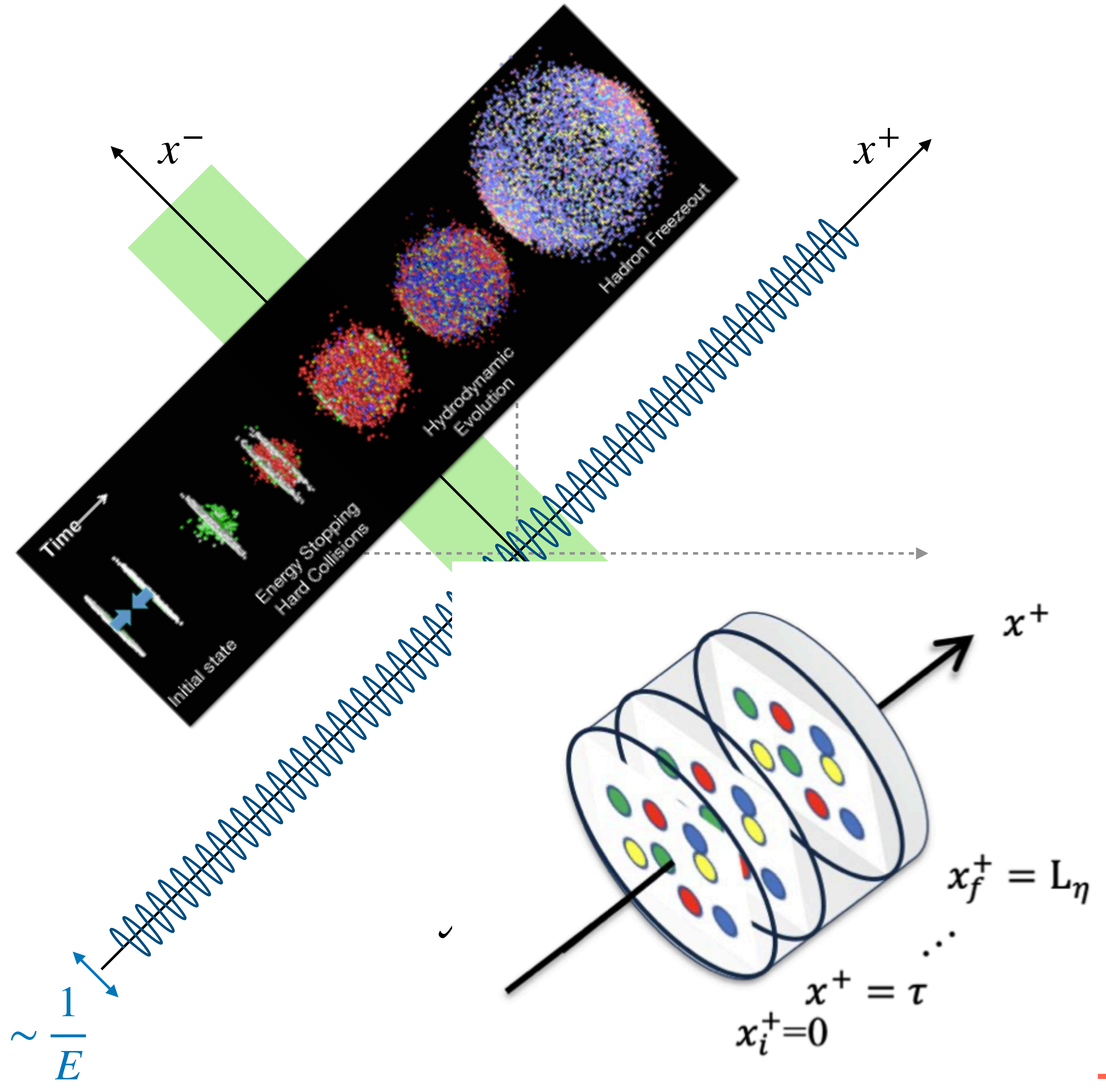

The background field satisfies reduced CYM eoms

$$(m_g^2 - \nabla_\perp^2)\mathcal{A}_a^-(x^+, \boldsymbol{x}) = \rho_a(x^+, \boldsymbol{x})$$

Source describes "hard" partons that generate classical field

We use Gaussian model to describe source statistics

$$\langle\langle \rho_a(x^+, \boldsymbol{x})\rho_b(y^+, \boldsymbol{y})\rangle\rangle = g^2\mu^2\delta_{ab}\,\delta^{(2)}(\boldsymbol{x}-\boldsymbol{y})\,\delta(x^+ - y^+)$$

Then, the time evolved state is given by

$$\begin{aligned}|\psi_{L_\eta}\rangle =& U(L_\eta;0)\,|\psi_0\rangle \\ \equiv& \mathcal{T}_+ e^{-i\int_0^{L_\eta} \mathrm{d}x^+\, P^-(x^+)}\,|\psi_0\rangle\end{aligned}$$

for each background field

→ Requires generating several matter layers + Trotter decomposition

Real-time simulation of hard probes

[JB et al, 2104.04661, 2208.06750, 2307.01792]
[Qian, Li, Salgado, Kreshchuk, 2411.09762]

Physical space   Computational space

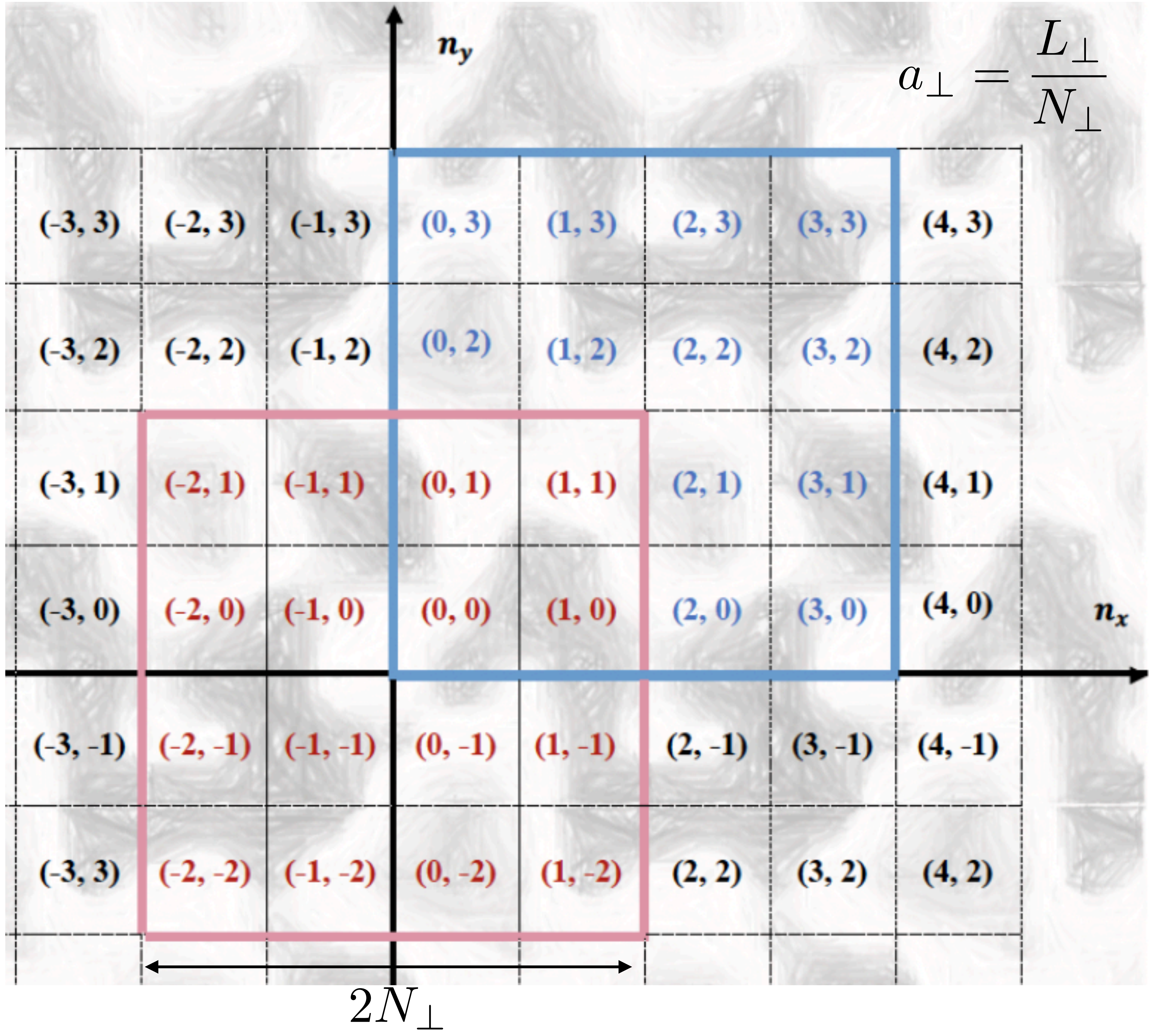

Number of qbits: $n_{\text{partons}} \log N_\perp$

In general, a quark or gluon state requires encoding

$$|\psi_{x^+}\rangle = \sum_\beta c_\beta(x^+)\,|\beta\rangle \qquad \beta_l = \{p_l^+, p_l^x, p_l^y, c_l, \not{\chi_l}\}$$

Since total energy is conserved, we can use

$$z = \{1, 2, \cdots K - 1/2\}$$

$$|\psi\rangle = |z\rangle \otimes \underbrace{\Big(|g_x\rangle\,|g_y\rangle\,|c_g\rangle\Big)}_{|g\rangle} \otimes \underbrace{\Big(|q_x\rangle\,|q_y\rangle\,|c_q\rangle\Big)}_{|q\rangle}$$

In transverse space we use periodic lattice

$$\vec{n} = (n_x, n_y) = (n_x + i2N_\perp, n_y + ji2N_\perp)$$

We discretize longitudinal momentum such that

$$p^+ = \frac{2\pi}{L_\eta} k_i^+ \qquad k_q^+ = \frac{1}{2}, \frac{3}{2}, \cdots \qquad k_g^+ = 1, 2, \cdots$$

$$K \equiv \sum_i k_i^+ = k_q^+ + k_g^+, \quad P^+ = \frac{2\pi}{L} K,$$

Real-time simulation of hard probes

[JB et al, 2104.04661, 2208.06750, 2307.01792]
[Qian, Li, Salgado, Kreshchuk, 2411.09762]

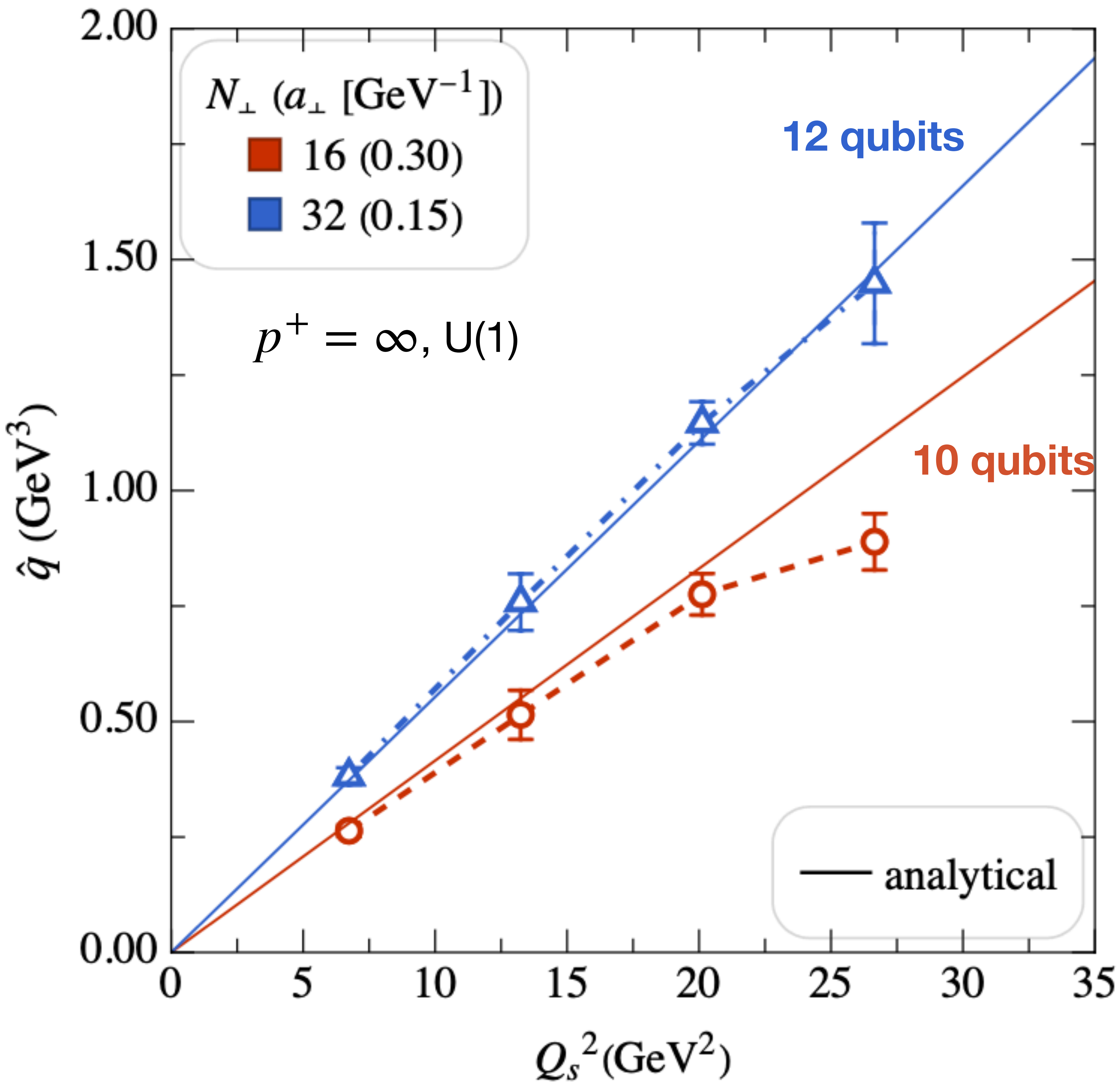

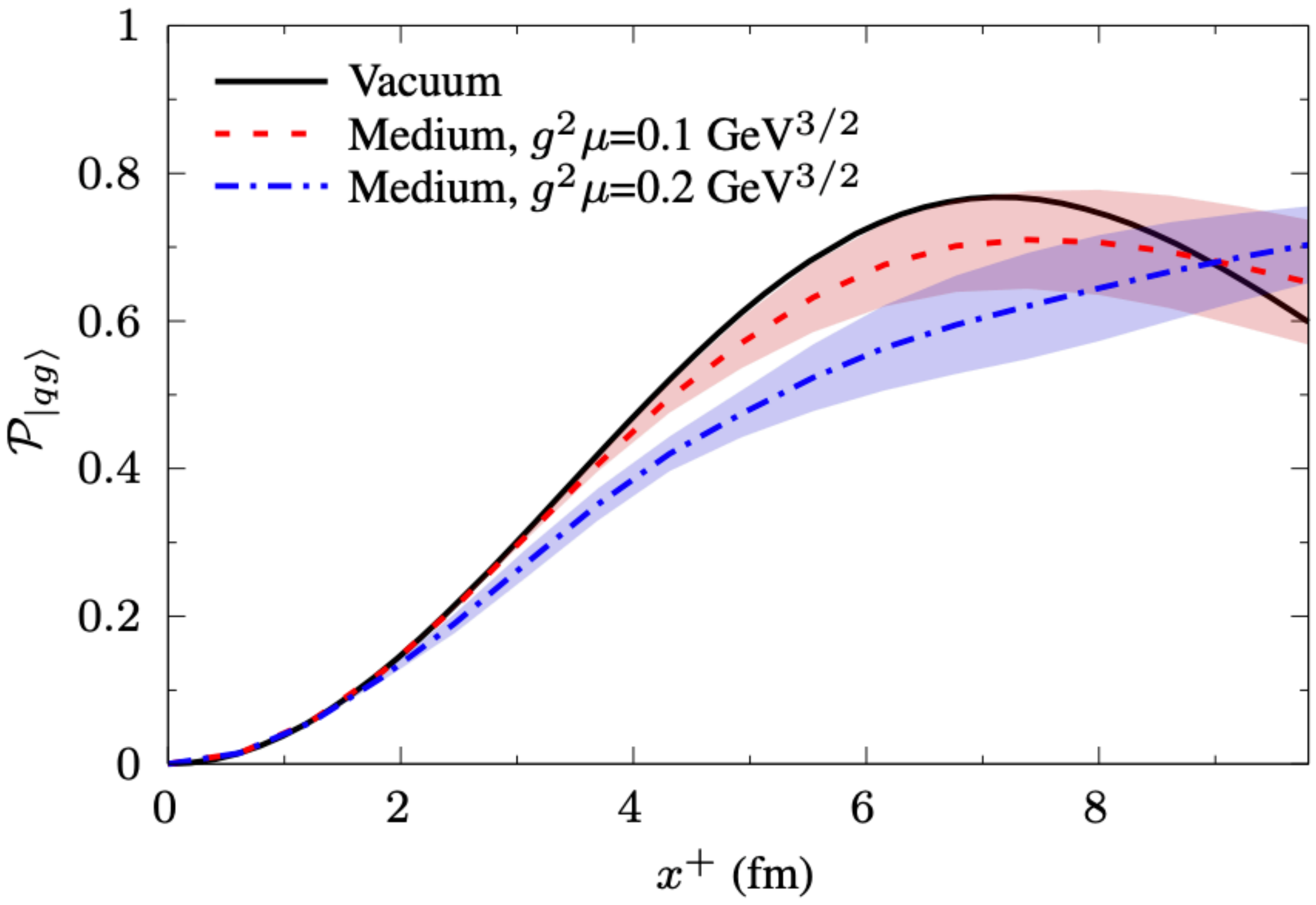

Real-time simulation of hard probes

[JB, Rico, 2502.17558]

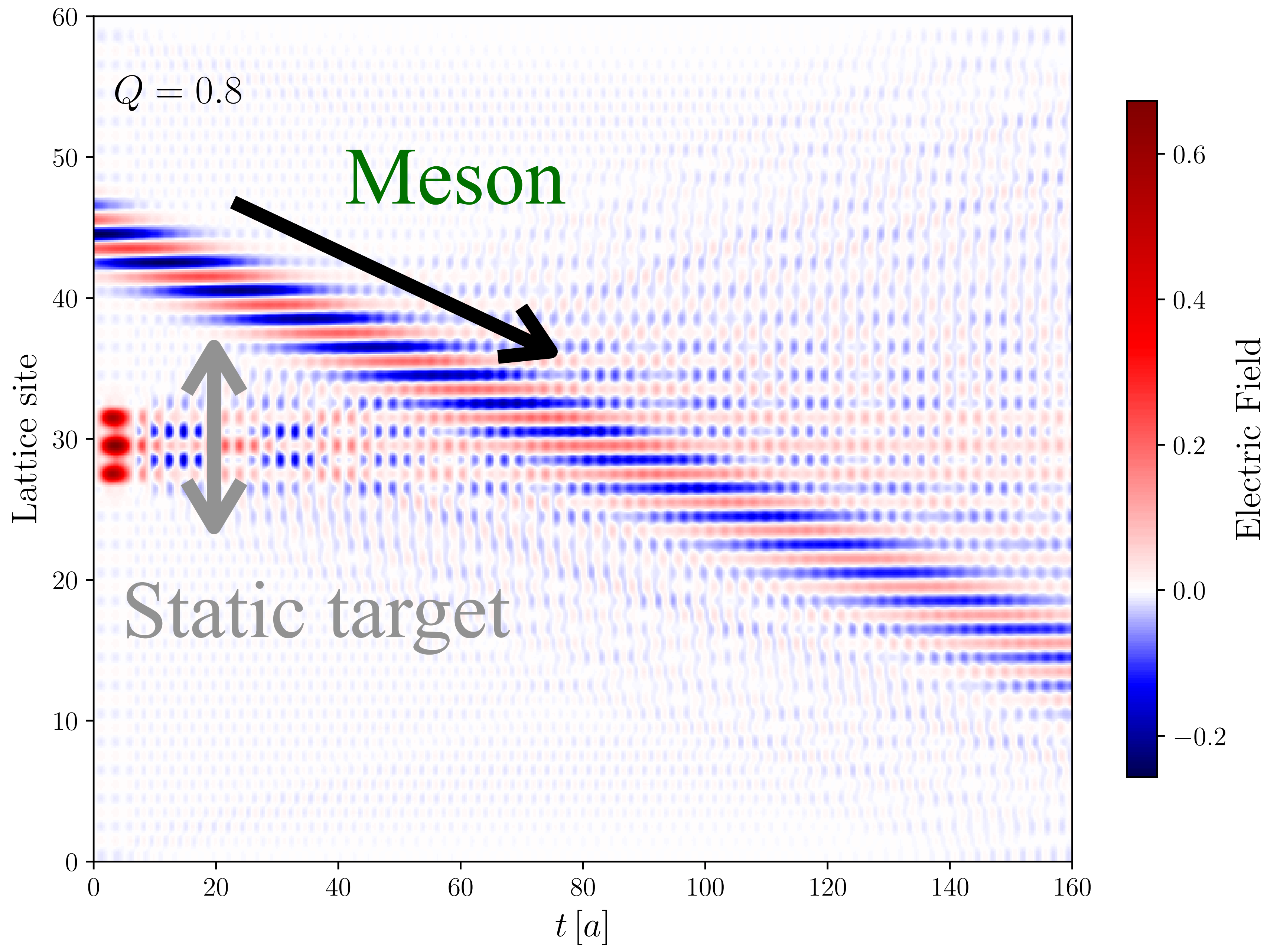

[Farrell, Illa, Savage, 2405.06620]

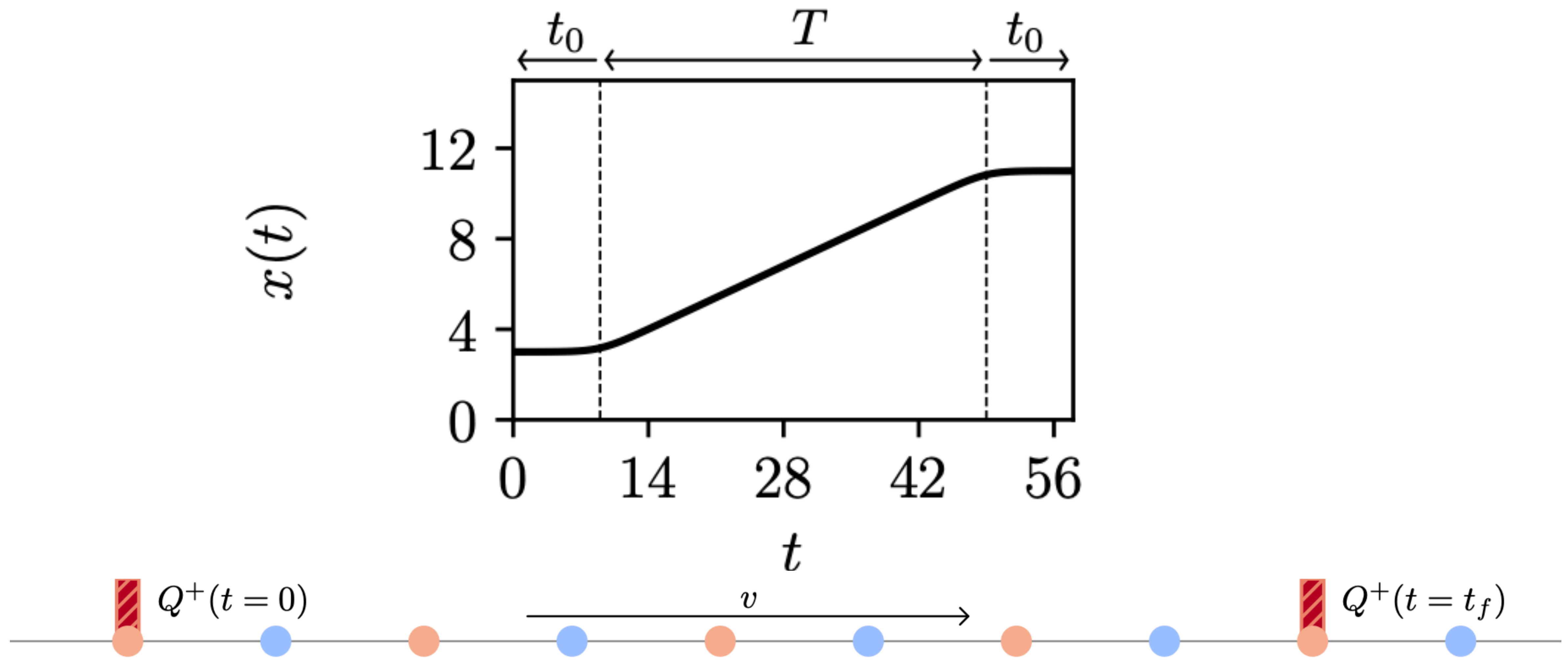

Real-time simulation of hard probes

[JB, Rico, 2502.17558]

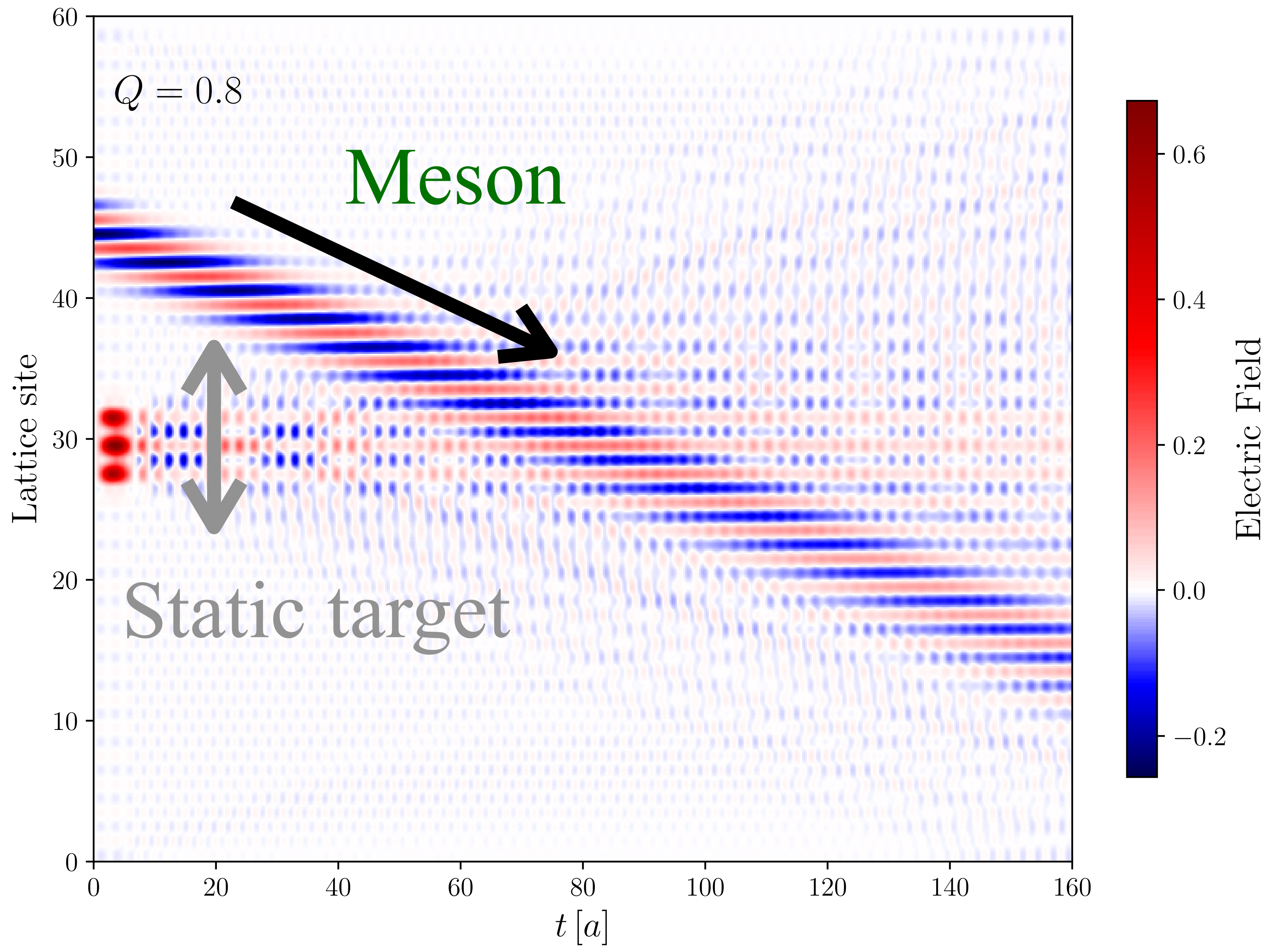

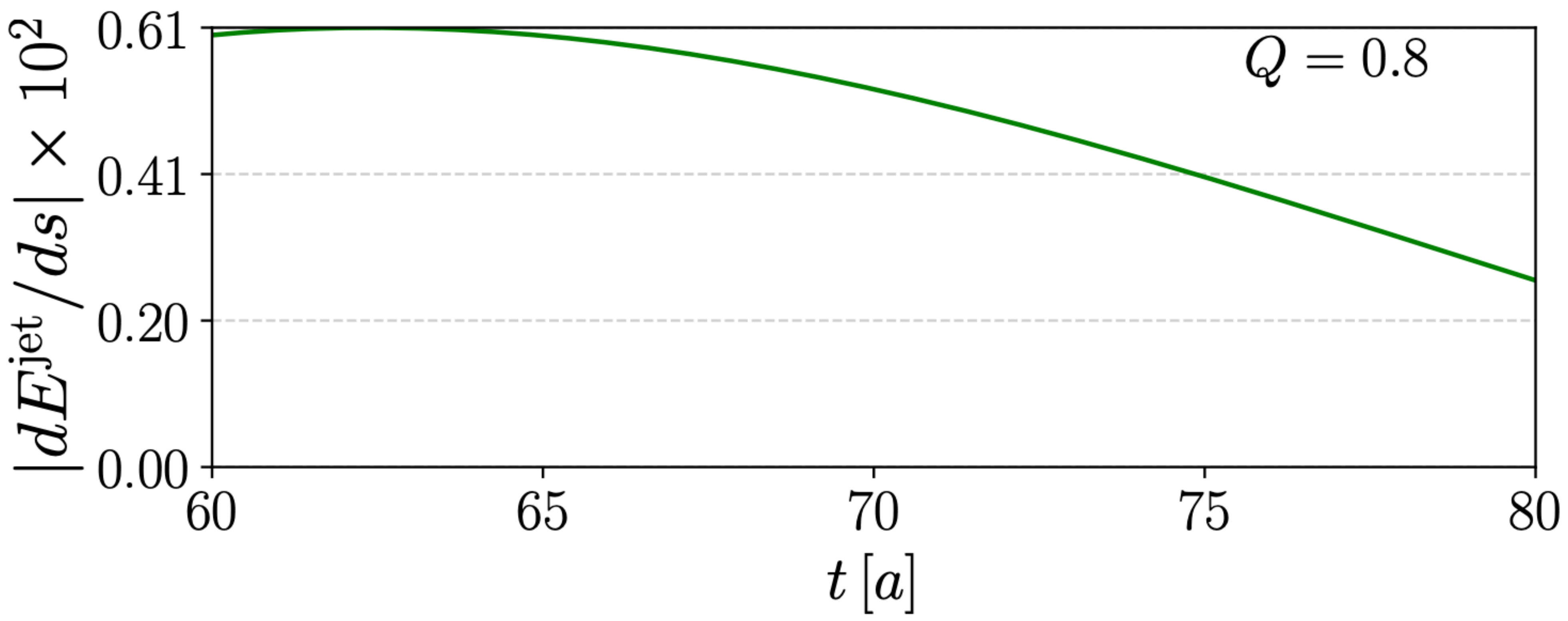

[Farrell, Illa, Savage, 2405.06620]

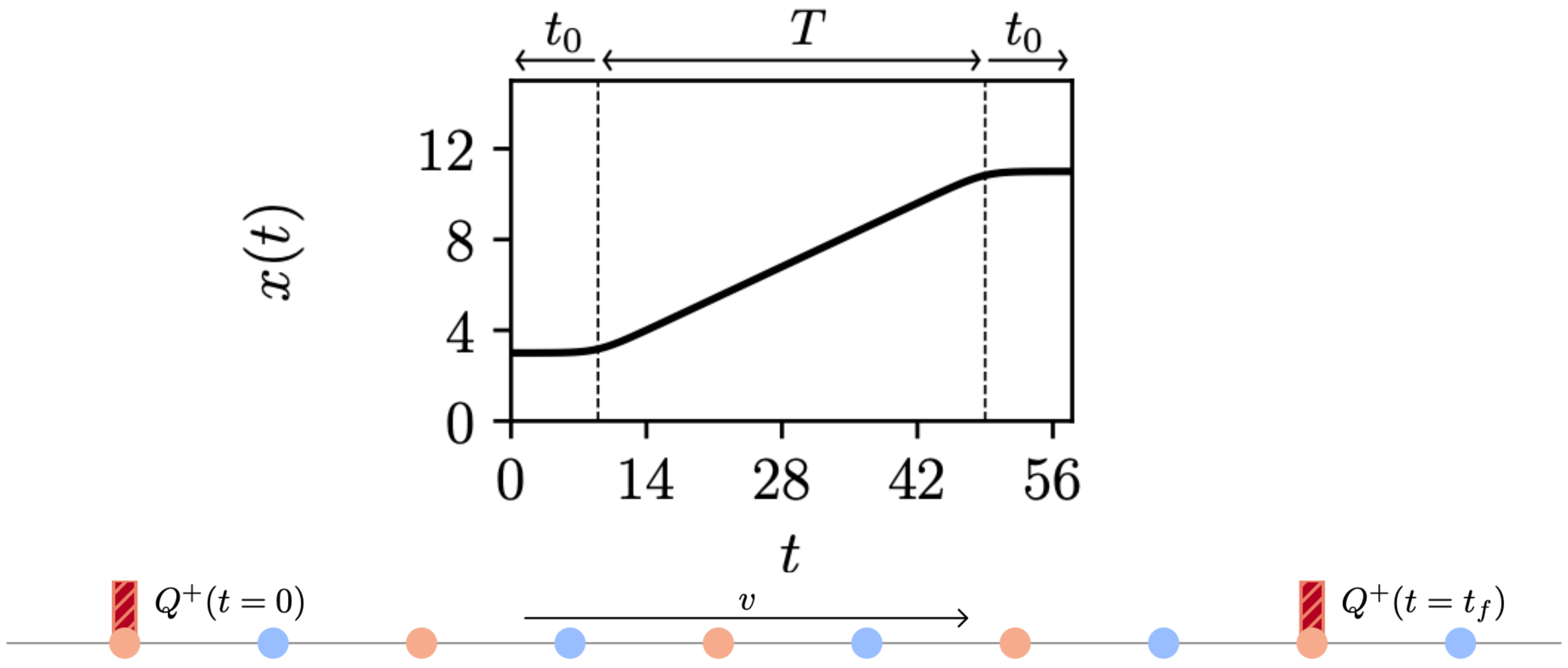

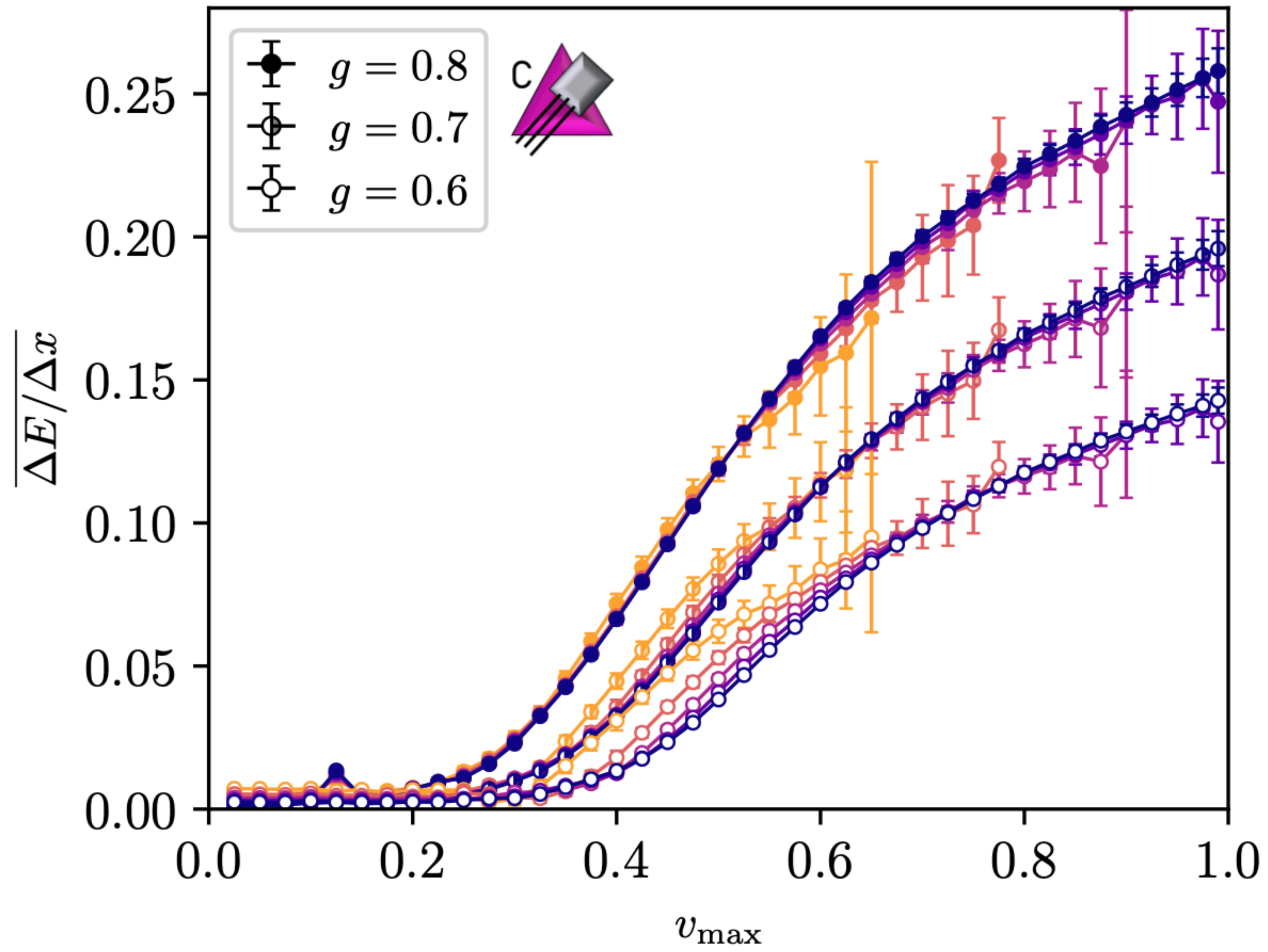

Real-time simulation of hard probes

[JB, Qian, Li, Salgado, Silva, 2604.11616]

The leading order cross-section can be written as

$$(2\pi)\frac{\mathrm{d}\sigma}{\mathrm{d}z\ \mathrm{d}^2\boldsymbol{p}} = (2\pi)\frac{\mathrm{d}\sigma^{\rm vac}}{\mathrm{d}z\ \mathrm{d}^2\boldsymbol{p}}(1+F_{\rm med}(\boldsymbol{p}^2,z))$$

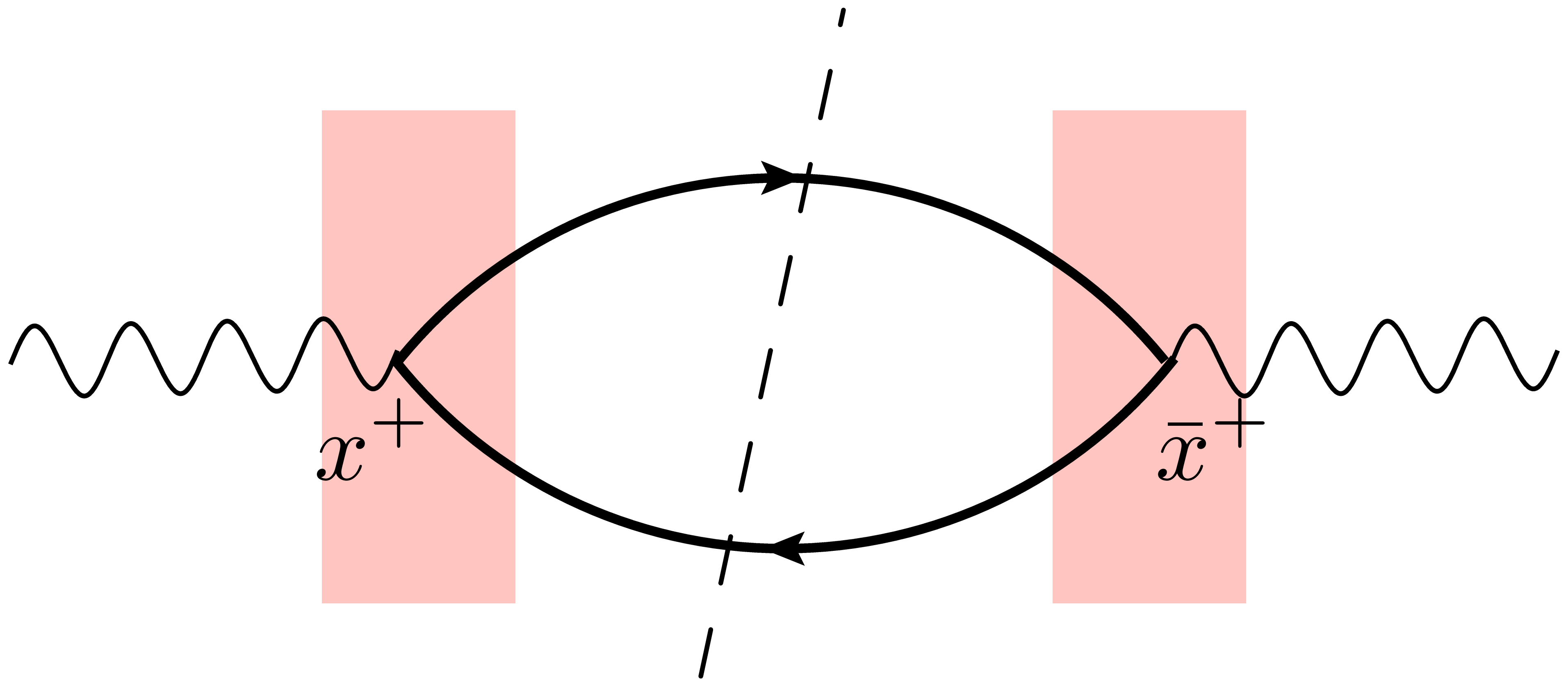

$$F_{\rm med}(\boldsymbol{p}^2,z) = \frac{\boldsymbol{p}^2}{2\omega^2}\mathrm{Re}\int_0^L \mathrm{d}x^+\int_{x^+}^L \mathrm{d}\bar{x}^+\int_{\boldsymbol{k}_1,\boldsymbol{k}_2,\bar{\boldsymbol{k}}_1,\bar{\boldsymbol{k}}_2}(\boldsymbol{\kappa}\cdot\bar{\boldsymbol{\kappa}})e^{i\boldsymbol{K}^2/2p_0^+(\bar{x}^+-x^+)}\ \mathcal{C}_4|_{\boldsymbol{P}=0} \ - \frac{1}{\omega}\mathrm{Re}\,i\int_0^L \mathrm{d}x^+\int_{\boldsymbol{k}_1,\boldsymbol{k}_2}(\boldsymbol{\kappa}\cdot\boldsymbol{p})\ \mathcal{C}_2|_{\boldsymbol{P}=0}$$

The non-trivial terms relate to the in-medium correlation functions

$$\int_{\boldsymbol{K},\bar{\boldsymbol{K}}} e^{i\boldsymbol{K}^2/2p_0^+(\bar{x}^+-x^+)}\ \mathcal{C}_4|_{\boldsymbol{P}=0} = \int_{\boldsymbol{q}} \mathcal{Q}(\boldsymbol{p},\boldsymbol{q},\bar{\boldsymbol{\kappa}};L,\bar{x}^+)\mathcal{K}(\boldsymbol{q},\boldsymbol{\kappa};\bar{x}^+,x^+)$$

$$\mathcal{Q}(\boldsymbol{p},\boldsymbol{q},\bar{\boldsymbol{\kappa}};L,\bar{x}^+) = \int_{\boldsymbol{u}_1,\boldsymbol{u}_2,\bar{\boldsymbol{u}}_1,\bar{\boldsymbol{u}}_2} e^{i\boldsymbol{u}_1\cdot\boldsymbol{q}}e^{-i\bar{\boldsymbol{u}}_1\cdot\bar{\boldsymbol{\kappa}}}e^{-i(\boldsymbol{u}_2-\bar{\boldsymbol{u}}_2)\cdot\boldsymbol{p}} \int_{\boldsymbol{u}_1}^{\boldsymbol{u}_2}\mathcal{D}\boldsymbol{u}\int_{\bar{\boldsymbol{u}}_1}^{\bar{\boldsymbol{u}}_2}\mathcal{D}\bar{\boldsymbol{u}}\, e^{\frac{i\omega}{2}\int_{\bar{x}^+}^L ds^+\,(\dot{\boldsymbol{u}}^2-\dot{\bar{\boldsymbol{u}}}^2)}\frac{1}{N_c}\left\langle \mathrm{Tr}\left(U_1U_2^\dagger U_{\bar{2}}U_{\bar{1}}^\dagger\right)\right\rangle$$

Real-time simulation of hard probes

[JB, Qian, Li, Salgado, Silva, 2604.11616]

There is a direct way to evaluate these correlators by evolving partonic systems in real-time

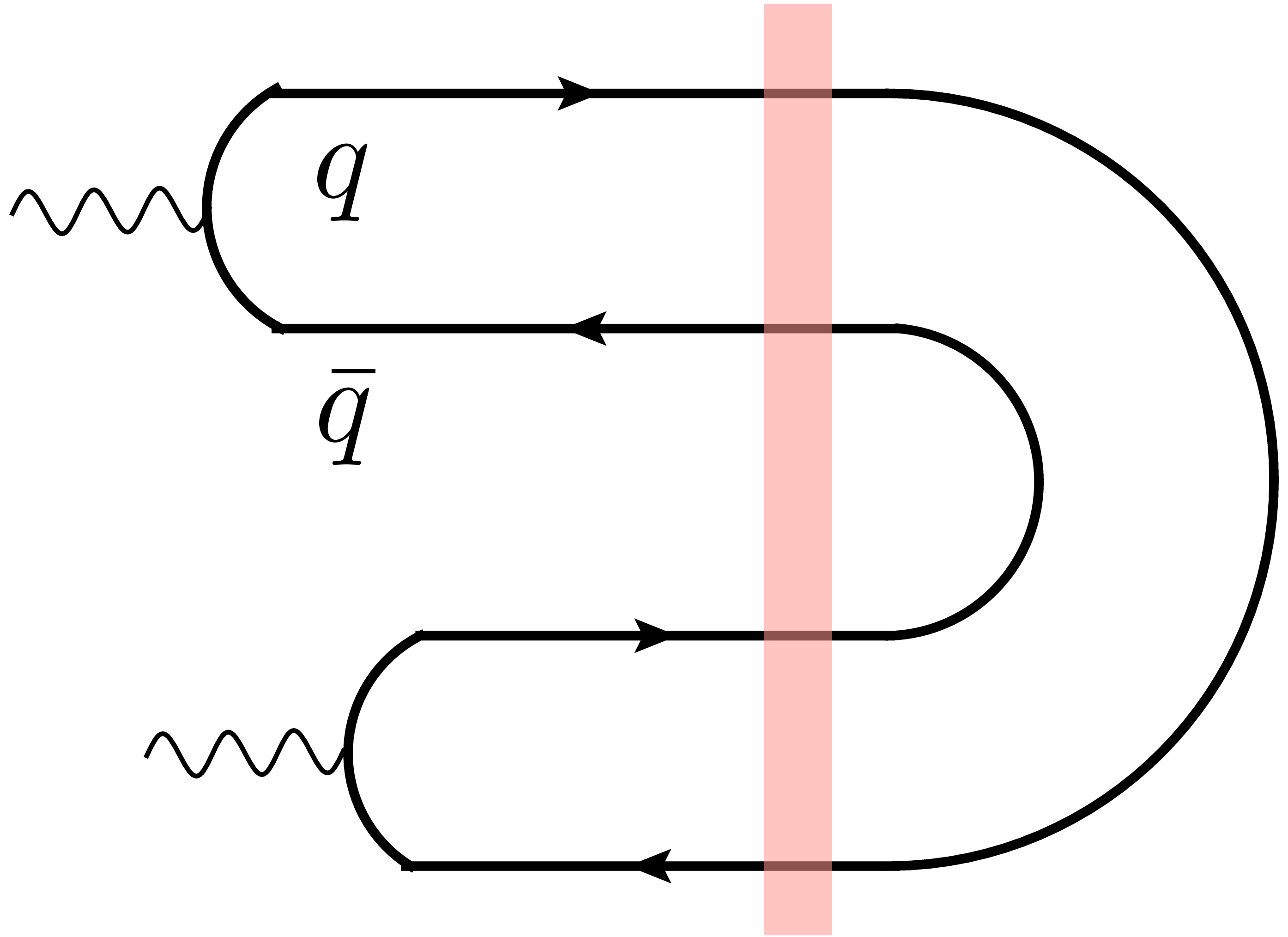

Above C4 correlator can be written as

$$\int_{\boldsymbol{q}_1,\boldsymbol{q}_2} \langle \, \mathrm{Tr} \langle \bar{\boldsymbol{k}}_1 \bar{\boldsymbol{k}}_2 | U^\dagger_{q\bar{q}}(L,\bar{x}^+) \, \mathtt{M} \, U_{q\bar{q}}(L,\bar{x}^+) | \boldsymbol{q}_1 \boldsymbol{q}_2 \rangle \, \rangle$$

with the projection operator

$$\mathtt{M} = |\boldsymbol{p}_1 \boldsymbol{p}_2\rangle\langle \boldsymbol{p}_1 \boldsymbol{p}_2|$$

This gives an immediate realization in terms of a quantum circuit language

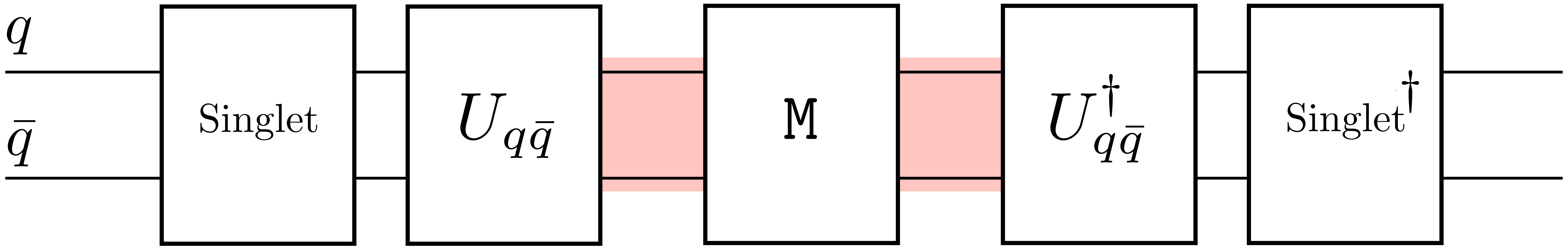

Some illustrative results ...

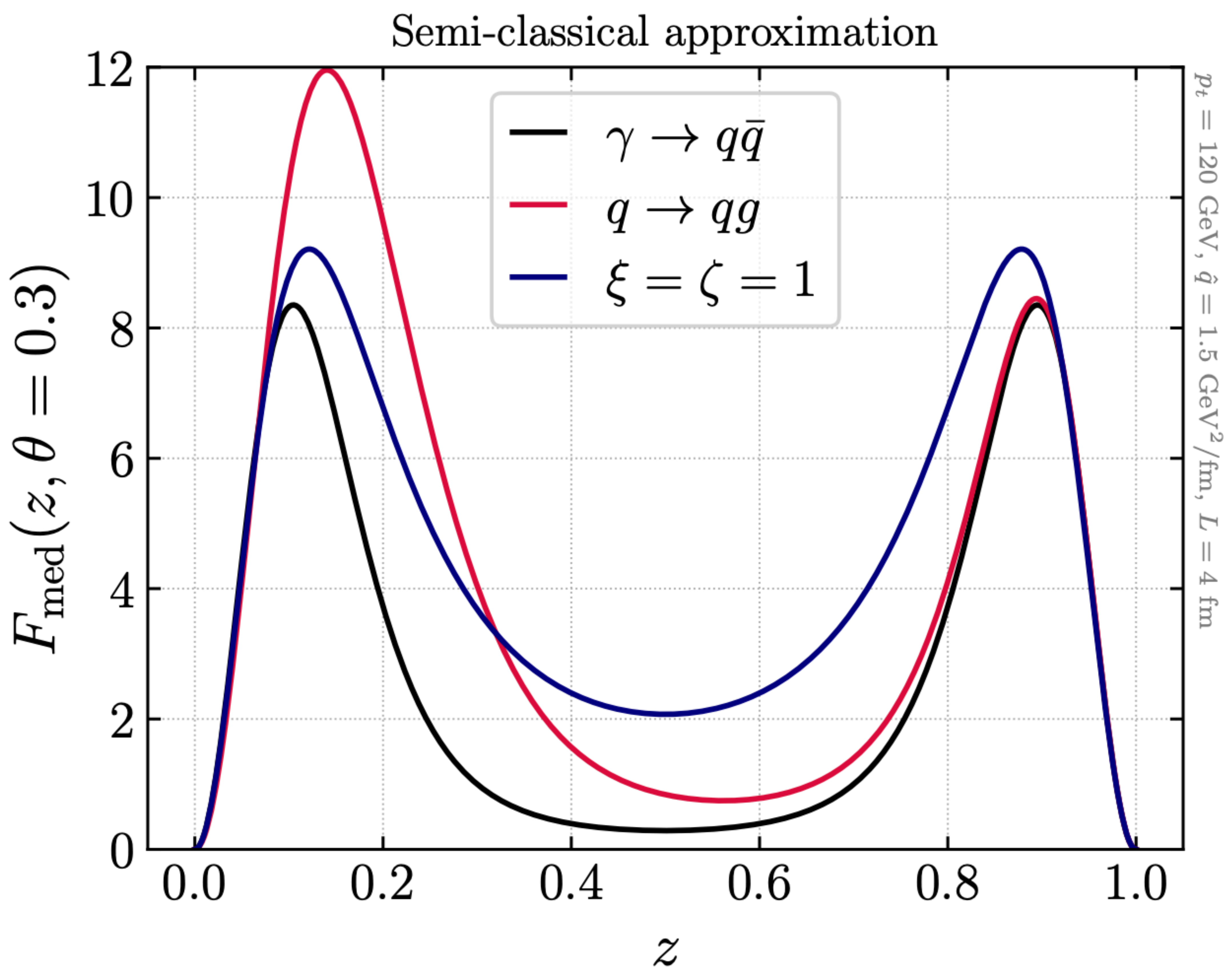

Averaging performed first

[Isaksen, Tywoniuk, 2303.12119]

Real-time simulation of hard probes

Some illustrative results ...

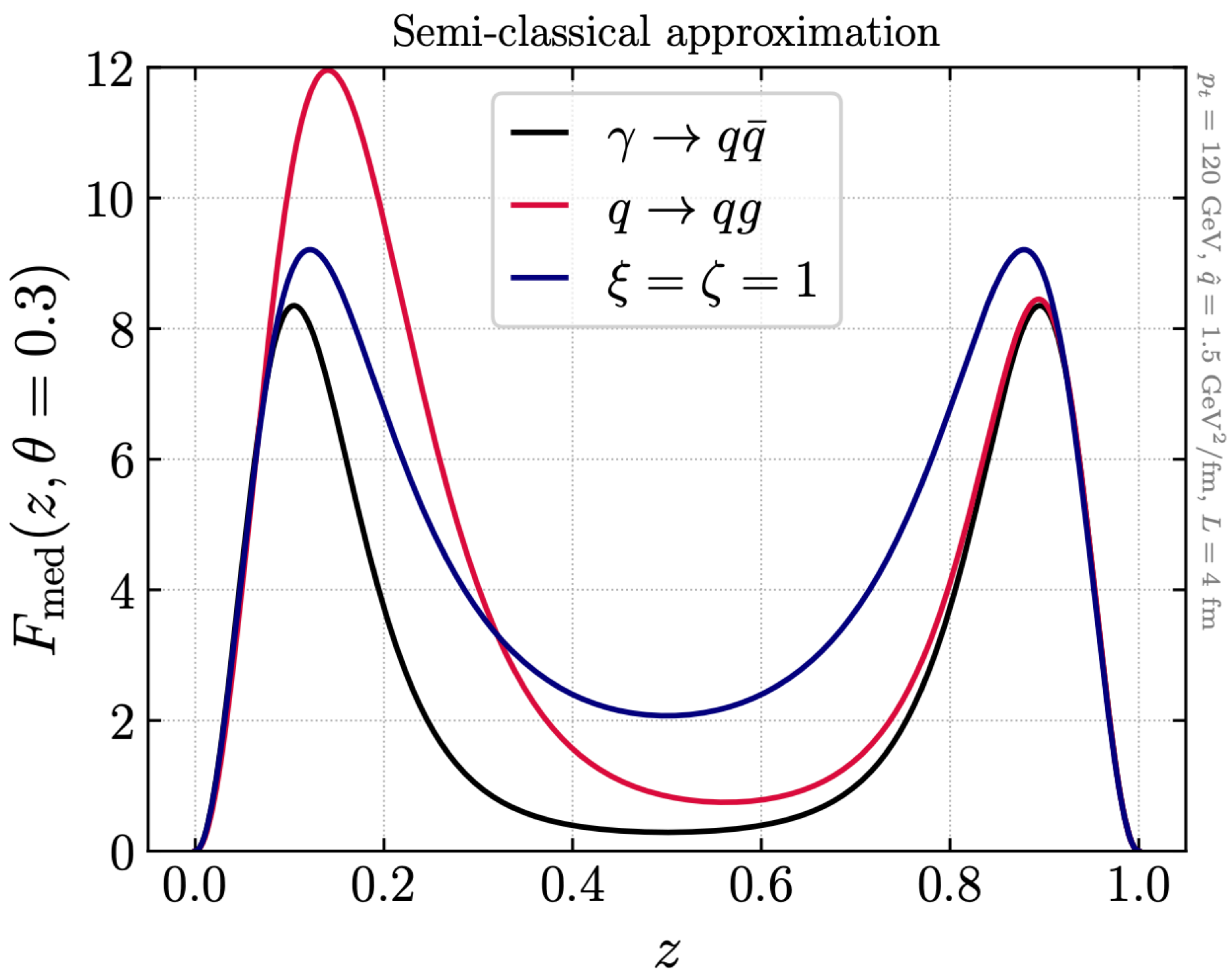

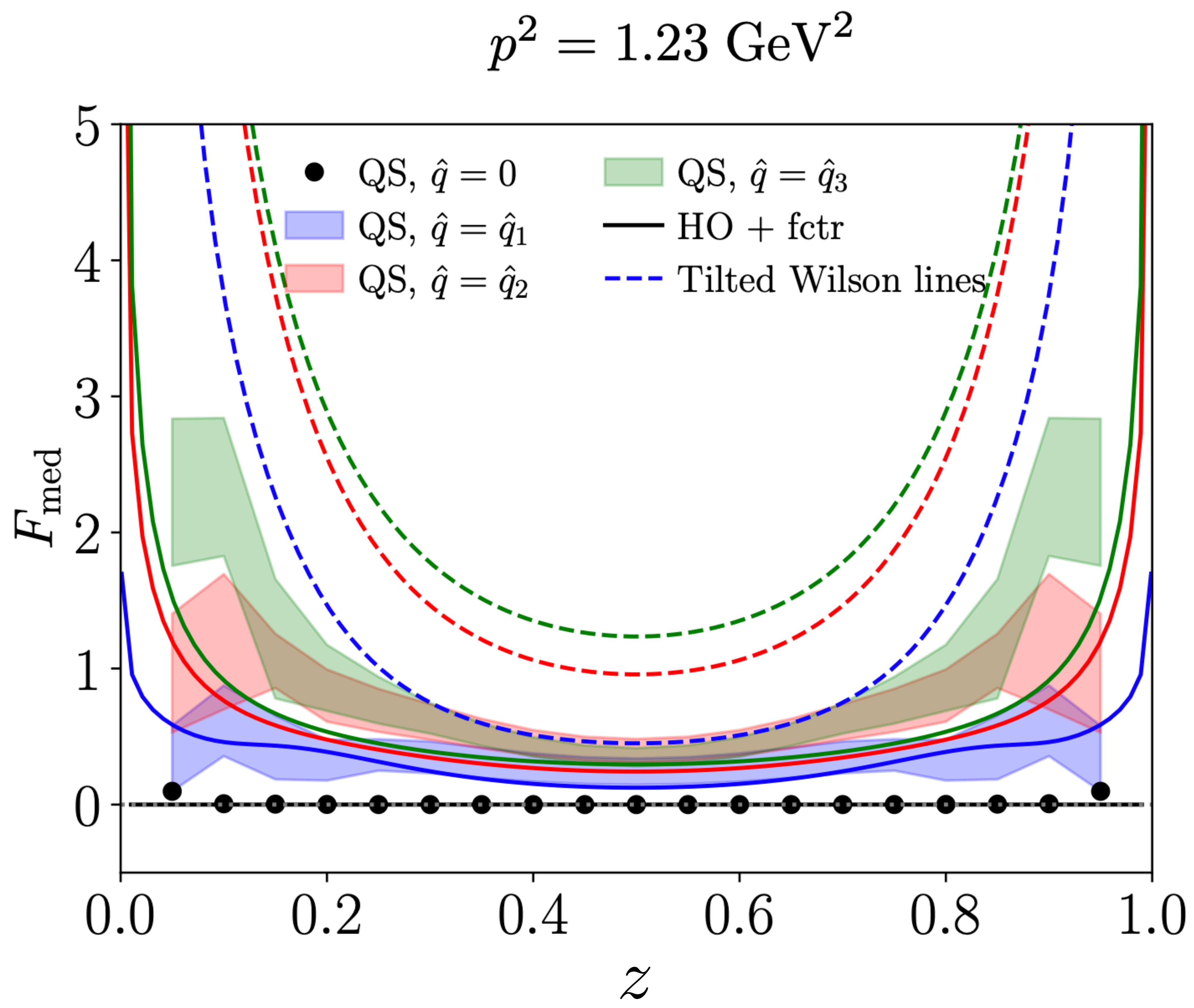

Averaging performed first

[Isaksen, Tywoniuk, 2303.12119]

Averaging performed at the end

Conclusions

Density matrix formulation of jets is useful to explore some intrinsic quantum effects

$$\rho_n\left(\{p_i\}_{i=1}^n, \{p_i'\}_{j=1}^m\right) = \sum_{\{a_i,\lambda_i,f_i\}_{i=1}^n} \sum_{\{a_j',\lambda_j',f_j'\}_{j=1}^m} C_H^\dagger\left(p_1^{a_1\lambda_1 f_1}, \ldots, p_n^{a_n\lambda_n f_n}\right) \times I\left(p_1^{a_1\lambda_1 f_1}, \ldots, p_n^{a_n\lambda_n f_n}; p_1'^{\,a_1'\lambda_1' f_1'}, \ldots, p_m'^{\,a_m'\lambda_m' f_m'}\right) \times C_H\left(p_1'^{\,a_1'\lambda_1' f_1'}, \ldots, p_m'^{\,a_m'\lambda_m' f_m'}\right) + \ldots$$

↔

Breuer, Petruccione; Neill, Waalewijn

$$I\left(p_1^{a_1\lambda_1 f_1}, \ldots, p_n^{a_n\lambda_n f_n}; p_1'^{\,a_1'\lambda_1' f_1'}, \ldots, p_m'^{\,a_m'\lambda_m' f_m'}\right) = 0$$

unless $n = m, p_i = p_i'$ and $a_i = a_i'$ for all i,

Hamiltonian formulation allows for novel calculational approach to physical observables

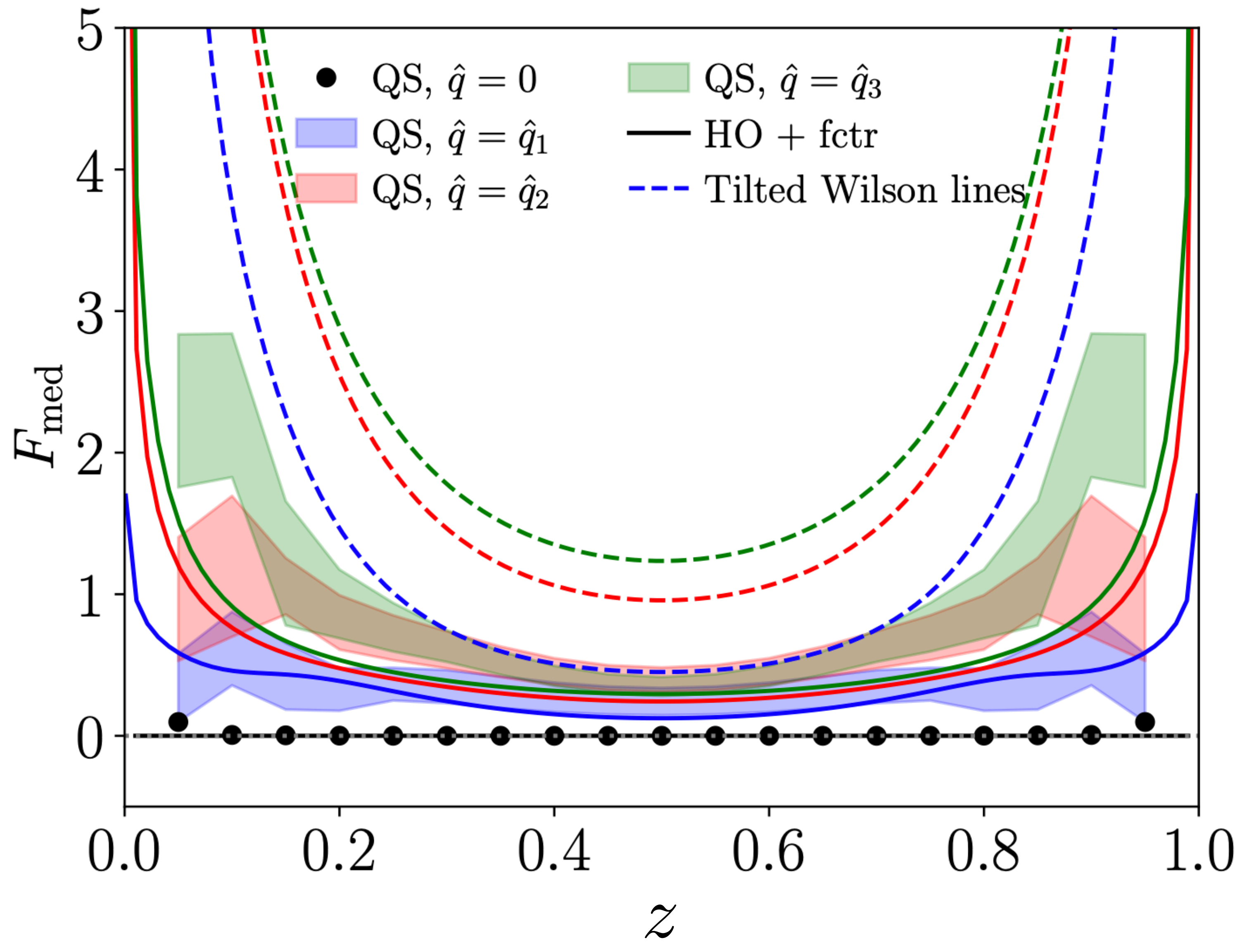

Thank you !

Extra slides

The Standard Model of heavy ion collisions

We have a good hydrodynamical description of the bulk comparing to the remnants of the QGP

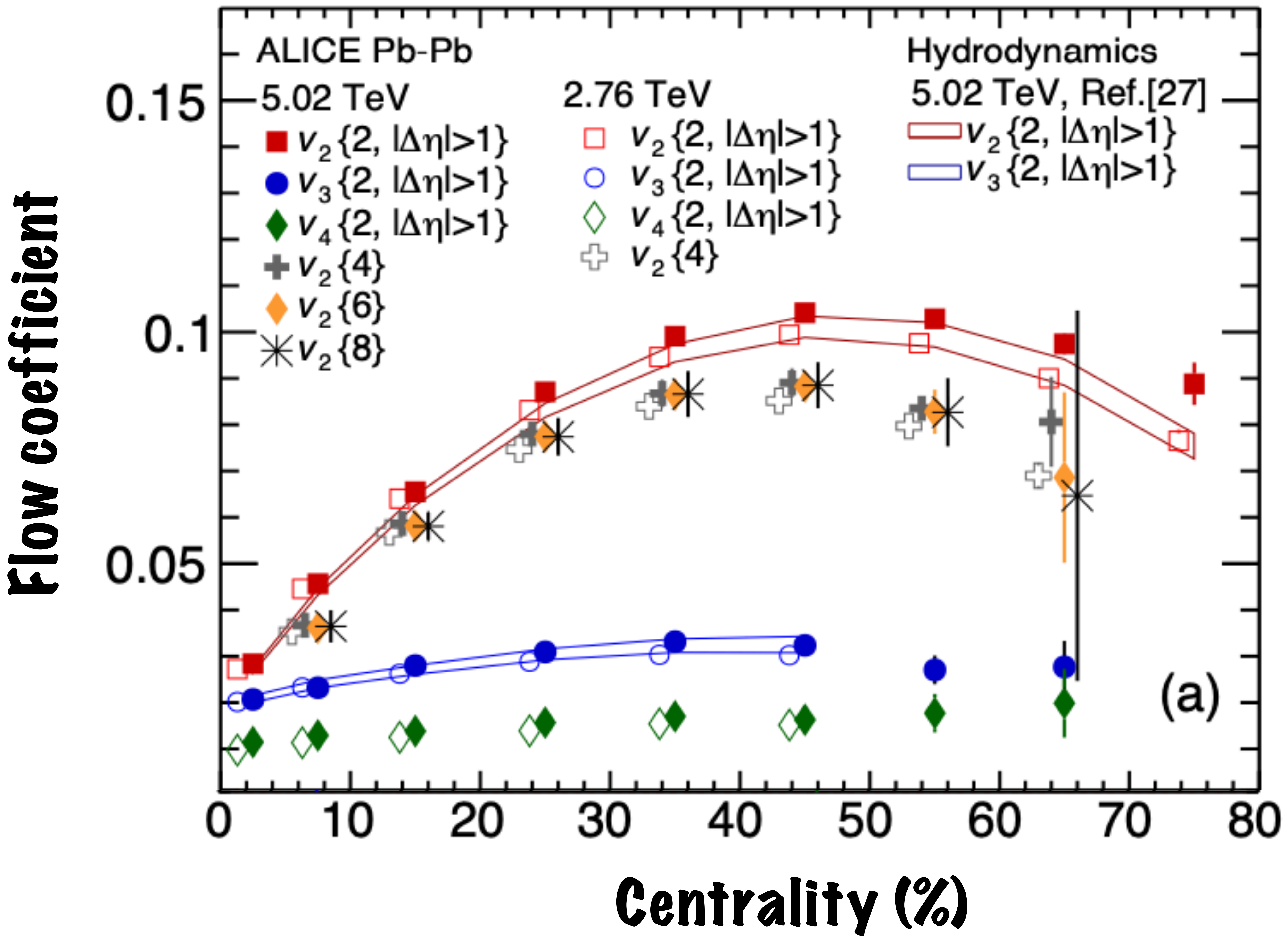

Jet density matrix

Example: density matrix of a QCD jet Breuer, Petruccione; Neill, Waalewijn

$$
\begin{aligned}
&\rho_n\left(\{p_i\}_{i=1}^n, \{p_i'\}_{j=1}^m\right) \\
&= \sum_{\{a_i,\lambda_i,f_i\}_{i=1}^n} \sum_{\{a_j',\lambda_j',f_j'\}_{j=1}^m} C_H^\dagger\left(p_1^{a_1\lambda_1 f_1},\ldots,p_n^{a_n\lambda_n f_n}\right) \\
&\times I\left(p_1^{a_1\lambda_1 f_1},\ldots,p_n^{a_n\lambda_n f_n}; p_1'^{\,a_1'\lambda_1' f_1'},\ldots,p_m'^{\,a_m'\lambda_m' f_m'}\right) \\
&\times C_H\left(p_1'^{\,a_1'\lambda_1' f_1'},\ldots,p_m'^{\,a_m'\lambda_m' f_m'}\right) + \ldots
\end{aligned}
$$

$$
I\left(p_1^{a_1\lambda_1 f_1},\ldots,p_n^{a_n\lambda_n f_n}; p_1'^{\,a_1'\lambda_1' f_1'},\ldots,p_m'^{\,a_m'\lambda_m' f_m'}\right) = 0
$$

unless $n = m, p_i = p_i'$ and $a_i = a_i'$ for all i,

This is result is well known for heavy non-relativistic particles in QED from decoherence theory; it is related to IRC safety. It trivially results that

$$
\rho = \sum_{n=1}^{\infty} \int_H \mathrm{d}\Pi_n(p_J) \frac{1}{\sigma} \frac{\mathrm{d}\sigma}{\mathrm{d}\Pi_n} |p_1, p_2, \ldots p_n\rangle\langle p_1, p_2, \ldots p_n|
$$

How does this mechanism work in the presence of a QCD medium ?

Light Front Hamiltonian

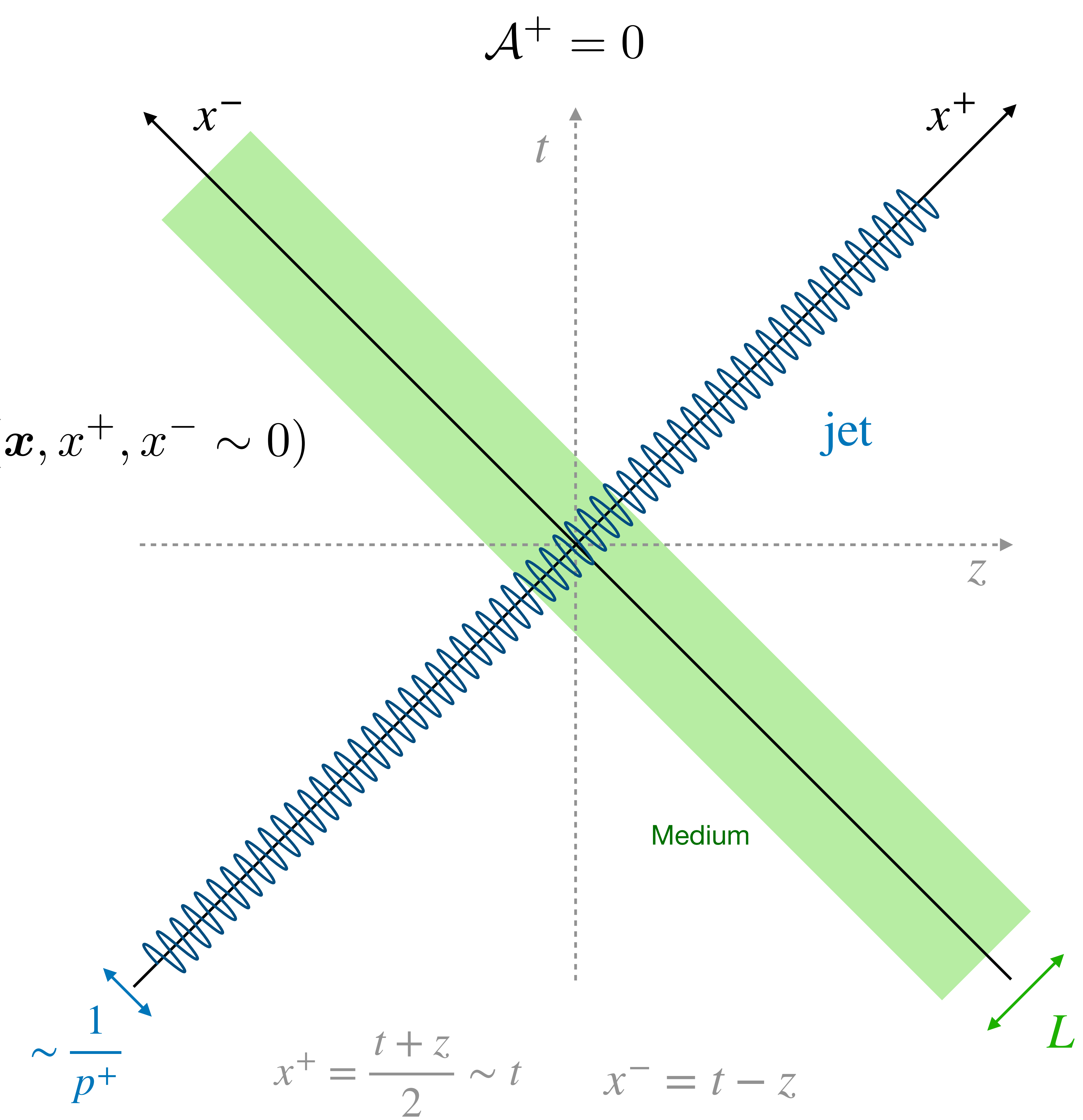

Restricting to $|\psi\rangle = c_q|q\rangle + c_{qg}|qg\rangle$ the Hamiltonian reads

$$H = P^- + V_{\mathcal{A}} + V_{qg}$$

$$F_a^{\mu\nu} \equiv \partial^\mu C_a^\nu - \partial^\nu C_a^\mu - g f^{abc} C_b^\mu C_c^\nu \qquad C^\mu = \underbrace{A^\mu}_{\text{quantum}} + \underbrace{\mathcal{A}^\mu}_{\text{stochastic}}$$

where

$$P^-_{KE} = P^-_{KE,g} + P^-_{KE,q} = \int \mathrm{d}x^- \, \mathrm{d}^2\boldsymbol{x} \left(-\frac{1}{2} A_a^j (i\nabla)_\perp^2 A_j^a + \frac{1}{2} \bar{\Psi} \gamma^+ \frac{m^2 - \nabla_\perp^2}{i\partial^+} \Psi \right)$$

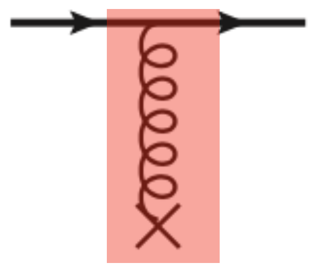

$$V_{\mathcal{A}}(x^+) = V_{\mathcal{A},q}(x^+) + V_{\mathcal{A},g}(x^+) =$$
$$= \int \mathrm{d}x^- \, \mathrm{d}^2\boldsymbol{x} \left(g \bar{\Psi} \gamma^+ T^a \Psi \mathcal{A}_+^a(x^+) + g f^{abc} \partial^+ A_i^c A^{bi} \mathcal{A}_+^a(x^+) \right)$$

$$V_{qg} = \int \mathrm{d}x^- \, \mathrm{d}^2\boldsymbol{x} \, \bar{\Psi} \gamma^\mu T^a \Psi A_\mu^a$$